2015-07-23

Aequorin Mutants with Site-Specifically Incorporated Non-Natural Amino Acids for Biomedical Applications

Kristen Marie Grinstead
University of Miami, k.grinstead1@umiami.edu

UNIVERSITY OF MIAMI

AEQUORIN MUTANTS WITH SITE-SPECIFICALLY INCORPORATED NON-NATURAL AMINO ACIDS FOR BIOMEDICAL APPLICATIONS

By

Kristen Marie Grinstead

A DISSERTATION

Submitted to the Faculty
of the University of Miami
in partial fulfillment of the requirements for
the degree of Doctor of Philosophy

Coral Gables, Florida

August 2015

UNIVERSITY OF MIAMI

A dissertation submitted in partial fulfillment of
the requirements for the degree of
Doctor of Philosophy

AEQUORIN MUTANTS WITH SITE-SPECIFICALLY INCORPORATED NON-NATURAL AMINO ACIDS FOR BIOMEDICAL APPLICATIONS

Kristen Marie Grinstead

Approved:

_____ Sylvia Daunert, Ph.D. Professor of Biochemistry and Molecular Biology	_____ Leonidas Bachas, Ph.D. Professor of Chemistry
_____ Roger LeBlanc, Ph.D. Professor of Chemistry	_____ Dean of the Graduate School
_____ Sapna Deo, Ph.D. Professor of Biochemistry and Molecular	

GRINSTEAD, KRISTEN MARIE (Ph.D., Chemistry)

Aequorin Mutants With Site-Specifically Incorporated Non-Natural Amino Acids For Biomedical Applications

(August 2015)

Abstract of a dissertation at the University of Miami.

Dissertation supervised by Professor Sylvia Daunert.
No. of pages in text. (150)

Light emitting molecules are an indispensable part of detection and reporting in many fields and are employed in a variety of biomedical applications. Bioluminescent light, or living light, from bioluminescent proteins in particular has many beneficial characteristics, including their lack of a need for an outside excitation source and detection at as low as subattomole levels. Aequorin is a well-characterized bioluminescent photoprotein that has found application in *in vitro* and *in vivo* studies. Despite the many advantages of aequorin, its application has been limited by the finite number of canonical amino acids restricting the engineering of aequorin. In order to increase the applications of aequorin, we have taken established methods that hijack the cellular machinery used to synthesize proteins to incorporate non-natural amino acids. By site-specifically incorporating the non-natural amino acids L-4-aminophenylalanine, L-4-bromophenylalanine, L-4-iodophenylalanine, and L-4-methoxyphenylalanine, into positions associated with the bioluminescence and charging them with analogs of coelenterazine, several red-shifted aequorins, including the most red-shifted aequorin to date, with half-lives of up to 60 s were developed, creating aequorin mutants suitable for multiplexing and for transparent and deep tissue imaging. An additional non-natural amino acid, L-4-azidophenylalanine, for bio-orthogonal linking via click chemistry was

incorporated at position 69 of aequorin. This form of orthogonal reaction can be reliably performed with any two molecules that contain the azide and alkyne reactive groups required for click reactions, even in complex samples, with no side reactions. The L-4-azidophenylalanine substituted aequorin was successfully covalently linked to a fluorophore via the azide to alkyne click reaction for BRET. Aequorin was also genetically linked to a VEGFA targeting molecule, a DARPin designated as MP0112, for the imaging of neovascularization *in vivo* using a wet age-related macular degeneration model in mice induced by laser exposure. By doing so, we developed the first bioluminescent imaging system using a DARPin to directly image VEGFA in the retina.

It's not that I'm so smart, it's just that I stay with problems longer.-Albert Einstein

Dedications

I have to thank many people in my life whose support and direction built a foundation on which achievements could be built. First and foremost, I thank my Ph.D. advisor Sylvia Daunert. She has provided an environment of drive and initiative and freedom backed up by practical resources to let me strive for the best I could achieve. I could not have accomplished what I have without her drive for the success of her students. I also thank my committee members Dr. Bachas, Dr. LeBlanc, and Dr. Deo. Your experience, concern, and critiques have helped me become the investigator that I am. I would also like to thank Dr. Mark Ensor for taking the time to teach me all the details of professionally conducting research and my much of my success is owed to that. I also thank Dr. Pirouz Daftarian and Dr. Jean-Marc Zingg for their insights and support in research and scientific communications.

Working in the Daunert Lab has allowed to meet a lot of people that made lab more than a just a research environment. First, I thank Dr. Laura Rowe, who mentored me when I was new and answered all my questions. She gave me the experience that was the basis for the rest of my research. Second, I have to thank Xiaowen Yu, Megan Gillespie, Greg O'Conner, Dave Broyles, Trajen Head, and Eric Hunt, for the fun and the science. Finally, I thank Dr. Emre Dikici for pushing me and brainstorming sessions.

My family gave me the start in the world that allowed me to seek everything thereafter. I am thankful to my mom and dad, Barbara and Randy Grinstead, for trying to provide me with all I need and always caring about how I'm doing and where I'm going.

Lastly, I want to thank my extended family, whose examples helped me determine where to go in life and what to do when I got there.

TABLE OF CONTENTS

LIST OF FIGURES

CHAPTER 1

CHAPTER 2

CHAPTER 3

CHAPTER 4

CHAPTER 6

LIST OF TABLES

List of Publications

1. Grinstead, K., Rowe, L., Ensor, CM., Dikici, E., Joel, S., Daftarian, P., Zingg, JM., Daunert, S. *Red-Shifted Aequorin Variants Incorporating Non-Canonical Amino Acids: Applications in In Vivo Imaging* (in preparation)

2. Grinstead, K., Dikici, E., Daftarian, P., Zingg, JM., Daunert, S. *In Vivo Imaging of Neovascualrization in the Retina Using an VEGFADARPIN-Aequorin Fusion Protein* (in preparation)

3. Grinstead, K., Dikici, E., Daftarian, P., Zingg, JM., Daunert, S. *Click Capable Non-Natural Aequorin for Bio-orthogonal Conjugation* (in preparation)

4. Grinstead, K., Joel, S., Dikici, E., Daunert, S. *The Photoprotein Aequorin in Biotechnology: Fundamental Properties and Genetic Engineering*. In Advances in Biochemical/Engineering Biotechnology-Bioluminescence: Fundamentals and Applications in Biotechnology, Springer (in preparation)

CHAPTER 1. INTRODUCTION

Protein engineering emerged as strategy to take advantage of the ability to modify the molecular machinery of living organisms following the increased understanding of DNA and development of recombinant DNA in the 1970's[1]. Genes could be pulled from nature to recreate the proteins they encode in a laboratory setting. The uses of such proteins ranged from rigid structural applications to molecular motors, from DNA editing to shuttling larger molecules, and as described in this thesis, from sensing small molecules to emitting light. Such luminescent molecules are valuable to many fields, including biochemistry, biophysics, cell biology, and immunology[2].

Light emitting molecules in nature include fluorescence, phosphorescence, and bioluminescence. Unlike fluorescence and phosphorescence, bioluminescence does not require an outside excitation source to excite the electrons in the molecule and stimulate light emission from the energy released from electronic relaxation, instead it uses a chemiluminescent reaction to generate light. Though the emission of bioluminescent light can be found in a wide variety of organisms, from plankton to fireflies, the location of much of the bioluminescent organisms in nature can be found in the ocean (Figure 1.1)[3]. In the absence of sunlight, either during the night or in the deep ocean, life forms provide their own light for tasks such as hunting and communicating danger[4].

Bioluminescence, or living light, provides several advantages over the fluorescence frequently found in nature and used in laboratories, in addition to the lack of a need for an

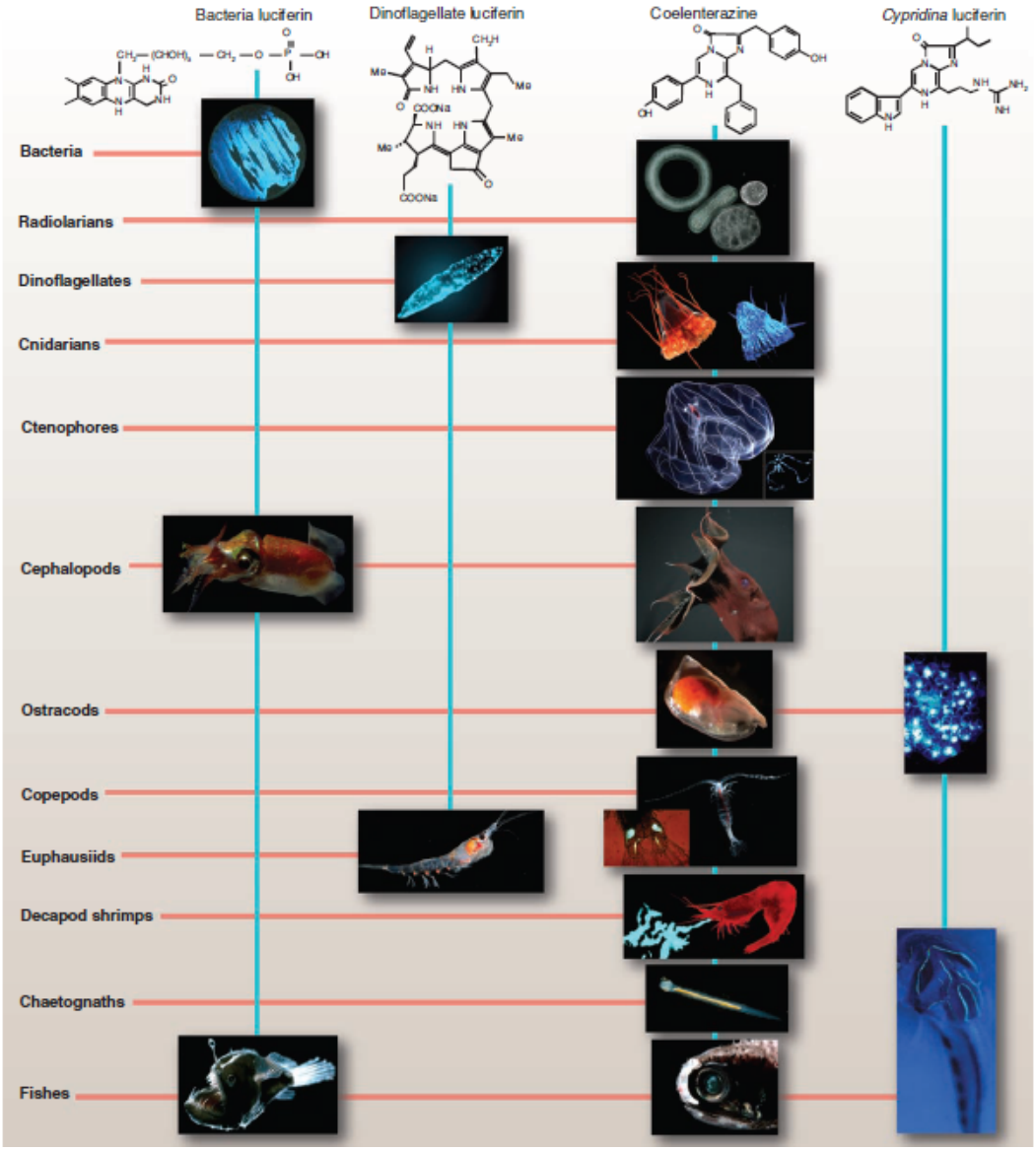

Figure 1.1. Chemical structures of well-known luciferins and their phylogenetic distribution. From Bioluminescence in the Ocean: Origins of Biological, Chemical, and Ecological Diversity, E. A. Widder, *Science* 7 May 2010: 328 (5979), 704-708. Reprinted with permission from AAAS.

fluorescence of common small molecules like the amino acid tryptophan. Furthermore, even samples with a low fluorescence background can be photobleached by repeated exposure to potentially damaging light sources like UV and lasers, a problem not encountered with bioluminescence[5].

Bioluminescent proteins can be divided into two categories: luciferases, or glow proteins, and photoproteins which display flash kinetics[6]. Both of these take advantage of the light emitting molecule, known as a luciferin, reaching the excited state necessary for light emission by becoming oxidized. Luciferases, including firefly luciferase (FLuc), *Renilla* Luciferase (RLuc) from the Sea Pansy, and *Gaussia* luciferase (GLuc) from the Deep Sea Copepod generate their bioluminescence using the enzymatic luciferase, their luciferin substrates, and any required cofactors such metal ions and hydrogen peroxide[7]. In contrast to the luciferases, photoproteins do not display standard enzyme-substrate enzyme kinetics, rather, there is a fast catalytic set followed by a slow regeneration step, allowing the light emission to be treated like a switch with "on" and "off" positions controlled by the addition of the luciferin and required cofactors. Therefore, the signal generated by the photoprotein is proportional to the amount of the protein present in the sample rather than the amount of substrate and can be detected at subattmole levels[8]. There are many photoproteins, frequently taking advantage of a particular luciferin known as coelenterazine, include those that use calcium ions as a cofactor. Of these, two well-characterized photoproteins include obelin and aequorin[9].

1.1 Aequorin

The photoprotein aequorin was originally isolated in the 1970's by Shimomura Osamu, who won the Noble Prize 2008 for his work with Green Fluorescent Protein isolated from the hydromedusa *Aequorea victoria,* also known as the Crystal Jelly (Figure 1.2)[10]. Aequorin is a globular 21 kDa protein consisting of 4 EF-hands. EF-hands

are made up of a pair of alpha helices connected by a stretch of amino acids that include a 12 amino acid loop with six invariant amino acids that are able to bind divalent cations in

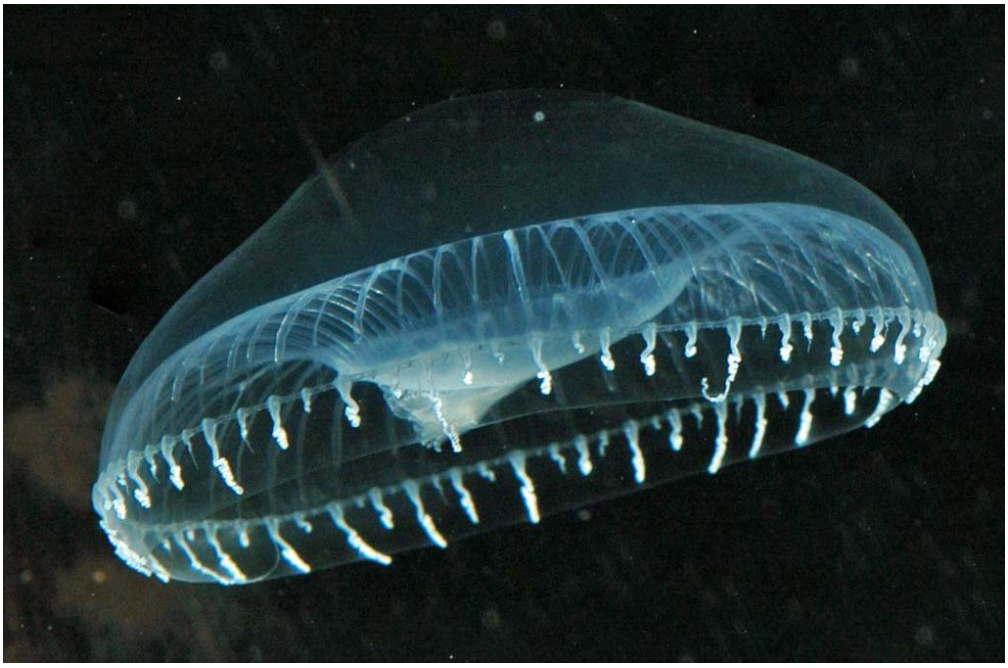

Figure 1.2. *Aequorea victoria*, the Crystal Jelly, and its light-emitting organs.
Attribution: Sierra Blakely.

a bipyramidal configuration[11]. Of aequorin's four hands, the hands designated I and III are capable of binding calcium ions, while II is unable to bind due to site-specific mutations in the binding loop and IV has a deformation of the loop[12]. Thus, two calcium ions are required for the activation of the aequorin signal.When coelenterazine is within the pocket, it forms a covalent bond with an oxygen to create a peroxide bond that is stabilized by a tryptophan at molecule at position 184 near the N-terminus of the protein, one of three tryptophans within the hydrophobic pocket that are part of Tyr-Trp-His triads that are key in stabilizing the peroxide form of the coelenterazine via H-bonds (Figure 1.3)[13]. The conformational change caused by the calcium binding moves the

Trp184 away from the peroxide to cause a rearrangement of the coelenterazine into an excited coelenteramide and a CO_2 molecule[9c].

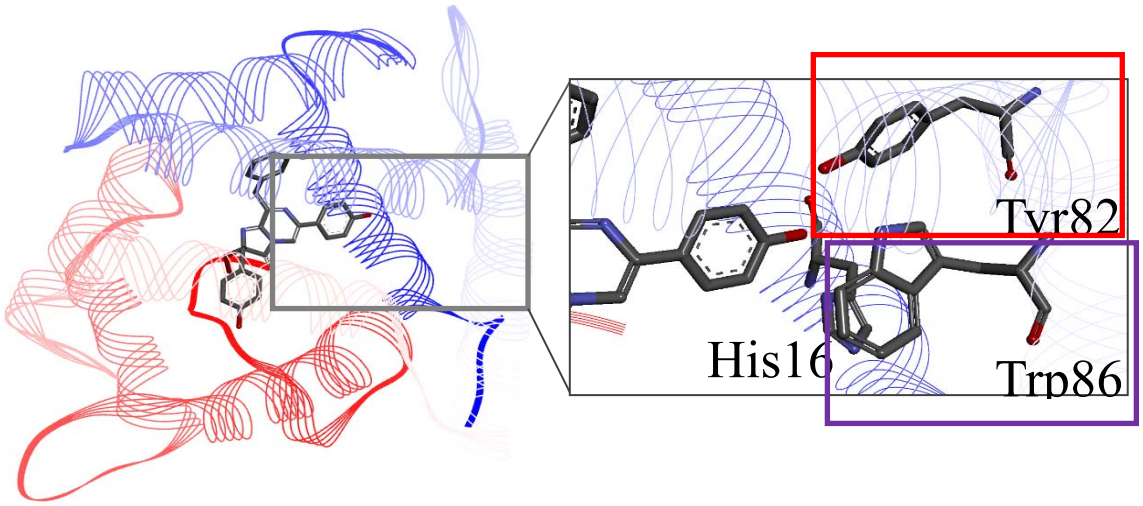

Figure 1.3. Crystal structure of aequorin around the active site with native coelenterazine.

It is the excited coelenteramide molecule in a singlet state that releases the half second flash of blue light associated with aequorin. The spent coelenteramide remains bound within the hydrophobic pocket of the aequorin, preventing the incorporation a new coelenterazine resulting in a slow regeneration rate[14]. The flash of aequorin is proportional to the amount of protein present and it's high sensitivity to calcium in to the sample has led to aequorin being applied in many biomedical applications including calcium sensing *in vivo*[15], in assays, and more recently in *in vivo* imaging[5, 8, 16].

1.2 Designed Ankyrin Repeat Proteins (DARPins)

Bioluminescent molecules such as aequorin are not the only protein type found in the ocean that can be used in assays. The *Agnatha* superclass of jawless fish uses leucine-rich

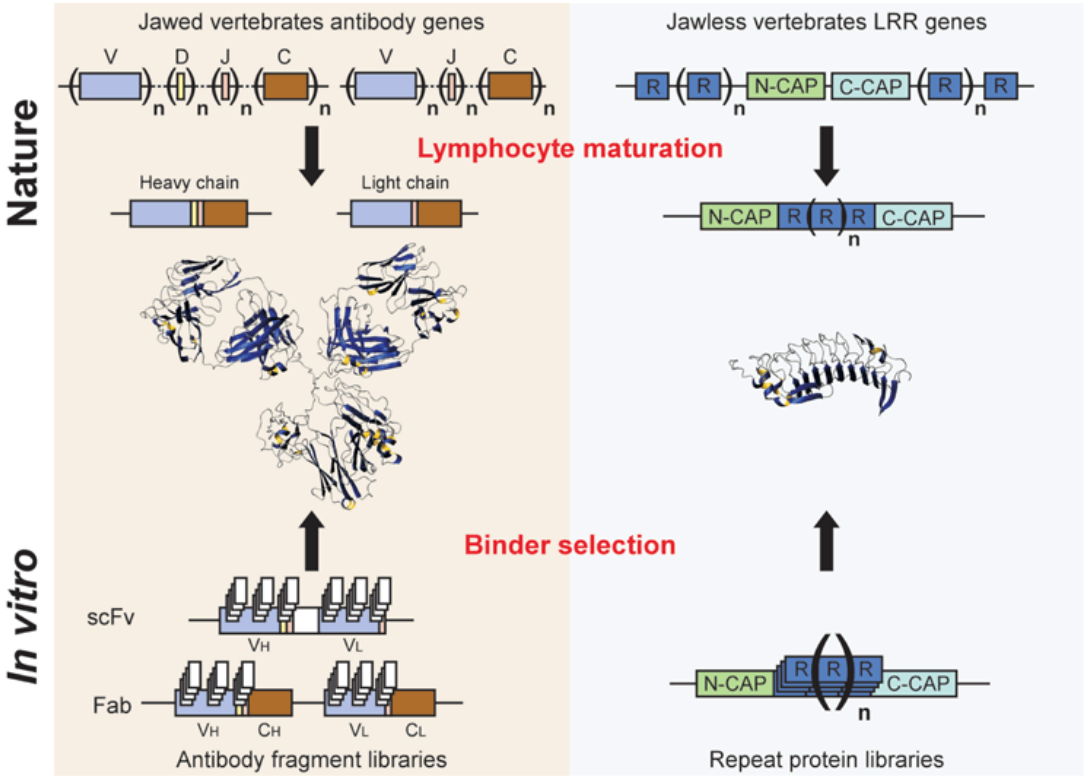

Figure 1.4. Schematic of the generation of antibodies and repeat proteins in nature and *in vitro*. *Left* The generation of antibodies in nature and the creation of antibody fragment libraries *in vitro*. *Right* The generation of leucine repeat proteins (LRR) in nature and engineered novel binding repeat proteins *in vitro*. Binz, H. Kaspar. Amstutz, P. Pluckthun, A. *Curr. Opin. Biotechnol*. 2005, 16: 459-69. Reprinted with permission from Nature Publishing Group.

repeat (LRR) proteins as an adaptive immune system in place of antibodies[17]. LRR, like other repeat proteins found in nature such as ARM, HEAT, and Ankyrins, are consist of repeat motifs that generate different types of protein architecture that drive protein-protein interactions and function as scaffolds for multi-protein complexes[18]. Designed Ankyrin Repeat Proteins (DARPins) are an engineered version of the ankyrin repeat protein motif, that like LRR, can be used as targeting proteins in the same manner as antibodies[19]. DARPins are composed of alpha-helical repeat modules that create a target interaction surface that can be modified, or designed, by deleting, substituting, or

inserting individual amino acids or entire modules without losing the tertiary structure of the protein, capped on end by flanking modules referred to as the N-cap and C-cap.DARPins repeats are usually 33 amino acids long, with four to six repeats of anti-parallel alpha-helices connected by a single beta-turn, though DARPins can have as many as 29 consecutive repeats [19-20] (Figure 1.4). Libraries created by semi-randomized methods are enormous, with a theoretical 5.2 x 10^{15} proteins available for two-module binders alone. Full consensus DARPins are especially stable and resistant to denaturation by boiling and guanidine hydrochloride, to the degree that DARPins with three internal repeats can resist temperatures of 37 ^{o}C for up to a year. DARPins of this type are expressed very well in *E. coli* as soluble monomers[21], making them easy to produce, and they can be genetically linked to other proteins. The specificity and affinities are comparable to those of antibodies, and can be even higher. A DARPin specific for human epidermal growth factor 2 (HER2) was tested by the US Food and Drug Association (FDA) and determined to have a similarly sensitive but significantly higher specificity than the FDA approved antibody in a tissue microarray[22]. DARPins have many characteristics that make them preferable to antibodies and antibody fragments as targeting molecules in biological imaging in addition to their specificity, robust nature, and modifiable structures. Antibodies have a high aggregation tendency made worse when conjugated to other molecules or when under reducing conditions. Most DARPins, as previously mentioned, are easy to express as soluble monomers in *E. coli* and therefore are expressed in their functional form inside the cell without aggregating.

In addition, the crystals structures of some DARPins bound to their targets have been obtained, confirming the location of the binding of the DARPin to targets and

providing additional information on not only how the DARPin binds, but where (Figure 1.5). DARPins can also be genetically fused to other proteins without compromising the binding. A study aiming to prove the effectiveness of DARPins as targeting molecules utilized DARPins targeting c-Jun-N-terminal kinase-1 (JNK-1) and c-Jun-N-terminal kinase-2 (JNK-2) fused to RLuc and GFP, respectively; these DARPin fusion proteins were expressed in living cells and acted as selective inhibitors of the kinases[23].

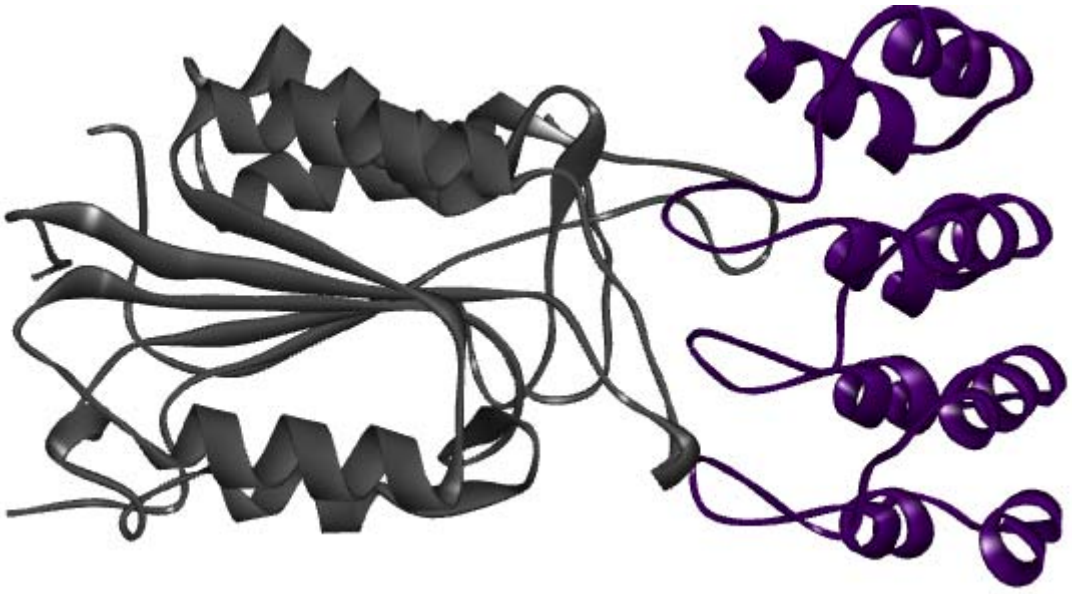

Figure 1.5. DARPin-3.4_178S (grey) in complex with caspase-3 (purple). (PMD Code: 2XZT)

1.3 Assays

The specific and high affinity binding of the DARPins make them suitable for use as a targeting molecule beyond the initial studies with the JNK enzymes. Assays make use of a biological element as the reporter molecule, which provides the signal, that is linked to a targeting molecule for the detection of the target molecule or ion, called an analyte.

Samples analyzed by biological assays include biochemical samples, individual cells or cells within an organism, and organic samples.

Clinical diagnostics have made use of biological based assays for the detection of target analytes for years. Sensitive and specific detection molecules for biological assays are typically antibodies, large multi-chain proteins created by the immune cells to target a single analyte, and DNA oligonucleotides that under optimal conditions only bind to their complementary sequence match. A greater variety is found in the different methods available for the quantitative reporting the detection of the analyte. Methods include visualization in the form of colorimetric, electrochemical, gravimetric, luminescent, magnetic, and radioisotopic signals. Each method has benefits and limitations, including increased variables from multiple added reagents effecting purity and reproducibility and reagents potential toxicity. Reporter molecules can either report by being linked to the targeting molecule, such as a fluorophore linked to an antibody, or the analyte itself in a competitive assay, such as a radioactive isotope in a small molecule, like glucose. Illumination based reporter molecules share this flexibility without some of the limitations of other reporting methods[5].

1.4 Linking Aequorin to Targeting Molecules

Aequorin, which is non-toxic and active at physiological pH, offers all the benefits of other bioluminescent reporter molecules when compared against fluorescence, and can be detected with attomolar sensitivity, an important characteristic when detecting low amounts of analytes[24]. Additionally, the aequorin luminescent signal can be tuned by protein engineering using genetic or chemical methods. Methods for

linking the aequorin to the targeting molecule or analyte can be via chemical conjugation or genetic fusion.

1.4.1 Chemical Conjugation for Assays

Methods of chemical conjugation use a linker molecule of any appropriate length that allows both the aequorin and the reporter molecule to maintain their functionality[25]. These linkers have reactive groups on each end that often target amino acids side groups. Commonly available reactive groups on linkers are NHS esters (succinimidyl esters) that allow for linking to the primary amines in lysine and maleimide groups for linking the sulfohydryl groups of cysteine. By keeping track of the number of times the amino acid group appears on the surface of the protein, the number of times the linker can be attached to the protein can be determined. Site-specific linking to the protein can be accomplished by restricting the target residue to only one location in the protein sequence. This requires manipulating the gene sequence of the protein, either by removing all but one of the target amino acid or using a protein that is naturally free of the target residue and introducing one into the sequence using site-directed mutations. However, many factors affect the efficiency of the linking reactions, including pH and temperature, and linking lysines or cysteines present in protein interiors can adversely affect protein activity. An alternative reaction is click chemistry, a reaction using an alkyne group on one molecule and an azide group on the other[26]. This reaction is orthogonal and readily useable in unpurified samples and *in vivo* since neither triple carbon bonds nor azide groups are found in biological fluids, though this requires the analyte to have an alkyne reactive group.

1.4.2 Genetic Fusions for Assays

Genetic fusion is an alternative to chemical conjugation. Genetic fusion guarantees 100% linking of the photoprotein to the second molecule by placing the two proteins into a single gene with any appropriate number of amino acids inserted between the two sequences to create a flexible linker sequence which often consists of serine and glycine. This fused gene is then inserted into a plasmid and placed into an expression cell line to be generated using the cellular machinery. This method has a drawback in that the targeting protein can only be fused to the C and N-terminals of the protein. Additionally, both the photoprotein and the targeting molecule need to be stable proteins that fold correctly when expressed in cells. Despite this drawback, if the fusion protein is to be used in large amounts, genetic fusion is often the most reproducible, efficient, and cost-effective method to produce large amounts of linked proteins.

1.4.3 Aequorin as a Reporter Molecule in ELISA

Enzyme-Linked Immunosorbent Assay's (ELISA) are a common type of photoprotein assay and can be homogenous (the sample contains only the analyte) or heterogeneous (the sample contains multiple molecules beside the analyte). These assays use antibody photoprotein conjugates to directly detect the analyte or use a competitive binding assay where the analyte and an analyte- photoprotein conjugate compete for available antibodies (Figure 1.6)[24, 27]. Assays require a platform for the antibody to bind to, such as beads, nanoparticles, filter paper, or microtiter plates made of plastic. In direct detection, the native analyte binds to the first layer of antibodies already bound to the platform, then the antibody-photoprotein conjugate is added to create the third layer that

generates the signal. In a competitive assay, the native analyte and analyte-photoprotein are added together, resulting in the displacement of the photoprotein bound analyte. Upon addition of calcium to an aequorin based photoprotein assay, the direct assay results in a directly proportional bioluminescent signal that increases as the amount of analyte increases while the competitive assay results in a signal that decreases as the amount of native analyte increases. Both methods require a standard dose-response curve created by plotting the bioluminescence signal observed against the concentration of the analyte to be created as a reference for the final value determination. Assays that use aequorin as a reporter include biotin, HIV protease, and HIV protease inhibitor[28].

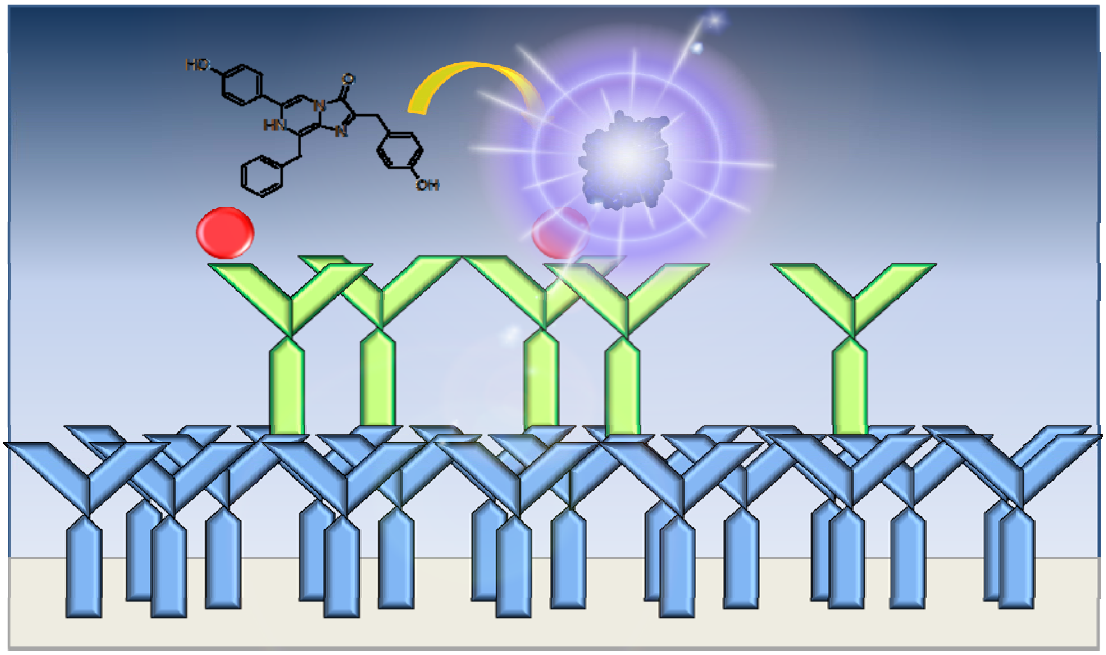

Figure 1.6. Schematic of a competitive bioluminescent ELISA assay with aequorin as the reporter molecule. The red target molecule is bound by the primary antibody, but only the competing red target conjugated to aequorin and paired with coelenterazine generates a signal.

Aequorin also has the potential to be used as a reporter molecule in assays that do not use antibodies as the targeting molecule. DARPins have been combined with other

reporter molecules, but not aequorin[23]. As investigated in this thesis using aequorin and DARPins together for detection is a promising pairing that has thus far been overlooked.

1.4.4 Aequorin as the Reporter in a Molecular Switch

Not all biological assays require a platform for immobilizing part of the assay. Assays that utilize a fusion protein known as a molecular switch do all the detection free in solution. Molecular switches utilize a hinge containing binding protein that capable of binding the target analyte. Hinge structures in proteins created a highly flexible point between the N and C-terminus of the protein that creates a conformational change that moved both halves of the protein together to hold the analyte in place in a non-enzymatic reaction. Aequorin can split into two halves that can be genetically fused at either end of the binding protein such that the aequorin is inactive when separated in the absence of the analyte and regains activity when the two halves are brought together by the closing of the hinge of the binding protein when the analyte is present. Alternatively, the aequorin halves can be together until the binding of the analyte, causing the hinge to open and the signal to be inversely proportional to the amount of analyte present[29].

1.5 *In Vivo* Imaging

Medical imaging is the optical recreation of the interior of the body for the purposes of analysis and intervention, including locations in deep tissues and hidden by other structures, such as bone. Unlike imaging of organs that have been removed, which is considered more the realm of pathology, medical imaging seeks to understand and discriminate healthy and unhealthy tissue while still in the body. Diagnostic imaging uses

the images of the interior to provide information about disease and suspected disease for the purposes of therapy. This is includes biomedical physics, engineering, and clinical medicine.

1.5.1 Imaging Techniques

The introduction of imaging techniques into medicine created ways to monitor disease at its location within the body and in increasingly detailed terms. Early imaging like X-rays were able to show the structure of bones in living people without invasive surgeries and early motion pictures created using X-rays showed healthy and unhealthy physiology in addition to the anatomical information. Increasingly sophisticated imaging techniques have been developed with the advancement of technology, including techniques that provide anatomical information such as ultrasonography that uses sound, magnetic resonance imaging (MRI) that uses magnets and radio frequency to polarize the hydrogens of water molecules, and nuclear based medicine such as single-photon emission computed tomography (SPECT) and positron emission tomography (PET) which use radioactive markers to provide physiological information[30]. Despite these advancements, each of the techniques listed includes drawbacks and limitations. X-rays and ultrasonography both can have limits in imaging structures behind dense tissue like bone. MRI can yield detailed 2D and 3D anatomical and physiological information and is generally considered safe, but cannot be used if patients with metal based implants including pace-makers and shrapnel, and concerns of overuse have brought up concerns of cost-effectiveness. The radioactive nature of nuclear medicine can be harmful to both patient and care-giver and therefore has to be monitored and disposed of carefully.

Despite the limitations, the usage, and costs, of these methods is expanding. Between 1996 and 2010, over 30.9 million imaging examinations were conducted in the US, with a 3.7% annual increase for ultrasounds, 10% annual increase for MRI, 57% annual increase for PET, among others, while Medicare expenditures for such services rose an average of 17% a year, from $3.6 to $7.6 billion from 2000-2006[30b, 31]. These imaging systems can also be time-consuming, costly, require special training to do or interpret, and most problematic, these techniques provide macroscopic or metabolic information, but not the microscopic molecular or even single ion interactions needed to have comprehensive information about disease states.

1.5.2 Molecular Probes

Optical based imaging systems have also been used in imaging though less commonly than the other forms of imaging mentioned above. Because optical images use fluorescent and bioluminescent signals a light emitting source has to be introduced to the body, referred to as a molecular probe[32]. Fluorescent molecular probes, such as green fluorescent protein (GFP), have been widely applied in imaging studies including molecule interaction studies based on BRET and gene expression[2b, 33]. However, as mentioned previously, fluorescence has the difficulties of background autofluorescence native to samples, the need for an outside excitation source, photobleaching, and possible toxicity that bioluminescence does not.

Bioluminescent studies *in vivo* have often used the luciferases *Renilla* luciferase (RLuc), Firefly luciferase (FLuc), and a bacterial luciferase (Lux) as reporter molecules[6, 34]. The FLuc protein requires ATP-Mg^{2+} for oxidative catalysis of reduced luciferin

resulting in the generation of yellow-green light (peak emission at 562 nm) that can be detected at levels as low as 10^{-19} moles. Rluc utilizes the same oxidative decarboxylation of coelenterazine to coelenteramide found in aequorin to generate blue light at 480 nm. In contrast to aequorin, Lux requires several genes to generate bioluminescence. The bacterial Lux operon consists of five genes (*luxCDABE*) that produce bioluminescence at 490 nm. The Lux consists is a heterodimer of two subunits encoded by the *luxA* and *luxB* genes, and the *luxCDE* genes that express enzymes required for the production and turnover of the luciferin. So far, these luciferases have only been introduced into samples by expression through reporter genes in cellular and animal imaging in mice, rabbits, and monkeys. The requirement of introducing new DNA into the host for the purposes of imaging would require DNA transfection or a tissue transplant for it to be attempted in humans. Another delivery method, the quantum dot, nanocrystals comprised of semi-conductors between 2-10 nm, has potential toxicity that makes it undesirable for medical applications[35].

The use of recombinant aequorin sensor proteins to tissues may be a solution to overcome the above concerns. The addition of protein that had been expressed and purified outside the body avoids the problem of human tissue transplant or transfection. In this thesis, aequorin variants have been designed and purified for *in vivo* imaging of VEGF overexpressing cells in the eye. Once introduced to specific sites in tissues, the non-bound protein was given time to diffuse away and be degraded, upon which the substrate , and the coelenterazine which is known to diffuse through cell membranes was added to activate specifically the bound form.

1.5.3 Photoprotein Applications in IVIS

Molecular probes based on aequorin can be monitored by the In Vivo Imaging System (IVIS) that allows for imaging at the microscopic level when combined with a bioluminescent reporter molecule such as aequorin providing the desired insights into disease states[36]. The IVIS imaging system gathers information faster than other imaging techniques. In IVIS, 3-5 mice can be imaged simultaneously with image acquisition times lasting no more than a few seconds to a few minutes. In contrast, techniques PET, SPECT, or MRI, require about 60 min for image acquisition and can image only one animal at a time, increasing the cost associated with imaging.

1.6 Protein Engineering Strategies

Molecular reporter proteins such as aequorin have been engineered like many other proteins. Characteristics selected for engineering include stability, spectral characteristics such as brightness, peak emission wavelength and bioluminescence half-life, and introducing amino acids for use in linking to targeting proteins for assays and BRET. The process of protein engineering utilizing genetic manipulation to insert, delete, or substitute amino acids in the protein sequence is known as mutagenesis, and can be either random or rational. The mutagenesis of aequorin takes two forms, random and rational.

1.6.1 Random Mutagenesis of Aequorin

Random mutagenesis takes advantage of established methods of random mutagenesis to quickly generate a library of aequorin variants that can then swiftly be

tested for desirable traits. Random mutagenesis can include signal point mutations in the gene or large changes throughout the sequence. Established methods for random mutagenesis include XL1-Red competent cells, error-prone PCR and degenerate oligonucleotides-Pfu (DOP)[37]. XL1-Red cells are engineered *E. coli* cells that have their ability to repair DNA mutations removed, resulting in random mutations of the transfected plasmid every time it undergoes replication. In error-prone PCR, the polymerase, which normally is very carefully selected and engineered to prevent error, a trait known as fidelity, instead incorporates errors during amplification when altering the ratio of nucleotides and the concentration of divalent cations. DOP mutagenesis involves the use of oligonucleotides primers with errors incorporated into the sequence, otherwise known as degenerate primers. To speed up the process of screening, aequorin mutants generated in this manner are first tested for bioluminescent activity before undergoing further characterization.

The random mutagenesis of aequorin by several groups has resulted in a large number of aequorin variants[38]. Among these, only a small portion maintain their activity, indicating just how important the correct amino acid sequence to generate the correct protein structure is for generating bioluminescent activity in aequorin[38c, 39]. Of those that maintain their bioluminescent activity, a handful of locations were revealed to be able to incorporate amino acids with similar properties such that the activity was maintained but the spectral characteristics were altered. For example the tyrosine at position 82 and the position at tryptophan 86 in the hydrophobic pocket were shown to be interchangeable with the other large hydrophobic amino acids, phenylalanine, tryptophan, and tyrosine, to effect the peak emission wavelength and bioluminescent half-life with suffering complete

activity loss, but did suffer activity loss when combined with smaller amino acids, such as alanine and valine.

1.6.2 Rational Mutagenesis of Aequorin

Rational mutagenesis uses a focused approach to generate proteins for specific purposes. For example, insulin has been altered using mutagenesis to provide variants with tailored characteristics that result in rapid or long acting types.

Rational forms of mutagenesis frequently use information obtained from X-ray crystallography and NMR to determine the tertiary structure of the protein and choose locations that might be mutated. In addition, candidate amino acid for mutations can be selected by looking at the interactions with the surrounding environment, including the solvent, the substrate and other amino acids. This can be combined with information gathered through random mutagenesis.

Early experiments with site-specific mutations in aequorin included that substitution of the tryptophan at position 86 with phenylalanine by Ohmiya *et al.*, resulting in a bimodal emission peak with the maxima a position 410 nm (later repeated using random mutagenesis as mentioned previously)[13], and the replacement of histidine causing activity loss[40]. Further site-specific mutations with aequorin focused on the removal of the three cysteine residues found in the wild-type aequorin to simplify purification by removing sulfide binds. Replacing the cysteine's one at a time with a serine revealed a large loss in activity; however, replacing each cysteine with a serine simultaneously yielded an increase in activity and generated the cysteine-free aequorin

used in this dissertation that do not require sulfohydryl reducing agents[41]. Additional studies that incorporated cysteine residues into new locations resulted into a mix of variants with lower activity, though a few maintained as much as 80% of their activity[42]. Rational site-directed mutagenesis of aequorin by our group replaced locations associated with bioluminescent activity to create variants with shifted emission characteristics and elongated half-lives without complete activity loss. In particular, Y82F and W86F revealed red-shifted peak emissions and elongated wavelengths that made these positions of interest in future studies[39b].

The linking ability of the sulfohydryl group of the single introduced cysteine at position 5 was exploited to create a BRET based molecule dubbed "artificial jellyfish". Artificial jellyfish use site-specific mutagenesis to mimic the role of aequorin in nature in relation to GFP wherein aequorin provides the excitation for the emission of GFP[43]. In nature, the emission wavelength of aequorin overlaps with the excitation wavelength of GFP. This is mimicked by choosing a fluorophore that also has an excitation wavelength that overlaps with aequorin's blue emission. By keeping a cysteine at either position 69 or 71 of the aequorin, fluorophores containing a maleimide side group can be covalently linked to the photoprotein. Fluorophores that have been used to create artificial jellyfish with aequorin include IANBD ester and Lucifer Yellow which emit their fluorescent signal at 428 nm and 531 nm[44]. Other BRET aequorin include aequorin linked to the tandem dimer Tomato fluorophore (tdT) created by Roger Tsien to create a chimera with a peak emission at 575 nm specifically designed for use in deep tissue[45].

1.6.3 Coelenterazine Analogs

The natural coelenterazine ligand that is incorporated into the aequorin and that is source of the chemiluminescence is taken up by the jellyfish as part of their diet of organisms such as the ctenophore *Bathocyroe fosteri*[46]. The coelenterazine can be chemically altered at the C2 and C8 positions to produce synthetic analogs that are stable and soluble and alter the emission spectra while maintaining the bioluminescent activity of aequorin[47]. Shimomura *et al.* began studies on the effects of these analogs on the specific activity, peak emission wavelength, and bioluminescence half-life of the wild-type aequorin, creating several active semi-synthetic mutants[48].

1.7 Non-Natural Amino Acid Incorporation

Protein engineering has been limited by the finite number of amino acids. Incorporating non-natural amino acids into a protein is made challenging by the fidelity of the biological machinery involved in the translation of RNA into peptides. This fidelity is important to the survival of living organisms as too many errors in translation would be fatal. To circumvent the many checks in place to guarantee the orthogonal incorporation of amino acids, several different methods have been invented created with the aim to expand the number of amino acids that can be incorporated.

By expanding the number of amino acids beyond the canonical number, new chemical interactions, including the influence of electronic environments and functional side groups, the biochemical applications greatly increase also for aequorin. Non-natural amino acids can theoretically be anything that includes that amino acid backbone. In

addition to providing access to new reactive groups, such a ketone groups , benzoyl, or cyano groups, non-natural amino acids can incorporate elements not found in the canonical amino acids, such as fluorine or iron, and radioactive isotopes[25, 49]. By incorporating these non-natural amino acids, their characteristics can be used to expand linking sites, reveal information about the protein structure through NMR, or be used to track the fate of peptides after introduction into a biological system[50]. Methods that can be used to incorporate non-natural amino acids include solid phase and semi-synthesis, global incorporation, *in vitro* site-specific non-natural amino acid incorporation, and *in vivo* site-specific incorporation.

1.7.1 Solid Phase and Semi-synthesis

One approach for the incorporation of non-natural amino acids bypasses the proof-reading found in biological systems by removing the synthesis from living systems and doing the work in the laboratory. The amino acids are immobilized on beads made of polystyrene or a polyamide. The amino acids have either a Fmoc[51] or Boc[52] group used to N-protect the amino acid to prevent polymerization. Subsequent cycles of deprotection and recoupling are used to synthesize the protein C-terminus to N-terminus, the opposite direction of the synthesis by ribosomes. After an amino acid links to an immobilized amino acid, the newly linked acid has its N group deprotected, allowing for a new amino acid to join the growing peptide. This method is fully automated, has high yields, but is limited to proteins of only around 100 peptides.

Semi-synthesis methods use chemical ligation to link together two or more smaller peptides into a larger structure[53]. These smaller peptides can be synthesized *in*

vivo or by solid phase synthesis. Native chemical ligation uses the C-terminal thioester of one peptide to link to the N-terminal cysteine of another peptide using an exogenous thiol catalyst. Expressed protein ligation exploits naturally occurring inteins, sections of peptides that are removed during protein splicing, in naturally synthesized peptides that contain C-terminal thioesters to link them to an N-terminal cysteine on the synthetic protein. These semi-synthetic methods create longer proteins than solid phase synthesis, but are still limited to around 400 amino acids in length.

While both methods allow for incorporation of non-natural amino acids, both methods have built in limits that prevent them for being universally useful. Non-natural amino acids can be incorporated into any location in a peptide synthesized using solid phase but only yield peptides of a limited length. Semi-synthetic approaches can generate longer peptides, but the sequence must contain at least one cysteine group, which is not always feasible. Additionally, peptides produced *in vivo* often undergo post translational modifications or require special conditions or chaperone proteins to fold properly, something that is not mimicked by solid phase synthesis or the synthetic portion semi-synthesis.

1.7.2 Global Incorporation

To overcome the limitations of these methods, techniques that use the molecular machinery found in biological systems have been developed. However, the complex system in place to prevent the incorporation of any amino acid other than the one encoded by the mRNA requires an understanding of transcription and translational and where the biology involved can be modified. One aspect of translation that can be

modified for incorporating amino acids other than the one that coded for is the tRNA molecule. The tRNA molecule becomes charged with the amino acid it is designed for and takes it to ribosomes to be placed in its appropriate location in the amino acid sequence. However, by manipulating the conditions under which translation is taking place *in vivo*, the tRNA can be forced to incorporate certain other amino acids that are similar in structure to the amino acid being replaced.

Global incorporation exploits this ability to replace one amino acid with another on the tRNA using selective pressure[54]. Selective pressure requires the removal of the endogenous amino acid from the sample so that the tRNA instead charges the similar non-natural amino acid that is introduced when the cells have reached a sufficient density. The incorporation is global as the substitution is forced and made in all peptides and in all locations in each peptide sequence, not just the target protein. This method requires a special strain of cells that have had their ability to synthesize the amino acid to be replaced by a non-natural amino acid referred to as an auxotrophic strain. The auxotrophic strain requires a supplement of the amino acid it cannot produce itself until it is time synthesize the non-natural amino acid containing peptide. This "medium shift method" had been used to globally incorporate norleucine in place of methionine, leading to a two-fold increase in peroxygenase activity by two-fold, and aminotryptophans in place of tryptophans in the inhibitor protein barstar [55].

This method can synthesize any protein for which the gene has been cloned into a plasmid. This also allows control over when the target protein is to be expressed to minimize the number of proteins that have endogenous amino acid instead of its non-

natural analog. Because the protein is synthesized by the molecular machinery in living cells, the protein can be of any length, be subjected to post-translational modification, and fold in natural conditions. However, because the incorporation is global, every time the amino acid appears in the peptide sequence it is replaced, potentially inhibiting folding and/or function. Furthermore, the incorporation of the non-natural amino acid into all proteins, as discovered with the early experiments using seleneomethionine, are usually toxic or fatal to the cell[56]. Finally, this method usually only yields about a 70-80% incorporation efficiency, which is attributed to proof-reading mechanisms, the availability of cofactors, and each peptides unique characteristics. Despite the restrictions, global incorporation studies have been conducted on aequorin. Global incorporation to replace Phe, Trp, and Tyr with six different non-natural amino acids to generate active aequorin mutants has been achieved (Dikici *et al.,* data unpublished).

1.7.3 *In Vitro* Site-Specific Non-Natural Amino Acid Incorporation

Among the restrictions of global incorporation, one the most problematic is the lack of specificity when incorporating the non-natural amino acid. To develop a technique to site-specifically incorporate non-natural amino acids into target peptides, the molecular mechanisms of transcription and translation were further exploited. Among the codons available in living organisms are three different "stop" nonsense codons that signal the termination of a peptide sequence: UGA (opal), UAG (amber), and UAA (ochre). The three nonsense codons occur at varying frequencies in different genomes. The amber codon is rarely seen in *E. coli* and was a chosen as the codon target for the incorporation of non-natural amino acids.

Rather than using selective pressure to charge tRNA with the non-natural amino acid, the Hecht laboratory truncated the tRNA that charges phenylalanine then covalently attached the non-natural amino acid using *in vitro* organic methods[57]. These two steps of this methods were modified into several similar approaches, but the basic two steps remain.

1.7.4 *In Vivo* Site-Specific Non-Natural Amino Acid Incorporation

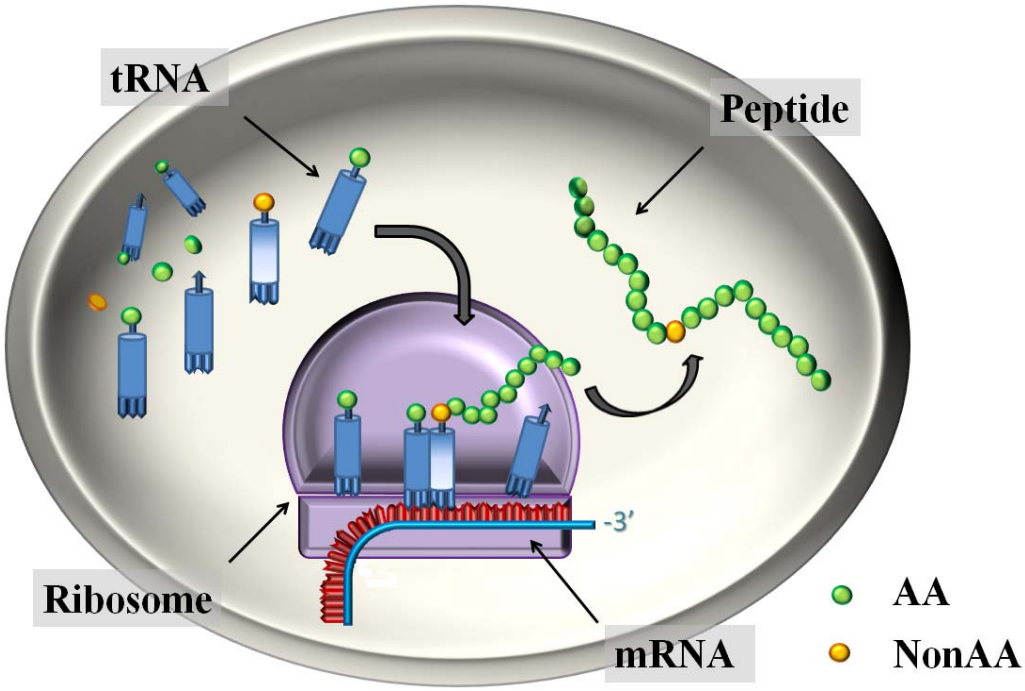

Figure 1.7. Schematic of the site-specific incorporation of amino acids (AA) and non-natural amino acids (NonAA) into a peptide.

Schultz and Chamberlain combined the amber codon, the tRNA, and a single nonsense mutation to create the first site-specific method for incorporating non-natural amino acids using the natural cellular machinery[49a, 58]. The codons used for incorporation where later expanded beyond the endogenous three letter codon with codons that contain

two, four, or five codons, but the three letter amber codon is still the most commonly used[59].

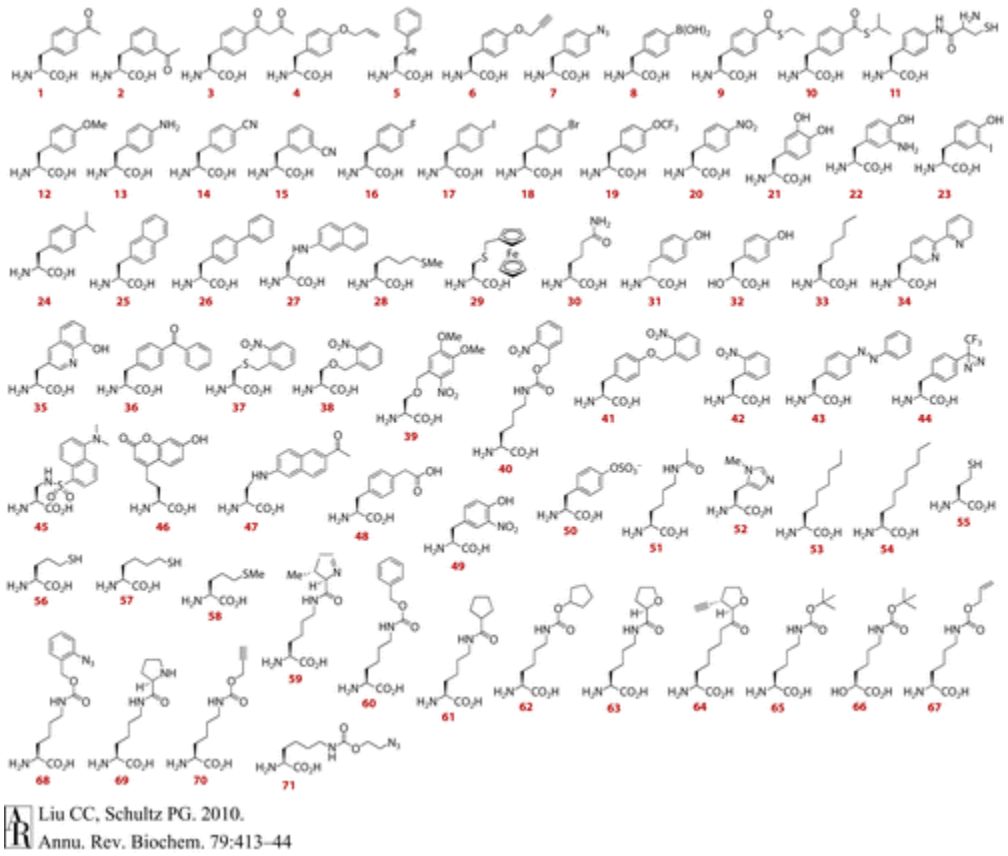

Figure 1.8. Structures of amino acids and hydroxy acids that can be incorporated genetically. Lin, CC. Schultz, P. G. Adding new chemistries to the genetic code. *Annu. Rev. Biochem.* 2010, 79: 413-44. Reprinted with permission from Annual Reviews.

These modified tRNA carrying artificial amino acids introduced into cells containing the amber codon in the desired gene to create a method that is partially *in vivo*. Using microinjection, the tRNA were introduced to Xenopus oocytes by Dougherty *et al.*, and later into CHO cells, and neurons[60]. However, this hybrid approach is work intensive, complex, and has a low yield, making it unsuitable for large scale applications. To streamline the process and increase yields, the site-specific incorporation of non-natural

amino acids site-specifically has been further refined and adapted for expression *in vivo* (Figure 1.7). To do so, the tRNA has to be designed such that it is able to become charged with the non-natural amino acid using cellular machinery, and the tRNA and accompanying tRNA-synthetase have to be expressed *in vivo*[61].

Schultz *et al.* developed a method to incorporate non-natural amino acids site-specifically *in vivo* by use of a tRNA/tRNA-synthetase from extremophile Methanococcus *janaschii* [58, 62]. By subjecting the tRNA/tRNA-synthetase for tyrosine to several rounds of positive and negative selection, the tRNA was modified to target the amber codon and charge non-natural amino acids (Figure 1.8). Each individual tRNA/tRNA-synthetase pair charges one and only one specific non-natural amino acid, and any new non-natural amino acid has to have a new tRNA/tRNA-synthetase designed. For example, incorporating a benzoylphenylalanine would require a tRNA/tRNA-synthetase pair designed for benzoylphenylalanine[63]. The genes encoding the pair are incorporated into a plasmid that must be contransformed into a cell line with another plasmid that contains the gene for the target protein with the amber codon incorporated into the desired locations. Alternatively, the gene may be inserted into the plasmid expressing the tRNA. Since the tRNA relies on the amber codon for insertion, auxotrophic stains are not required. The non-natural amino acid is added to the culture unless the bacteria has been modified to synthesize that non-natural amino acid. The target protein and tRNA/tRNA-synthetase are induced by the addition of the appropriate molecule for the plasmid. The protein can then be isolated from the culture and undergo further purification as necessary to remove truncated versions of the protein that failed to incorporated non-natural amino acid(s). Inteins are used in lieu of N-terminal purification

tags when the codon is near the C-terminus, to help with purification when the truncated protein and the full-length protein as close in length[64]. This technique results in high yields of protein with non-natural amino acid. This method of incorporation has been adapted to eukaryotic and mammalian cells, increasing their applications[61b]. Non-natural amino acids have been incorporated into GFP for the purposes of changing the emission characteristics with positive results[65]. In contrast photoproteins, in particular aequorin, this far have not had as much attention. Rowe *et al*. incorporated L-4-aminophenylalanine, L-4-bromophenylalanine, L-4-iodophenylalanine, and L-4-methoxyphenylalanine into aequorin at position 82, replacing the native tyrosine yielding aequorin with unique emission characteristics that were further diversified by the addition of coelenterazine analogs, opening an avenue into the development of further variants[66].

1.8 Age-Related Macular Degeneration

As the world population grows and ages, the number of cases of diseases associated with aging will increase. Age-related macular degeneration (AMD) is a leading cause of blindness world-wide and the most common form of blindness in the developed world. Studies tracking the number of cases begin analyzing patients as young as 40, and over 10% of all people 80 years old or older have late-stage macular degeneration in countries such as the US, France, Australia, Singapore, and Japan[67]. The total annual direct costs of age-related macular degeneration in the US alone are $575-733 million as of 2009, the additional costs from the consequence of blindness, such as reduced quality of life and depression[31]. Prevention of macular degeneration is challenging. Genetic factors,

nutritional factors, and life-style decisions such as smoking all contribute to age-related macular degeneration[68].

There are several types of macular degeneration, but all current drug-based therapies target the vascular endothelial growth factor A (VEGFA) and this anti-VEGFA therapy is the established standard of care[69]. VEGFA is a protein that is a key regulator of angiogenesis and blocking the binding of VEGFA to its receptor molecule prevents neovascular growth and causes neovascular regression[70]. The two dominant VEGFA antagonists are ranibizumab (Lucentis)[71] and bevacizumab (Avastin)[72], both of which are antibodies and the latter of which was originally developed as treatment for colon cancer by preventing angiogenesis in tumors. Both treatments are less than ten years old, introduced in 2006 and 2011, respectively, and require intravitreal injection for delivery. Neovascular age-related macular degeneration ("wet" MD) results in rapid visual loss as fibrous scarring forms on the retina as neovascularization breaks through from the underlying choroidal layer[73]. This neovascularization causes blood and other fluids to leak from the retina. It is this vascular leakage that the most current forms of imaging related to macular degeneration use for both diagnosis and monitoring of treatment.

Angiographies are used to map the changes in the neovascular architecture of the eye, particularly the leakage is used to determine the location of the lesion within the retina and choroidal layers. Fundus fluorescein angiography (FFA) and indocyanine green angiography both use dyes to map the leakage[74], whereas a newer method, optical coherence tomography (OCT)[75], uses near-infrared light scattering. Both methods have their limits. Fluorescence requires an outside excitation source that can cause background

fluorescence from the melanin and other native fluorescent molecules present in the eye. OCT provides a cross-sectional or volumetric tomographic visualization, but does not allow for the clear differentiation of neovascular components from scarring, hemorrhage, or exudates. Neither approach yields information about macular degeneration at the molecular level.

A DARPin molecule given the identifier MP0112 was developed by for use as an anti-VEGFA antagonist molecule by Stahl *et al.* in early 2013[76]. Like other DARPins, it consists of several highly stable anti-parallel helices that stack modularly, is cysteine-free, and readily expresses in *E. coli*. Preliminary studies *in vivo* showed the VEGFADARPin to be an effective inhibitor of neovascularization[17b, 77]. Furthermore, human trials demonstrated the safety and efficacy of the VEGFADARPin as treatment for wet macular degeneration and diabetic macular edema (DME) by preventing neovascularization and it is now known by the pharmaceutical name Abicipar[76b].

1.9 Statement of Research

The goal in the following dissertation was to first alter the bioluminescent properties of aequorin, including peak emission wavelength, half-life, and specific activity using non-natural amino acid incorporation and coelenterazine analogs for use *in vivo*. Secondly, the goal of this work was to use non-natural amino acids to enable facile, orthogonal linking of aequorin to amino acid containing targeting molecules using click chemistry. Thirdly, the goal of this work was to use aequorin as a reporter in ELISA for the purpose of creating a bioluminescence based assay for molecules such as serotonin. The final goal of this work was to express a VEGFADARPin-Aequorin fusion protein to

create a novel method of *in vivo* imaging of neovascularization in the eye. The overall hypothesis for this work is that: *By combining several rational protein engineering strategies, such as site-directed non-natural amino acid incorporation and coelenterazine analog substitutions, a greater diversity of aequorin variants could be created and applied* in vivo*. Additionally, aequorin could be further utilized in new applications including bioluminescent ELISA and DARPin based* in vivo *imaging.*

As discussed above, though bioluminescent proteins have many benefits over their fluorescent counterparts as reporters molecules, the variations and applications of aequorin created via protein engineering has only just been tapped. By continuing to expand the catalog of aequorin in terms of their emissions characteristics, linking groups, and the applications of aequorin as a reporter molecule and *in vivo* biosensor, we hope to increase the utility of aequorin for bioengineering applications.

- Chapter Two discusses several aequorin mutants paired with coelenterazine analogs designed to have novel emission characteristics

- Chapter Three shows the results of the *in vivo* application of select aequorin variants using a mouse model

- Chapter Four discusses the creation of an aequorin mutant containing a site-specifically incorporated L-4-azidophenylalanine for use in click chemistry

- Chapter Five details the development of a VEGFADARPin-Aequorin fusion protein for the *in vivo* imaging of neovascularization in the retina using a wet MD mouse model

- Chapter Six describes the development of an ELISA based bioluminescent assay using aequorin for the detection of serotonin

CHAPTER 2. DEVELOPMENT OF AEQUORIN MUTANTS WITH NOVEL EMISSION CHARACTERISITCS USING SITE-SPECIFIC MUTAGENSIS AND COELENTERAZINE ANALOGS

2.1 Overview

Naturally occurring luminescent proteins harvested from nature are applied in a wide variety of scientific techniques, from the development of miniaturized biosensors for deployment in the field to multiplex detection in number of assays, to the noninvasive imaging of the molecular aspects of disease states *in vivo*[78]. Of these luminescent proteins, fluorescent proteins, such as Green Fluorescent Protein (GFP [65a]), have become common in their usage both *in vitro* and *in vivo* as reporter molecules[2b, 79]. Numerous GFP variants have been engineered using methods such as random and site-directed mutagenesis, however, the drawbacks associated with fluorescent signals remain[65b]. Fluorescence requires an outside excitation source, creating a background signal and possibly causing undesirable consequences such as photobleaching. In biological samples, these limitations are further compounded by the inherent fluorescence found in many biological samples through molecules such as the amino acid tryptophan and the lipid lipofuscin, and the sensitivity of tissues to radiation, such as the retina of the eye.

In contrast, bioluminescent proteins offer a luminescent signal without the drawbacks of their fluorescent counterparts. Bioluminescent proteins do not require an outside excitation source. Additionally, there is little bioluminescence is many biological samples of research interest, including humans, leading to a lower signal background and increased sensitivity compared to fluorescence[5, 33a]. Though a variety of bioluminescent

proteins exist, the number of mutants with unique spectral characteristics has been limited by the number of canonical amino acids present in nature. The incorporation of non-natural amino acids offers a way to overcome of this limitation.

Aequorin is a 22 kDa, 189 amino acid long globular protein originally isolated from the jellyfish *Aequorea victoria* where it is involved in a bioluminescence resonance energy transfer (BRET) with GFP. Aequorin is a photoprotein that utilizes the luciferin coelenterazine to generate light via a chemiluminescent reaction. Coelenterazine is incorporated the hydrophobic pocket of the protein by four EF-hands motifs, where it is stabilized in a hyperperoxide form with an oxygen molecule by a series of H-bonds, including those provided by three Tyr-Trp-His triads. Upon the addition of calcium, two of the EF-hands bind the calcium resulting in conformational changes that destabilize the coelenterazine, resulting in a bound coelenteramide, CO_2, and the emission a half second flash of blue light[9c, 12c]. Aequorin is also non-toxic, stable, and can be subjected to protein engineering to alter its emission characteristics without losing bioluminescent activity. A previously published paper by our group demonstrated the first application of the incorporation of non-natural amino acids into aequorin using the methods developed by Schultz *et al.* that utilizes engineered tRNA/tRNA-synthetase combinations to insert non-natural amino acids site-specifically at the location of the amber codon TAG codon[61a].

In this thesis tyrosine at position 82, part of a Tyr-Trp-His triad with tryptophan 86 and histidine 16, was replaced with four non-natural amino acids that were also large, hydrophobic molecules, L-4-aminophenylalanine, L-4-bromophenylalanine, L-4-iodophenylalanine, and L-4-methoxyphenylalanine, and then charged with several

coelenterazine analogs in addition to native coelenterazine yielding active mutants[26, 66] (Figure 2.1).

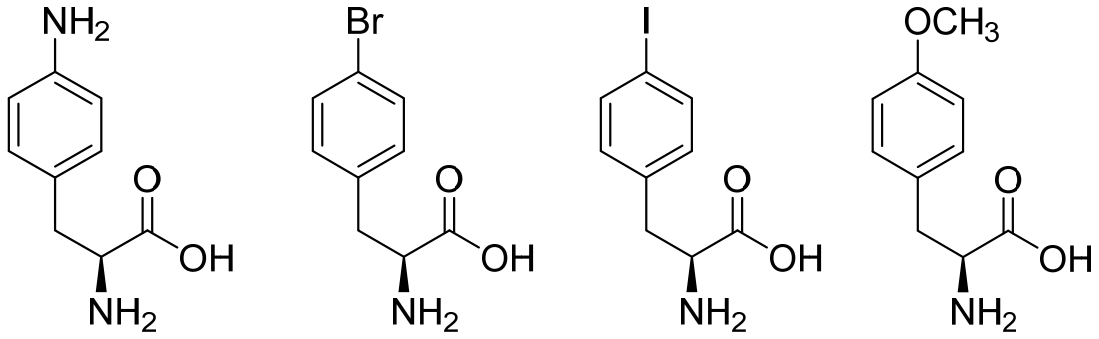

Figure 2.1. The four non-natural amino acids used for Amber replacement in this study. *Left to Right*: L-4-aminophenylalanine, L-4-bromophenylalanine, L-4-iodophenylalanine, L-4-methoxyphenylalanine.

These mutants showed red-shifted emission wavelengths, a characteristic desired to minimize scattering in tissue, and increased bioluminescent half-lives. To increase the range of spectral characteristics even further, aequorin was engineered to undergo site-specific non-natural amino incorporation at position 86, and the first example of double incorporation of non-natural amino acids into aequorin to the best of our knowledge, at positions 82 and 86 simultaneously. The expressed and purified substituted aequorin were then charged with several different coelenterazine analogs: *cp*, *f*, *fcp*, *h*, *hcp*, *i*, *ip*, and *n*. These mutants generated even greater bioluminescent half-lives and even greater red-shifted emission peaks, including the most red-shifted aequorin and longest lasting half-lives yet reported.

In addition to the full-length aequorin, preliminary data in our laboratory (Hamorsky, unpublished) lead to investigation of truncated aequorin using amino acids 48-189 as

possible mutant reporter molecules. However, the activity of these truncated, non-natural amino acid substituted aequorin showed only minimal activity, and the data is included here for the sake of completeness.

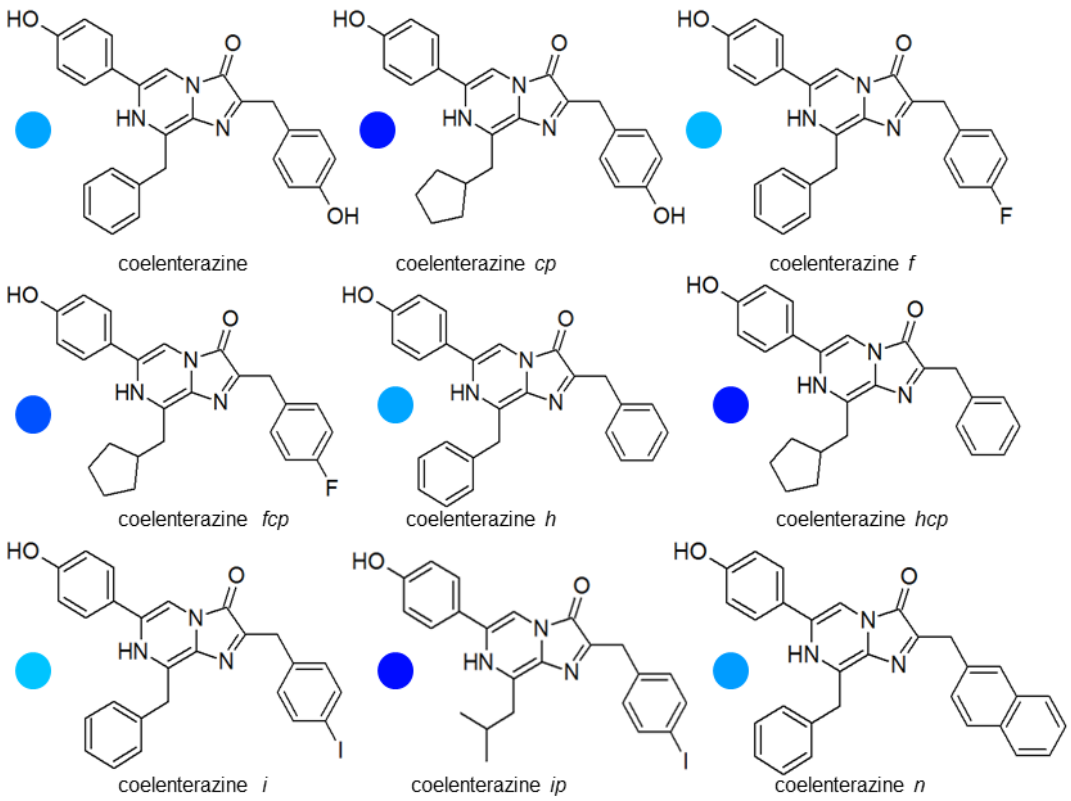

Figure 2.2. The coelenterazine analogs in this study and the color of their peak emission spectra in wild-type aequorin.

2.2 Materials and Methods

2.2.1 Reagents

The pBAD/His A and Terrific Broth (TB) are from Invitrogen (Carlsbad, CA). The PET30 Xa/LIC Kit and Xa Factor Cleavage Capture Kit are from Novagen

(Madison, WI). NcoI and Hind III restriction endonucleases are from New England Biolabs (Boston, MA). All natural amino acids, and all antibiotics, are from Sigma-Aldrich (St. Louis, MO). LB agar and LB broth are from Fischer Scientific (Fair Lawn, NJ). The coelenterazines are from Gold Biotechnology (St. Louis, MO). The L-4-aminophenylalanine, L-4-bromophenylalanine, L-4-iodophenylalanine, and L-4-methoxyphenylalanine are from Peptech (Burlington, MA).

2.2.2 Apparatus

Cells were grown in a Thermo-Fisher Scientific orbital shaker incubator at 37^{o}C. Cell cultures were harvested using a Beckman J2-MI centrifuge. The proteins were purified using a BioCad Sprint Perfusion Chromatography System (Perspective Biosystems, Farmington, MA) using 20 mL DEAE Waters AP-2 Anion Exchange Column (Waters Corporation, Milford, MA). The buffers for the purification of the protein were 30 mM Tris-HCl, pH 7.5, containing 2 mM EDTA (Buffer A) and a 30 mM Tris-HCl, pH 7.5, containing 2 mM EDTA, and 1 M NaCl (Buffer B). Diafiltration was performed using a tangential flow separation module with hollow fiber filter membrane (Spectrum Labs, Rancho Dominguez, CA) using 30 mM Tris-HCl, pH 7.5, containing 2 mM EDTA. Ni-NTA Agarose beads are from Qiagen (Venlo, Netherlands). Amiron Ultra-15 Centrifugal Filter Units are from EMD (Billerica, MA). Purity of the proteins was confirmed by sodium dodecyl sulfate-polyacrylamide gel electrophoresis (SDS-PAGE) using a Novex Mini-cell apparatus from Invitrogen and staining with Coomassie Brilliant Blue by the appearance of a single band. Aequorin activity was measured using an Optocomp I luminometer (MGM Biomedical Hamden, CT). The emission spectra of

the aequorins were determined using a custom made SpectroScan instrument (ScienceWares, Falmouth, MA), which is capable of obtaining spectra from flash reactions of luminescent samples that emit in the 400-700 nm range. Half-life scans were taken using a Polarstar Optima 96 well microplate reading luminometer (BMG Labtech, Ortenberg, Germany).

2.2.3 Construction of the pDULE-pBADHisA-AEQTAG86 expression strains

Four pDULE vectors which allow for the site-specific incorporation of four different non-natural amino acids were obtained from Dr. Peter Schultz (Scripps Research Institute, La Jolla CA) and Dr. Ryan Mehl (Franklyn and Marshall College, Lancaster, PA)[49a].Each of these pDULE plasmids coded for a $tRNA_{CUA}$ and $tRNA_{CUA}$ - synthetase specific for the TAG codon and a single non-natural amino acid, either L-4-aminophenylalanine, L-4-bromophenylalanine, L-4-iodophenylalanine, or L-4-methoxyphenylalanine. These plasmids were transformed into *E. coli* DH10B cells and transformants were selected by plating on LB agar medium containing ampicillin (100 μg/mL) and tetracycline (12 μg/mL). The presence of the pDULE plasmid was confirmed by plasmid isolation, restriction enzyme digestion and DNA gel electrophoresis.

2.2.4 Construction of the pDULE-pET30AEQ8286TAG expression strains

The four pDULE plasmids were transformed into *E. coli* DH10B cells with pET30AEQ8286TAG and transformants were selected by plating on LB agar medium containing tetracycline (12 μg/mL) and kanamycin (35 μg/mL). The presence of the

pDULE plasmid was confirmed by plasmid isolation, restriction enzyme digestion and DNA gel electrophoresis.

pBADAEQ86TAG was prepared by inserting the AEQTAG86 gene with the OmpA leader sequence attached into pBAD/His A. The pIN4AEQ86TAG vector containing the cysteine-free aequorin gene fused to the OmpA leader sequence was used as a template. The primers were designed so the resulting DNA sequence contained an NcoI site at the 5' end and a HindIII site at the 3' end.

The following primers were used for the cloning of ompA:AEQ86TAG fusion into pBAD/HisA vector (restriction sites for cloning are underlined).

AEQforpBAD

5'-CCATGGGTATGAAAAAGACAGCTATCGCGATTGC-3'

And *AEQrevpBAD*

5'AAGCTTAGGGGACAGCTCCACCGTAGAGCTTTTCGGAAGCAGGATCCATTG TGTAC-3'

The resulting PCR product was gel purified and cloned into the pCR®II-TOPO® vector by using the TOPO TA cloning kit (Invitrogen, Carlsbad, CA). The plasmid from the TA clone was then isolated and sequenced to confirm the presence of the insert. The ompA:AEQ86TAG insert from the TOPO TA clone was then ligated into the NcoI and HindIII sites of pBAD/His A to create pBADHisA-AEQ86TAG.

The AEQTAG86 gene was also cloned into a pET30 Xa/LIC Vector using primers designed according to the manufacturer's instructions. pET30AEQ8286TAG was then prepared by using a pair of primers to create a site-specific mutation consisting of a TAG at position 82 (underlined).

Oligo HPLCTAG8286for

5'-GGAAACTGATTGGCCTGCATAGATTGAAGG-3'

And *HPLCTAG8286rev*

5'-CCTTCAATCTATGCAGGCCAATCAGTTTCC-3'

pBADHisA-AEQ86TAG and pET30AEQ8286TAG vectors were transformed into chemically competent E. *coli* DH10B cells that already contained the pDULE plasmids to produce four different strains, each specific for the incorporation one of the four non-natural amino acids mentioned above. Selection for transformants was performed by plating on LB agar medium containing both tetracycline (12 μg/mL) and kanamycin (35 μg/mL).

2.2.5 Expression and Isolation of Aequorins Mutants from pBADHisA-AEQ86TAG

The cells harboring the pDULE systems with pBADHisA-AEQ86TAG vector were grown in 25 mL of LB broth containing ampicillin (100 μg/mL) and tetracycline (12 μg/mL). All cultures, unless specified otherwise, were grown overnight at 37 ºC with shaking at 250 rpm. These overnight cultures were used to inoculate 500 mL of LB broth containing the appropriate antibiotics and the cultures were grown at 37 ºC at 250 rpm to

an OD_{600} between 0.4-0.6. The corresponding non-natural amino acid was then added to a final concentration of 1 mM. The culture was allowed to grow for 1 hour and then induced with arabinose (0.2% final concentration) overnight.

2.2.6 Expression and Isolation of Aequorin Mutants from pET30AEQ8286TAG

The cells were grown in 25 mL of Terrific broth (TB) containing tetracycline (12 μg /mL) and kanamycin (35 μg/mL) overnight at 37 ^{o}C at 250 rpm. The overnight cultures were used to inoculate 500 mL of TB broth containing the appropriate antibiotics and the cultures were grown at 37 ^{o}C at 250 rpm. After growing to an OD_{600} between 0.4-0.6, the corresponding non-natural amino acid was added to a final concentration of 1 mM. The culture was allowed to grow for 1 hour and then induced with 1 mM IPTG and left to grow overnight.

The culture was centrifuged at 15,300 xg for 20 min and the pellet was boiled for 5 min in lysis buffer. The boiled pellet was centrifuged again and the supernatant added to 1 mL of suspended Ni-NTA agarose beads and rotated on a Mini Labroller (Labnet, Woodridge, NJ) at room temperature for 2 hours. The protein was eluted off the column using a PBS Buffer with 20 mM Imidazole at pH=8.0 and digested with Xa factor according to manufacturer's instructions until all the His tag was cleaved from the protein. The Xa factor was removed with Xa factor Agarose capture beads. The cleaved aequorin was then concentrated using Amicron Ultra spin columns.

2.2.7 Determination of Activities of Aequorin Variants

Aequorin was diluted with 30 mM Tris-HCl, pH 7.5, containing 2 mM EDTA, to 1 x 10^{-7} M and charged with 1x10^{-4} M coelenterazine overnight. Aequorin activity was triggered by injecting 100 µL of 100 mM Tris-HCl, pH 7.5, containing 100 mM $CaCl_2$. Bioluminescence intensity was measured at 0.1 s intervals for up to 6 s on an Optocomp I luminometer (MGM Biomedical Hamden, CT).

2.2.8 Emission Spectra of Aequorin Variants

A 1 x 10^{-6} M sample of each aequorin was charged by incubating overnight at 4 °C with 1 x 10^{-4} M of each of the different coelenterazines and 150µL of each charged aequorin was pipetted into a 96-well microtiter plate and following injection of 100 µL of 100 mM Tris-HCl, pH 7.5, containing 100 mM $CaCl_2$, the emission spectra was collected for 10 s from 400-700 nm in 1.5 nm increments on a custom made SpectroScan instrument (ScienceWares, Falmouth, MA).

2.2.9 Half-life Determination of Aequorin Variants

A 1 x 10^{-6} M sample of each aequorin variant was charged overnight at 4 ^{o}C with the 1 x 10^{-4} M of the coelenterazine analog used during the collection of emission spectra. A Polarstar Optima 96 well microplate luminometer (BMG Labtech, Ortenberg, Germany) was utilized for the half-life measurements. The bioluminescence signal of a 50 µL sample was collected between 30 s to 150 s, depending on the expected half-life of the aequorin analog, following the injection of 100 µL of triggering buffer (100 mM Tris-HCl, pH 7.5, containing 100 mM $CaCl_2$). The mean bioluminescence decay spectra was

fit with an exponential decay equation using GraphPad Prism 5.0 (GraphPad Software, San Diego, CA), and an equation for first order decay kinetics was used to calculate the bioluminescence half-life of each aequorin-coelenterazine pair.

2.2.10 Thermostability Studies of Aequorin Variants

A 1 x 10^{-6} M sample of each aequorin was charged by incubating overnight at 4 °C with 2 x 10^{-6} M of native coelenterazines. One mL of was then placed in a sealed Eppendorf tube and heated in a block until the sample was at 37 °C. Activity was determined as mentioned above.

2.2.11 Mass Spectrometry

Proteins were run on SDS-PAGE and cut out of the stained gels with Coomassie Blue. Gel pieces were digested with trypsin, and an LC-ESI-MS-MS was performed using a ThermoFinnigan LTQ. Resulting MS-MS spectra were searched against proteins in the Swiss-Prot database using the X!Tandem search engine to look for the presence of the substitution of the non-natural amino acid at and only at the target positions.

2.3 Results and Discussion

The usefulness of fluorescent molecules has resulted in their frequent application as detection molecules in small molecular sensors and as part of larger multi-molecule assays such as ELISA. Despite the appeal of fluorescent proteins, fluorescence as signal source has many undesirable limitations. Fluorescence requires an outside excitation source, causing an increased background signal and causing competing signals from

molecules commonly found in biological samples that have their own intrinsic fluorescent signal.

Bioluminescent photoproteins such as aequorin generate their own light using chemiluminescence. Aequorin is a stable, non-toxic globular protein that has been shown to exhibit tunable emission characteristics when subjected to site-directed mutagenesis, but the number of variants available was limited by the number of canonical amino acids available. Utilizing a method developed by Schultz and colleagues to site-specifically incorporate non-natural amino acids using specially engineered tRNA/tRNA-synthetase combinations and an inserted amber stop codon, the number of aequorin with unique spectral characteristics can be expanded to include any mutant for which there is tRNA/tRNA-synthetase available.

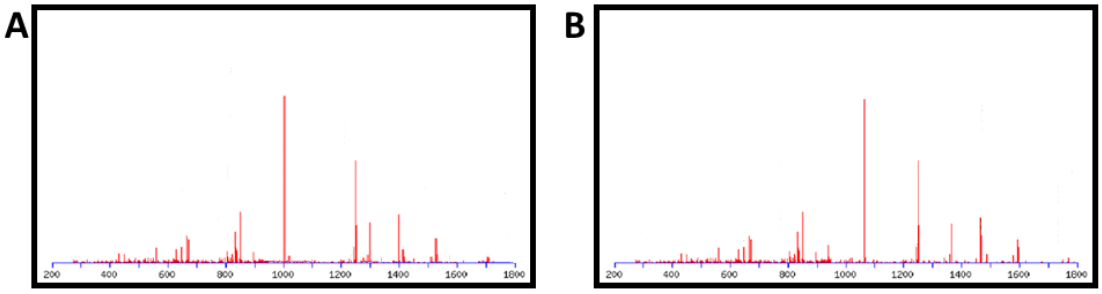

Figure 2.3. Mass spectrometry data confirming the incorporation of L-4-bromophenylalanine. (A) L-4-bromophenylalanine at position 86 and at (B) L-4-bromophenylalanine position 82 and 86 concurrently. Data is representative of all mass spectrometry data.

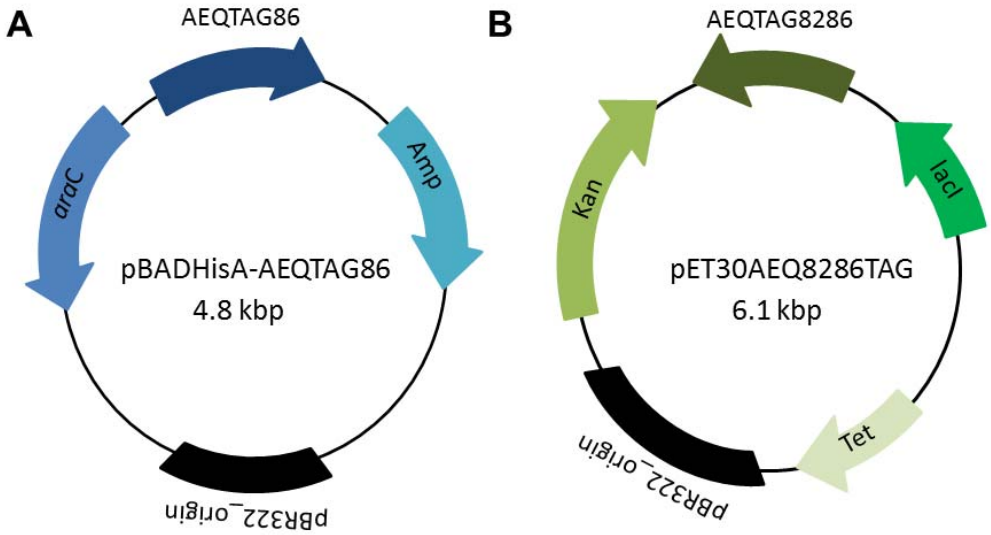

Figure 2.4. Plasmids used to express the aequorin mutant proteins. (A) pBAD based plasmid inducible by arabinose for the expression of cysteine-free mutant aequorin with a singular amber mutation at position 86. (B) pET30 based plasmid inducible by IPTG for the expression of cysteine-free aequorin with an amber mutation at positions 82 and 86.

Our lab had already shown the positions 82 in aequorin could incorporate four non-natural amino acids L-4-aminophenylalanine, L-4-bromophenylalanine, L-4-iodophenylalanine, and L-4-methoxyphenylalanine, chosen due to their large, hydrophobic structures to be as similar to the replaced tyrosine as possible, and maintain activity while showing new spectral characteristics[80]. Here, these four amino acids were site-specifically at position 86 and position 82 and 86 in tandem to push the number of available mutants with unique characteristics even further. Two systems were developed to express the mutant aequorin with incorporated non-natural amino acids. The first system incorporated the non-natural amino acids into position 86 using a pBAD/His A vector by using well-established molecular biology protocols[81] that was cotransformed with pDULE vectors engineered for each non-natural amino acid procured from the Schultz lab[49a]. This resulted in a system in which the expression of aequorin is tightly

regulated by the *ara*BAD promoter and protein expression is induced by the addition of arabinose to the culture medium. The culture was then spun down and the aequorin isolated from the supernatant with acid precipitation. Low-level expression of the L-4-aminophenylalanine aequorin prompted the use of the cysteine-free aequorin gene with a TAG codon at position 86 and was inserted into a pET30Xa/LIC plasmid by IPTG which is inducible. This construct gave a good yield of the 86 mutant aequorin and is used in all subsequent experiments (Figure 2.4).

The pET30Xa/LIC plasmid uses a T7 promoter and contains the gene for His6x Tag on the N-terminus to allow for purification via immobilized metal affinity chromatography. The gene was site-specifically mutated a second time to include an additional TAG codon and position 82, yielding the constructpET30AEQ8286TAG that was also cotransformed with the pDULE plasmids. An overnight culture of pET30AEQ8286TAG in E.coli containing the pDULE plasmids was induced with IPTG in the presence of the non-natural amino acid analogs, lysed and the protein was purified using a Ni-NTA column.

Table 2.1. Tables of mass spectrometry data. (A) Mass spectrometry data for the aequorin variants with a single substitution. Tryptophan 86 is located at the end of the peptide fragment (W*). (B) Mass spectrometry data for the aequorin variants with a double substitution. Tyrosine 82 is located near the middle of the fragment (Y*).

A

Aequorin	Peptide Fragment	Aequorin Mass	Actual Mass	Delta Mass
AminoPhe	YGVETDWPAYIEGW*K	1813.96	1789.94	-23
BromoPhe	YGVETDWPAYIEGW*K	1813.96	1851.54	+38
IodoPhe	YGVETDWPAYIEGW*K	1813.96	1899.72	+86
MethoxyPhe	YGVETDWPAYIEGW*K	1813.96	1804.84	-9

B

Aequorin	Peptide Fragment	Aequorin Mass	Actual Mass	Delta Mass
AminoPhe	YGVETDWPAY*IEGW*K	1813.96	1788.94	-25
BromoPhe	YGVETDWPAY*IEGW*K	1813.96	1916.72	+103
IodoPhe	YGVETDWPAY*IEGW*K	1813.96	2010.72	+197
MethoxyPhe	YGVETDWPAY*IEGW*K	1813.96	1818.94	-5

Table 2.2. The specific activity of aequorin mutants. (A) The single substitution at position 86 and (B) the specific activity of the double substitution aequorin variants at position 82 and 86. The literature value for the specific activity of recombinant aequorin is $5.1x10^{17}$ RLU/mole [13].

A

Aequorin	CTZ native	*cp*	*f*	*fcp*	*h*	*hcp*	*i*	*ip*	*n*
Cysteine-free	$9.7x10^{19}$	$5.9x10^{19}$	$3.6x10^{19}$	$3.9x10^{18}$	$3.5x10^{19}$	$9.9x10^{18}$	$4.4x10^{18}$	$2.6x10^{19}$	$3.7x10^{18}$
AminoPhe	$1.1x10^{16}$	$7.9x10^{15}$	$1.7x10^{16}$	$5.5x10^{14}$	$7.8x10^{15}$	$3.0x10^{15}$	$1.5x10^{15}$	$8.2x10^{14}$	$7.0x10^{14}$
BromoPhe	$4.0x10^{17}$	$1.9x10^{18}$	$3.6x10^{17}$	$1.2x10^{17}$	$4.3x10^{17}$	$1.9x10^{17}$	$2.9x10^{17}$	$1.2x10^{17}$	$2.0x10^{16}$
IodoPhe	$9.7x10^{15}$	$1.4x10^{16}$	$2.2x10^{16}$	$6.8x10^{15}$	$1.5x10^{16}$	$6.7x10^{15}$	$2.3x10^{15}$	$8.0x10^{15}$	$8.6x10^{14}$
MethoxyPhe	$1.1x10^{17}$	$3.6x10^{17}$	$1.3x10^{16}$	$7.6x10^{15}$	$4.9x10^{16}$	$2.5x10^{16}$	$2.1x10^{15}$	$7.0x10^{14}$	$7.5x10^{14}$

B

Aequorin	CTZ native	*cp*	*f*	*fcp*	*h*	*hcp*	*i*	*ip*	*n*
Cysteine-free	$9.7x10^{19}$	$5.9x10^{19}$	$3.6x10^{19}$	$3.9x10^{18}$	$3.5x10^{19}$	$9.9x10^{18}$	$4.4x10^{18}$	$2.6x10^{19}$	$3.7x10^{18}$
AminoPhe	$2.8x10^{14}$	$2.5x10^{14}$	$5.6x10^{14}$	$1.5x10^{14}$	$3.8x10^{14}$	$1.9x10^{14}$	$1.6x10^{14}$	$1.0x10^{14}$	$1.5x10^{14}$
BromoPhe	$4.5x10^{12}$	$3.1x10^{13}$	$1.3x10^{13}$	$4.9x10^{12}$	$1.7x10^{12}$	$1.9x10^{12}$	$3.1x10^{12}$	$1.5x10^{12}$	$1.6x10^{12}$
IodoPhe	$1.2x10^{13}$	$2.8x10^{12}$	$3.4x10^{12}$	$1.0x10^{12}$	$4.6x10^{12}$	$1.0x10^{12}$	$6.8x10^{11}$	$2.1x10^{11}$	$9.5x10^{11}$
MethoxyPhe	$8.0x10^{13}$	$4.8x10^{13}$	$6.5x10^{13}$	$4.6x10^{13}$	$5.1x10^{13}$	$2.2x10^{13}$	$6.2x10^{13}$	$3.4x10^{13}$	$1.4x10^{14}$

Table 2.3 The emission maxima of aequorin mutants. (A) The single substitution at position 86 and (B) the double substitution at 82 and 86 in nm.

A

Aequorin	CTZ native	*cp*	*f*	*fcp*	*h*	*hcp*	*i*	*ip*	*n*
Cysteine-free	472	454	480	463	472	454	484	454	475
AminoPhe	488	465	494	476	489	470	496	480	489
BromoPhe	489	468	495	481	489	474	499	467	492
IodoPhe	499	492	507	496	506	483	508	492	494
MethoxyPhe	489	471	497	477	493	474	502	470	496

B

Aequorin	CTZ native	*cp*	*f*	*fcp*	*h*	*hcp*	*i*	*ip*	*n*
Cysteine-free	472	454	480	463	472	454	484	454	475
AminoPhe	496	487	502	486	494	480	515	479	509
BromoPhe	500	477	507	483	503	481	514	476	518
IodoPhe	503	475	498	484	493	475	500	477	492
MethoxyPhe	513	490	522	495	513	478	526	482	519

Table 2.4 The half-lives of aequorin mutants. (A) Single substitution at position 86 and (B) the double substitution at 82 and 86. The half-life values of the bioluminescence are in s.

A

Aequorin	CTZ native	*cp*	*f*	*fcp*	*h*	*hcp*	*i*	*ip*	*n*
Cysteine-free	0.59	0.17	0.59	0.37	0.23	0.13	14.3	0.67	1.66
AminoPhe	4.9	0.61	2.01	0.96	1.20	0.47	33.28	2.67	8.37
BromoPhe	2.83	0.51	2.21	1.0	0.64	0.34	22.51	2.64	8.51
IodoPhe	4.49	0.70	2.09	1.04	0.79	0.50	38.01	2.37	1.68
MethoxyPhe	9.56	3.71	10.34	1.32	11.66	0.52	30.88	2.97	8.83

B

Aequorin	CTZ native	*cp*	*f*	*fcp*	*h*	*hcp*	*i*	*ip*	*n*
Cysteine-free	0.59	0.17	0.59	0.37	0.23	0.13	14.3	0.67	1.66
AminoPhe	3.37	0.77	2.68	1.40	1.20	0.56	58.68	4.20	8.37
BromoPhe	3.21	0.94	2.57	1.01	0.68	0.36	55.62	3.50	8.04
IodoPhe	4.19	0.87	3.67	1.26	1.77	0.94	64.74	5.38	8.42
MethoxyPhe	3.53	0.82	3.79	1.35	0.81	0.42	48.73	5.39	9.48

Additional studies were conducted on truncated aequorin incorporating non-natural amino acids, but these were found to be almost completely without activity (data not shown).

All aequorin mutants showed red-shifted emission wavelengths and longer half-lives compared to the cysteine-free aequorin with additional mutations. The data in Table

2.1 show a decrease in specific activity for all mutants as well as cysteine-free aequorin. This was observed previously with aequorin mutants that contain non-natural amino acids at position 82 [66]. Some of the aequorin mutants also displayed a marked increase in their half-lives of light emission. The results of the emission characteristics studies, namely wavelength emission maxima and time of emission half-lives, are shown in Tables 2.2 and 2.3. The emission half-lives of the single substitutions at position 86 are longer than those found in our previous study with a cysteine-free aequorin single non-natural incorporation at position 82, and the double non-natural incorporation produces variants with a marked increase in the red-shift of emission [66]. Most significantly, cysteine-free aequorin with L-4-methoxyphenylalanine at positions 82 and 86 complexed with coelenterazine *i* emits bioluminescence at 526 nm, which is the largest red-shift of any aequorin variant reported thus far and 11 nm longer than the previous most red shifted aequorin, 4-methoxyphenylalanine at position 82 (Figure 2.3A)[66]. Notably, the aequorin variant with a single L-4-methoxyphenylalanine non-natural amino acid incorporation at position 86 paired with coelenterazine *i* has the longest half-life emission time reported as well at approximately 60 seconds, versus our labs previously reported 14 s (Figure 2.5B)[66]. These emission characteristics allow for the differentiation of signal by peak emission wavelength or time scale[47b]. It is known that the tryptophan residue at position 86 is involved in the stabilization of the coelenterazine molecule in the protein's

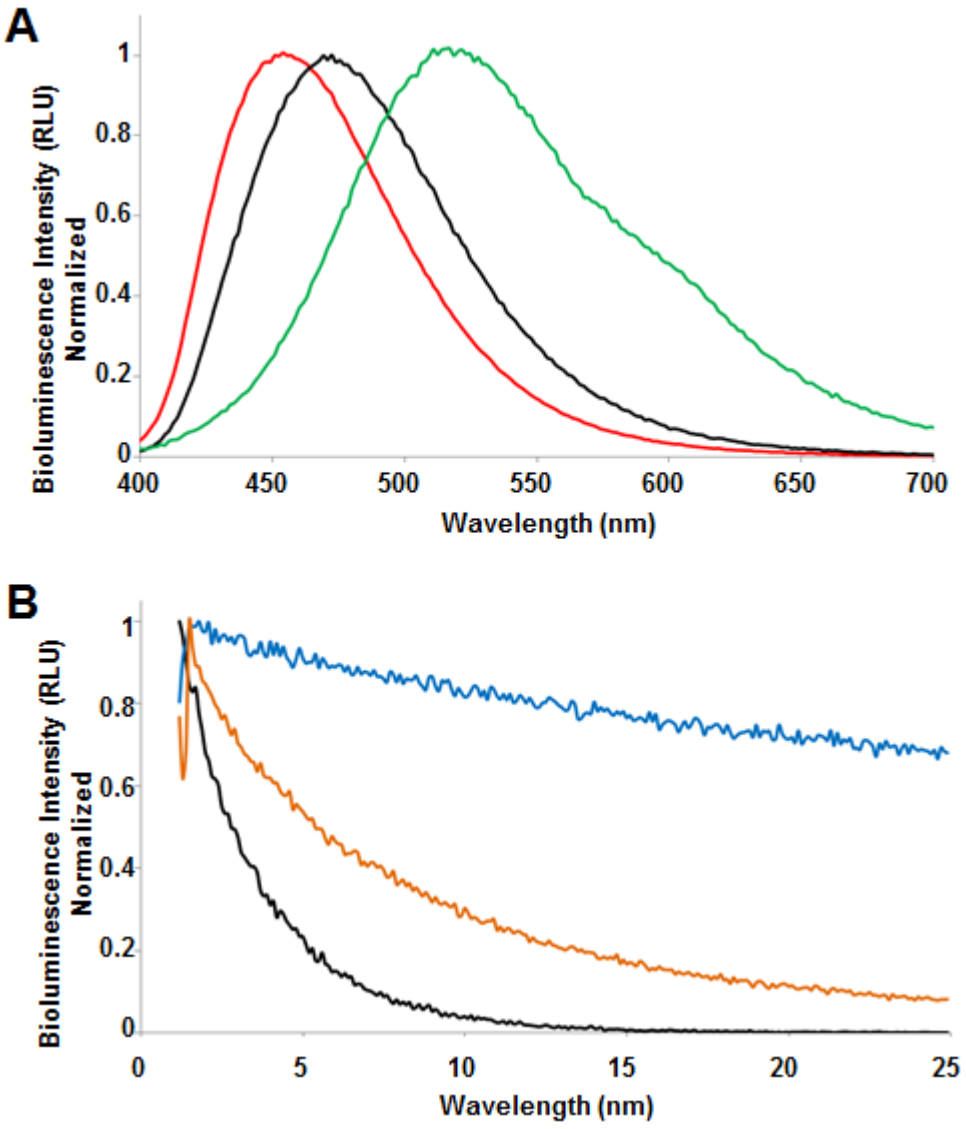

Figure 2.5. Peak emission wavelengths and half-lives of select aequorin mutants. (A) Bioluminescence emission spectra of cysteine-free aequorin with L-4-aminophenylalanine at position 86 with coelenterazine *cp* (red), cysteine-free aequorin with native coelenterazine (black) and L-4-methoxyphenylalanine at position 82 and 86 with coelenterazine *i* (green). (B) Half-life decay of cysteine-free aequorin with native coelenterazine (black), L-4-methoxyphenylalanine with coelenterazine *n* (orange), and L-4-iodophenylalanine with coelenterazine *i* (blue).

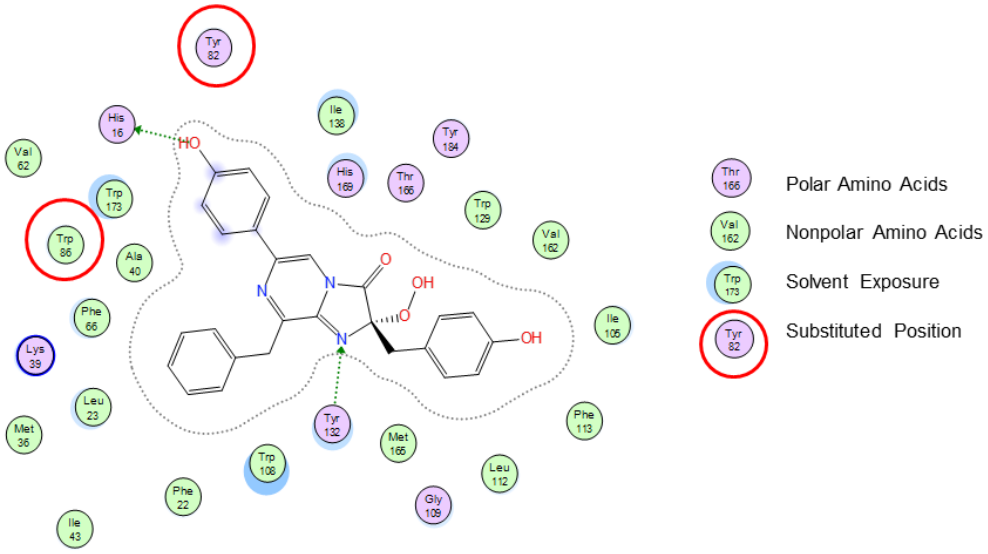

Figure 2.6. Figure shows native coelenterazine in the binding pocket of aequorin based on the crystal structure[12c]. The grey dashed lines represent the Van der Waal surface of the ligand. Green dashed lines with an arrowhead represent an H-bond going from donor to recipient.

hydrophobic binding pocket[12c, 82]. By mutating this residue, the stability of the phenol ring moiety associated with the Tyr82-His16-Trp86 triad is thus affected.

Figure 2.6 show the interactions of the tryptophan residue at position 86 with the coelenterazine molecule. In examining the binding interactions of the amino acids in the binding pocket with the newly prepared mutant aequorin with L-4-aminophenylalanine and L-4-methoxyphenylalanine, it is evident that these non-natural amino acids, which have an amino group and methoxy group, respectively, are capable of maintaining a polar interaction with coelenterazine, while L-4-bromophenylalanine and L-4-iodophenylanine are not.

We postulate that the presence of additional non-covalent bond interactions between the substituted amino acid residue(s) of the Tyr82-His16-Trp86 triad and the chromophore alters the stability of the chromophore in the binding pocket. This change in the stability of the chromophore could explain red shifted emission wavelengths of the latter two halogenated aequorin variants. The aequorin variant that showed the largest red shift is the double substituted L-4-methoxyphenylalanine complexed with coelenterazine *i*, with a maximum shift of Δ56 nm when compared to cysteine-free aequorin complexed with native coelenterazine. Conversely, the substitution of a cyclopentyl group instead of a phenyl group of coelenterazine causes a Δ20 nm blue-shift in both Trp86 single substitution and Trp86 and Tyr82 double substitution relative to these same mutants complexed with native coelenterazine.

While all novel non-natural amino acid-modified aequorins show an increase in half-lives of the bioluminescence emission, the most notable half-life changes are associated with the variants resulting from the pairing of the modified aequorins with the coelenterazine analog containing iodine, coelenterazine *i*. The presence of iodine in a molecule can increase the transition probability of an electron in an excited singlet state to an excited triplet state, creating a shift in emission spectra as well as the half-life [83]. All variants with coelenterazine *i* display the longest decay half-lives with an average of approximately 1 minute, while the half-life of cysteine-free aequorin with native coelenterazine is approximately a half second (Table 2.3). The increased probability of transition of the excited electron from singlet state to triplet state due to the heavy atom

can explain the differences in half-lives of the coelenterazines that have iodine *vs* the ones that do not possess a heavy atom[83]. This trend is also present in the modified aequorins with an L-4-bromophenylalanine substitution, though to a lesser extent. Interestingly, in our previous work, the single substitution of tyrosine82 did not display as great an increase in the half-life of the bioluminescence emission as the single substitution at position Trp86, even with coelenterazine *i*, but, in contrast, they did exhibit greater red-shift in emission wavelength. The variants with non-natural amino acid substitutions at both positions, Tyr82 and Trp86, show a mixed influence of both substitutions, with longer emission half-lives as well as greater red-shifted emission spectra.

2.4 Conclusions

While fluorescence is frequently used in luminescent applications, bioluminescence has several advantages in the form of a lower background, greater sensitivity, and no need for outside excitation. Bioluminescent proteins provide all these advantages. Aequorin is such a protein, with the additional advantage of fine tuning in the form of several synthetic coelenterazine analogs and the site-specific incorporation of non-natural amino acids to create mutants suitable for *in vitro* and *in vivo*. Our data demonstrated that we could consistently express and purify aequorin variants that contain non-natural amino acid analogs in place of the tryptophan residue at position 86 alone and simultaneously with the tyrosine at position 82. The four non-natural amino acid

analogs, namely, L-4-aminophenylalanine, L-4-bromophenylalanine, L-4-iodophenylalanine, and L-4-methoxyphenylalanine all showed bioluminescence activity when paired with native coelenterazine as well as several analogs. We have shown that one of these aequorin variants displays a 56 nm red-shift in bioluminescence emission wavelength, the greatest red-shift yet reported for an aequorin variant. Moreover, half-lives of the bioluminescence emission have been tuned to range from 0.1 seconds to approximately 60 seconds which can be useful in selectively imaging separate areas simultaneously or two different targets within the same location by resolving the separate signals temporally. Truncated aequorin with the first 47 amino acids removed were found to be almost entirely inactive. These newly developed red-shifted flash aequorin offer improved characteristics over our previously reported aequorin, and provide new bioluminescent molecules for applications *in vitro* and *in vivo*.

CHAPTER 3. ACTIVITY OF AEQUORIN CONTAINING SITE-SPECIFICALLY SUBSTITUTED NON-NATURAL AMINO ACIDS AND COELENTERAZINE ANALOGS *IN VIVO* USING A MOUSE MODEL

3.1 Overview

Imaging is an invaluable part of medical research and clinical practice[78]. The importance of imaging to understanding both normal biology and disease states can be seen in the large and growing number of imaging techniques available, from the relatively simple X-ray to complex methods like single-photon emission computed tomography (SPECT) and combined positron emission tomography and magnetic resonance imaging (PET-MRI)[30c, 31]. Despite the many different approaches to imaging, much of the focus has been on anatomical structures and physiology or on changes in metabolism, neither of which provide a comprehensive reconstruction of the molecular-level changes associated with disease states. With an aim towards improving early diagnosis and tailoring more accurate disease therapies, molecular imagining using molecular probes such as genes and proteins has an emerged as a valuable approach.

Bioluminescent proteins have proven to be a reliable, widely applied type of reporter for *in vivo* imaging[34c, 34d, 78, 84]. Unlike their fluorescent counterparts, bioluminescent proteins do not require and outside excitation source, cutting down on background signal from outside illumination and the intrinsic fluorescence in many biological samples, and making them more suitable for light-sensitive tissues such as the

retina. Furthermore, bioluminescence has shown to be cost-effective. Methods such as SPECT, PET, and MRI can take approximately one hour for image acquisition of a single target, while the IVIS [30a, 34c] imaging system using a bioluminescent reporter can imaging several mice at once in only three to five minutes. Combined with the non-toxic nature of bioluminescent proteins, bioluminescence offers a fast, high through put method capable of non-invasive form of imaging.

Imaging using bioluminescence has frequently utilized luciferases such as firefly luciferase (FLuc), *Renilla* luciferase (RLuc), and bacterial luciferase (Lux)[6, 7b, 34e, 43]. While having all the advantages of bioluminescence, the proteins have been introduced into the targets using plasmid DNA, requiring a tissue transplant for animal imaging, not desirable in clinical applications[84]. To overcome this restriction, the photoprotein aequorin offers a flexible, non-invasive alternative with the potential for a quantifiable signal through the photon count from the coelenterazine molecules. Aequorin is a 22 kDa globular protein that uses the luciferin coelenterazine to generate light that can be expressed in a bacterial culture and then purified for introduction as a sensor or imaging protein into a living animal. Aequorin is a popular subject for protein engineering to create red-shifted variants used *in vivo*, but these methods require conjugation to fluorophores[45]. However, the limited number of aequorin variants available had restricted its use *in vivo*. By increasing the number of amino acids available beyond the canonical number using site-specific non-natural amino acid incorporation, aequorin with improved emission characteristics for *in vivo* imaging have been developed (see Chapter 2).

Using the method developed by Shultz and colleagues to incorporated non-natural amino acid using amber suppression and specially engineered tRNA/tRNA-synthetase combinations, non-natural amino acids can be incorporated into any position in a protein sequence where the TAG stop codon has been introduced. Previous work in our lab showed that four non-natural amino acids L-4-aminophenylalaine, L-4-bromophenylalanine, L-4-iodophenylalanine, and L-4-methoxyphenylalanine, could replace a tyrosine and position 82 and be combined with several coelenterazine analogs to yield active mutants with red-shifted peak emission wavelengths and lengthened bioluminescence half-lives, desirable characteristics for imaging in tissues. To push the emission characteristics even further, the same four non-natural amino acids were incorporated at position 86 to replace a tryptophan and at both positions simultaneously, and then combined with coelenterazine analogs. The most promising of these aequorin variants, aequorin withL-4-methoxyphenylalanine at position 82 and 86 selected for its 56 nm red shift and aequorin with L-4-iodophenylalanine at positions 82 and 86 chosen for its 60 s long half-life, were then injected intrasomally into the eye of a 6-8 weeks old ICR (CD1) outbred female mouse. The eye was chosen for suitability for visualization studies, including its optical transparency, simple anatomy and well-defined structure, and easy accessibility, and to apply aequorin to imaging in proximity to a light sensitive tissue, the retina, a likely target for future studies with aequorin.

3.2 Materials and Methods

3.2.1 Reagents

The pBAD/His A and Terrific Broth (TB) are from Invitrogen (Carlsbad, CA). The PET30 Xa/LIC Kit and Xa Factor Cleavage Capture Kit are from Novagen (Madison, WI). NcoI and Hind III restriction endonucleases are from New England Biolabs (Boston, MA). All natural amino acids, and all antibiotics, are from Sigma-Aldrich (St. Louis, MO). LB agar and LB broth are from Fischer Scientific (Fair Lawn, NJ). The coelenterazines are from Gold Biotechnology (St. Louis, MO). The L-4-aminophenylalanine, L-4-bromophenylalanine, L-4-iodophenylalanine, and L-4-methoxyphenylalanine are from Peptech (Burlington, MA).

3.2.2 Apparatus

Cells were grown in a Thermo-Fisher Scientific orbital shaker incubator at 37^{o}C. Cell cultures were harvested using a Beckman J2-MI centrifuge. The proteins were purified using a BioCad Sprint Perfusion Chromatography System (Perspective Biosystems, Farmington, MA) using 20 mL DEAE Waters AP-2 Anion Exchange Column (Waters Corporation, Milford, MA). The buffers for the purification of the protein were 30 mM Tris-HCl, pH 7.5, containing 2 mM EDTA (Buffer A) and a 30 mM Tris-HCl, pH 7.5, containing 2 mM EDTA, and 1 M NaCl (Buffer B). Diafiltration was performed using a tangential flow separation module with hollow fiber filter membrane (Spectrum Labs, Rancho Dominguez, CA) using 30 mM Tris-HCl, pH 7.5, containing 2 mM EDTA. Ni-NTA Agarose beads are from Qiagen (Venlo, Netherlands). Amiron

Ultra-15 Centrifugal Filter Units are from EMD (Billerica, MA). Purity of the proteins was confirmed by sodium dodecyl sulfate-polyacrylamide gel electrophoresis (SDS-PAGE) using a Novex Mini-cell apparatus from Invitrogen and staining with Coomassie Brilliant Blue by the appearance of a single band. Aequorin activity was measured using an Optocomp I luminometer (MGM Biomedical Hamden, CT). The emission spectra of the aequorins were determined using a custom made SpectroScan instrument (ScienceWares, Falmouth, MA), which is capable of obtaining spectra from flash reactions of luminescent samples that emit in the 400-700 nm range. Half-life scans were taken using a Polarstar Optima 96 well microplate reading luminometer (BMG Labtech, Ortenberg, Germany).

3.2.3 Construction of the pDULE-pBADHisA-AEQTAG86 Expression Strains

Four pDULE vectors which allow for the site-specific incorporation of four different non-natural amino acids were obtained from Dr. Peter Schultz (Scripps Research Institute, La Jolla CA) and Dr. Ryan Mehl (Franklyn and Marshall College, Lancaster, PA)[49a].Each of these pDULE plasmids coded for a $tRNA_{CUA}$ and $tRNA_{CUA}$-synthetase specific for the TAG codon and a single non-natural amino acid, either L-4-aminophenylalanine, L-4-bromophenylalanine, L-4-iodophenylalanine, or L-4-methoxyphenylalanine. These plasmids were transformed into *E. coli* DH10B cells and transformants were selected by plating on LB agar medium containing ampicillin (100 μg/mL) and tetracycline (12 μg/mL). The presence of the pDULE plasmid was confirmed by plasmid isolation, restriction enzyme digestion and DNA gel electrophoresis.

3.2.4 Construction of the pDULE-pET30AEQ8286TAG Expression Strains

The four pDULE plasmids were transformed into *E. coli* DH10B cells with pET30AEQ8286TAG and transformants were selected by plating on LB agar medium containing tetracycline (12 μg/mL) and kanamycin (35 μg/mL). The presence of the pDULE plasmid was confirmed by plasmid isolation, restriction enzyme digestion and DNA gel electrophoresis.

pBADAEQ86TAG was prepared by inserting the AEQTAG86 gene with the OmpA leader sequence attached into pBAD/His A. The pIN4AEQ86TAG vector containing the cysteine-free aequorin gene fused to the OmpA leader sequence was used as a template. The primers were designed so the resulting DNA sequence contained an NcoI site at the 5' end and a HindIII site at the 3' end.

The following primers were used for the cloning of ompA:AEQ86TAG fusion into pBAD/HisA vector (restriction sites for cloning are underlined).

AEQforpBAD

5'-<u>CCATGG</u>GTATGAAAAAGACAGCTATCGCGATTGC-3'

And *AEQrevpBAD*

5'-
<u>AAGCTT</u>AGGGGACAGCTCCACCGTAGAGCTTTTCGGAAGCAGGATCCATTGT
GTAC-3'

The resulting PCR product was gel purified and cloned into the pCR®II-TOPO® vector by using the TOPO TA cloning kit (Invitrogen, Carlsbad, CA). The plasmid from the TA clone was then isolated and sequenced to confirm the presence of the insert. The

ompA:AEQ86TAG insert from the TOPO TA clone was then ligated into the NcoI and HindIII sites of pBAD/His A to create pBADHisA-AEQ86TAG.

The AEQTAG86 gene was also cloned into a pET30 Xa/LIC Vector using primers designed according to the manufacturer's instructions. pET30AEQ8286TAG was then prepared by using a pair of primers to create a site-specific mutation consisting of a TAG at position 82 (underlined).

Oligo HPLCTAG8286for

5'-GGAAACTGATTGGCCTGCATAGATTGAAGG-3'

And *HPLCTAG8286rev*

5'-CCTTCAATCTATGCAGGCCAATCAGTTTCC-3'

pBADHisA-AEQ86TAG and pET30AEQ8286TAG vectors were transformed into chemically competent *E. coli* DH10B cells that already contained the pDULE plasmids to produce four different strains, each specific for the incorporation one of the four non-natural amino acids mentioned above. Selection for transformants was performed by plating on LB agar medium containing both tetracycline (12 μg/mL) and kanamycin (35 μg/mL).

3.2.5 Expression and Isolation of Aequorins Mutants from pBADHisA-AEQ86TAG

The cells harboring the pDULE systems with pBADHisA-AEQ86TAG vector were grown in 25 mL of LB broth containing ampicillin (100 μg/mL) and tetracycline (12 μg/mL). All cultures, unless specified otherwise, were grown overnight at 37 ºC with

shaking at 250 rpm. These overnight cultures were used to inoculate 500 mL of LB broth containing the appropriate antibiotics and the cultures were grown at 37 ^{o}C at 250 rpm to an OD_{600} between 0.4-0.6. The corresponding non-natural amino acid was then added to a final concentration of 1 mM. The culture was allowed to grow for 1 hour and then induced with arabinose (0.2% final concentration) overnight.

3.2.6 Expression and Isolation of Aequorin Mutants from pET30AEQ8286TAG

The cells were grown in 25 mL of Terrific broth (TB) containing tetracycline (12 μg /mL) and kanamycin (35 μg/mL) overnight at 37 ^{o}C at 250 rpm. The overnight cultures were used to inoculate 500 mL of TB broth containing the appropriate antibiotics and the cultures were grown at 37 ^{o}C at 250 rpm. After growing to an OD_{600} between 0.4-0.6, the corresponding non-natural amino acid was added to a final concentration of 1 mM. The culture was allowed to grow for 1 hour and then induced with 1 mM IPTG and left to grow overnight.

The culture was centrifuged at 15,300 xg for 20 min and the pellet was boiled for 5 min in Native Purification Buffer (50 mM NaH_2PO_4, 0.5 M NaCl, 1 mM Imidazole, pH = 8.0). The boiled pellet was centrifuged again and the supernatant added to 1 mL of suspended Ni-NTA agarose beads and rotated on a Mini Labroller (Labnet, Woodridge, NJ) at room temperature for 2 hours. The protein was eluted off the column using a PBS Buffer with 20 mM Imidazole at pH=8.0 and digested with Xa factor according to manufacturer's instructions until all the His6x tag was cleaved from the protein. The Xa factor was removed with Xa factor Agarose capture beads. The cleaved aequorin was then concentrated using Amicon Ultra spin columns.

3.2.7 Determination of Activities of Aequorin Variants

Aequorin was diluted with 30 mM Tris-HCl, pH 7.5, containing 2 mM EDTA, to $1x10^{-7}$ M and charged with $1x10^{-4}$ M coelenterazine overnight. Aequorin activity was triggered by injecting 100 µL of 100 mM Tris-HCl, pH 7.5, containing 100 mM $CaCl_2$. Bioluminescence intensity was measured at 0.1 s intervals for up to 6 s on an Optocomp I luminometer (MGM Biomedical Hamden, CT).

3.2.8 Emission Spectra of Aequorin Variants

A 1 x 10^{-6} M sample of each aequorin was charged by incubating overnight at 4 °C with $1x10^{-4}$ M of each of the different coelenterazines and 150µL of each charged aequorin was pipetted into a 96-well microtiter plate and following injection of 100 µL of 100 mM Tris-HCl, pH 7.5, containing 100 mM $CaCl_2$, the emission spectra was collected for 10 seconds from 400-700 nm in 1.5 nm increments on a custom made SpectroScan instrument (ScienceWares, Falmouth, MA).

3.2.9 Half-life Determination of Aequorin Variants

A $1x10^{-6}$ M sample of each aequorin variant was charged overnight at 4 ºC with the $1x10^{-4}$ M of the coelenterazine analog used during the collection of emission spectra. A Polarstar Optima 96 well microplate luminometer (BMG Labtech, Ortenberg, Germany) was utilized for the half-life measurements. The bioluminescence signal of a 50 µL sample was collected between 30 s to 150 s, depending on the expected half-life of the aequorin analog, following the injection of 100 µL of triggering buffer (100 mM Tris-HCl, pH 7.5, containing 100 mM $CaCl_2$). The mean bioluminescence decay spectra was

fit with an exponential decay equation using GraphPad Prism 5.0 (GraphPad Software, San Diego, CA), and an equation for first order decay kinetics was used to calculate the bioluminescence half-life of each aequorin-coelenterazine pair.

3.2.10 Mass Spectrometry

Proteins were run on SDS-PAGE and cut out of the stained gels with Coomassie Blue. Gel pieces were digested with trypsin, and an LC-ESI-MS-MS was performed using a ThermoFinnigan LTQ. Resulting MS-MS spectra were searched against proteins in the Swiss-Prot database using the X!Tandem search engine to look for the presence of the substitution of the non-natural amino acid at and only at the target positions.

3.2.11 *In Vivo* Imaging

The aequorin variants were dissolved in a HEPES Buffer (10 mM HEPES, 0.15 M NaCl, 5 mM $MgCl_2$, 1.8 mM $CaCl_2$, at pH=7.4) at concentrations from 9.1 x 10^{-6} M to 4.5 x 10^{-5} M. All mice were anesthetized with a 100 µL ketamine/xylazine (1.5 mg/0.3 mg) intraperitonal injection before the injection of the sample. The aequorin samples were injected into one eye of six mice via intrastromal injection in 5 µL volumes, or into the antechamber at a volume of 10 µL, of each of the ICR (CD1) outbred female mouse 6-8 weeks old purchased from Taconic (Germantown, NY). The same volumes of plain HEPES were injected into the other eye to serve as an internal control. Native coelenterazine was diluted in PBS Buffer to a volume of 2.3 x 10^{-4} M and applied to the surface of each eye in 1 µL volumes. The mice were then placed in a Caliper/Xenogen IVIS® SPECTRUM (Caliper, Hopkinton, MA) in the IVIS Small Animal Imaging

Facility at the Oncogenomics Core Facility, Miller School of Medicine, with oxygen flowing into the imaging chamber. Images were taken over 30 s to 60 s. All animal experiments were conducted based on protocols approved by Institutional Animal Care and Use Committee of the University of Miami.

3.3 Results and Discussion

In vivo imaging is a powerful tool employed in the diagnosis and understanding of disease. The *in vivo* imaging system (IVIS) provides a technique for imaging that uses fluorescence and bioluminescence probes to obtain *in vivo* images from one or more target body locations in whole animals. Bioluminescent reporters such as FLuc and RLuc have been introduced into target systems through transgenic gene expression, but such techniques are not suitable for humans. To overcome this limitation, we propose to use bioluminescent proteins with emission characteristics suitable for surface and, in future studies, deep tissue imaging. To broaden the applicability to imaging in humans, aequorin can be modified to tune its bioluminescence emission by preparing variants via genetic engineering followed by pairing with coelenterazine analogs[2a, 24, 66, 85]. To create aequorin mutants with emission characteristics suited for *in vivo* imaging, particularly aequorin mutants with red-shifted emission spectra for use in deep tissue imaging, we site-specifically incorporated non-natural amino acids into selected sites of the catalytic pocket of aequorin using "Amber Suppression" [2c, 86]. Developed by Schultz *et al.*, Amber Suppression utilizes specifically engineered $tRNA^{CUA}_{CUA}$/$tRNA^{CUA}_{CUA}$-synthetase encoded into plasmids that take advantage of the naturally low occurrence of the nonsense TAG codon in *E. coli* so as not to interfere with cell growth and prevent the

expression of the full length protein in the absence of non-natural amino acid[49a, 86c]. Previous work in our group replaced a tyrosine residue at position 82 with using an introduced TAG codon to create functional non-natural mutants of aequorin with red-shifted peak emission and longer half-lives. Our group individually incorporated four different non-natural amino acids, specifically, L-4-aminophenylalanine (AminoPhe), L-4-bromophenylalanine (BromoPhe), L-4-iodophenylalanine (IodoPhe), and L-4-methoxyphenylalanine (MethoxyPhe), into a cysteine-free aequorin a position 82 and 86 simultaneously. These non-natural amino acid residues were selected for their hydrophobicity, aromaticity, and their size similarity to tyrosine and tryptophan[2c, 12c, 87]. Of these, two mutants, L-4-iodophenylalanine and L-4-methoxyphenylalanine (MethoxyPhe) were chosen for *in vivo* studies.

An overnight culture of the transfected cells were refreshed and induced with IPTG in the presence of the non-natural amino acid analogs. The cells were lysed and the protein was purified using a Ni-NTA column. Incorporation of the non-natural amino acids by the mutant tRNA/tRNA-synthetase, was verified by mass spectrometry.

The resulting aequorins modified with non-natural amino acids were complexed with one of the nine different coelenterazine analogs: *native, cp, f, fcp, h, hcp, i, ip*, or *n*. The bioluminescence emission characteristics of the aequorin variants were then analyzed, and the specific activity, emission maximum, and half-life of each variant was determined and the mass spectrometry acquired.

Aequorin variants modified with L-4-aminophenylalanine, L-4-bromophenylalanine, L-4-iodophenylalanine, and L-4-methoxyphenylalanine were all

active and they all showed changes in the spectral characteristics that resulted in red-shifted emission wavelengths and longer half-lives compared to the cysteine-free aequorin. The specific activity data (previous chapter) shows a decrease in specific activity for all variants compared to cysteine-free aequorin. This was observed previously with aequorin variants that contain non-natural amino acids at position 82. The activity of the aequorin mutants *in vivo* was confirmed by the injection of aequorin into the eyes of anesthetized mice that were imaged using IVIS. The mutants with L-4-methoxyphenylalanine at position 82 and 86 and L-4-iodophenylalanine at position 82 and 84 were chosen for their red shift and long bioluminescent half-life, respectively. Control mice with no aequorin injected were also run in each experiment, and displayed no bioluminescence. Figure 3.1A, B, and C shows the cysteine-free aequorin and L-4-methoxyphenylalanine variant at the same concentration injected intrastromally. Native coelenterazine was added to the surface of the eye dropwise and the bioluminescence emission was then recorded immediately. External addition of calcium ions was not necessary since the cells and tissues of the eye already contain an abundance of calcium ions. Figure 3.2D, E, and F shows cysteine-free aequorin and the L-4-iodophenylalanine variant injected into the antechamber of the eye. The L-4-iodophenylalanine variant was added at a greater concentration due to the lower specific activity exhibited in the *in vitro* studies. The mice were observed for up to an hour and half after the addition of the coelenterazine and still displayed bioluminescence. The intensity of the bioluminescence emission continued to increase for some minutes after the addition of the coelenterazine, caused by the time taken for coelenterazine to diffuse to the aequorin. To our knowledge,

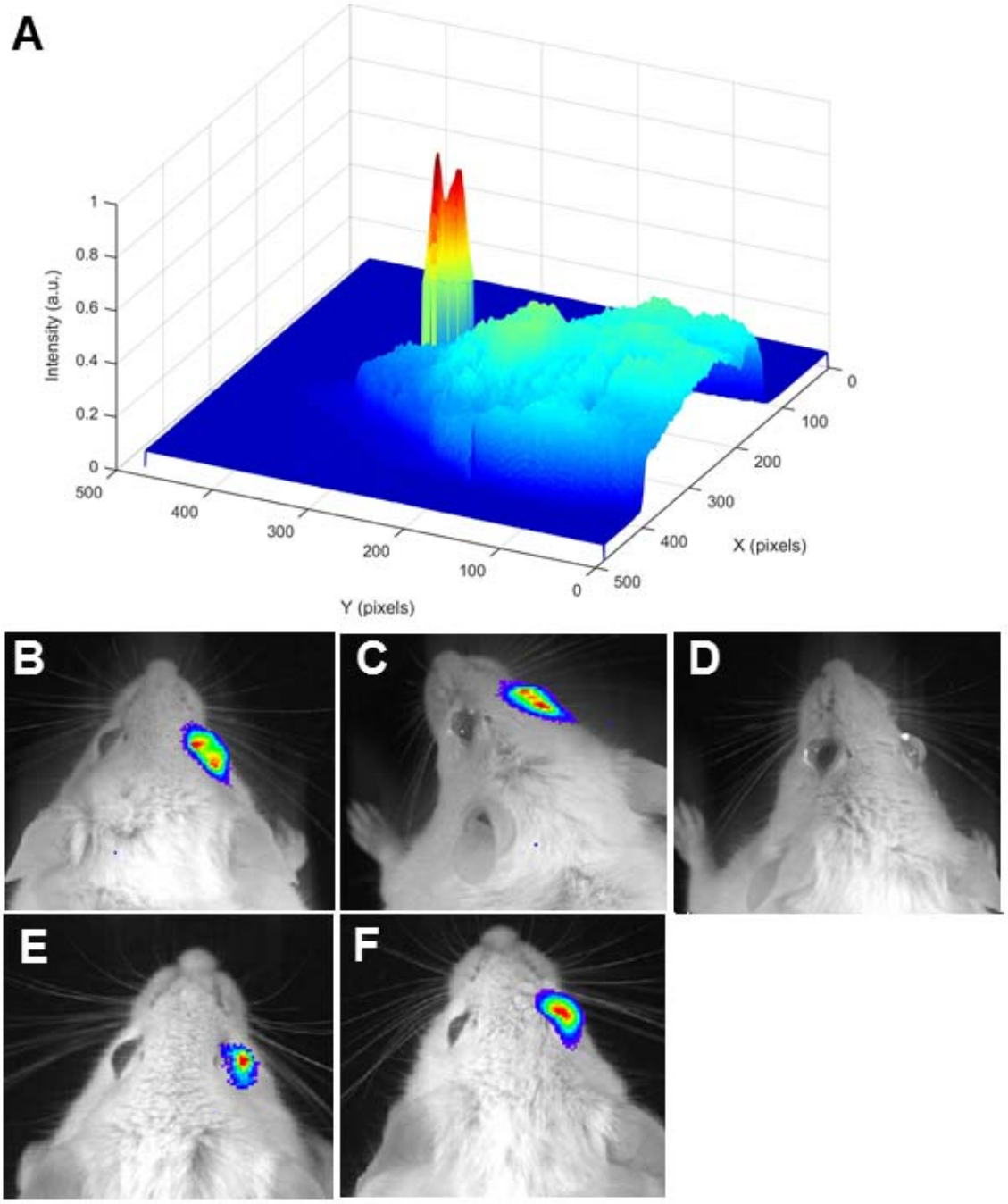

Figure 3.1 Bioluminescent activity of select aequorin mutants *in vivo.* Mice have a 5 µL intrastromal or antechamber injection in the right eye with mutant aequorin and the left eye with HEPES Buffer. (A,B) Cysteine-free aequorin injected intrastromally at a concentration of 2.7 x 10^{-5} M, 30 s exposure. (C) Cysteine-free aequorin with L-4-methoxyphenylalanine at positions 82 and 8. (D) HEPES Buffer only in both eyes. (E) Cysteine-free aequorin injected in the antechamber at a concentration of 3.2 x 10^{-5} M, 60 s exposure. (F) Cysteine-free aequorin with L-4-iodophenylalanine at positions 82 and 86. Images made in Mathlab R2014b and LivingImage 4.4.

this is the first time that a non-natural aequorin mutant has been shown to be active *in vivo*.

3.4 Conclusion

Despite a large number of imaging technologies, including MRI, PET, and fluorescent optical imaging, a method that provides a comprehensive look at the molecular basis of disease states is needed for diagnosis and the monitoring of therapy progression in research and clinical settings. IVIS provide a means of observing biological activity at the molecular level using luminescent signals. While fluorescence is frequently used in optical imaging, bioluminescence has several advantages in the form of a lower background, greater sensitivity, and no need for outside excitation. Bioluminescent proteins have been used for optical imaging, but typically using transgenic tissue[88]. This limitation can be circumvented by using a protein that can be added directly *in vivo*. Aequorin is such a protein, with the additional advantage of fine tuning in the form of several synthetic coelenterazine analogs and the site-specific incorporation of non-natural amino acids to create mutants suitable for imaging in deep tissue as well as surface cells (see Chapter 2). We have shown that one of these aequorin variants displays a 56 nm red-shift in bioluminescence emission wavelength, the greatest red-shift yet reported for an aequorin variant. The use of this variant can be more advantageous for *in vivo* studies since a red shifted photons can penetrate deeper in a tissue allowing for imaging tissues that are located deep within the organism. Moreover, half-lives of the bioluminescence emission have been tuned to range from 0.1 seconds to approximately 60 seconds which can be useful in selectively imaging separate areas

simultaneously or two different targets within the same location by resolving the separate signals temporally. The eye was selected for testing the *in vivo* activity of the aequorin due to its clarity, well-known simple anatomy, and the light sensitivity of the retina that makes it unsuitable for optical studies with fluorescent probes as the excitation source could damage light-sensitive proteins within the retina. Two of these aequorin mutants, aequorin with L-4-methoxyphenylalanine at positions 82 and 86 chosen for its red shift, and aequorin with L-4-iodophenylalanine at positions 82 and 86, chosen for its long bioluminescent half-life, were injected intrastromally to the eyes of CD1 mice with coelenterazine added dropwise to the eye surface. These newly prepared and characterized aequorin variants demonstrated improved characteristics with regard to our previously reported photoproteins, thus broadening the potential use of aequorin in bioanalysis and imaging applications.

CHAPTER 4. DEVELOPMENT OF "CLICK" AEQUORIN SITE-SPECIFICALLY INCOPORATING L-4-AZIDOPHENYLALANINE FOR BIO-ORTHOGONAL COPPER-FREE CLICK CHEMISTRY

4.1 Overview

The ability to selectively and specifically modify target molecules is a valuable tool for biological and chemical studies[26]. In particular, the ability to modify biomolecules, in the complex environment of biological samples, is a prerequisite to further studies and applications in biological engineering. Common methods for labeling molecules include linking covalently via native reactive side groups, such as primary amine reactive side groups with NHS-esters (N-hydroxysuccinimide esters), sulfohydryl reactive side groups with maleimide, and carboxylates to primary amines using sulfo-NHS. Methods that use non-native groups include photolinking using photoreactive side groups such as benzophenone. However, both these methods result in unavoidable non-specific targeting in biological samples. In contrast, orthogonal methods of labeling react only to their specific target, regardless of other molecules present. One of these bio-orthogonal methods, known as "click chemistry", has already found broad application in materials science, *in situ* drug development, and biomolecular labeling and imaging[89].

Click chemistry reactions utilizes two reactive groups, an azide and an alkyne[26, 90]. Both groups are stable in water and non-reactive in biological samples, and the azide is highly reactive when in close proximity to the alkyne, resulting in an irreversible cycloaddition. Since the development of click chemistry, several different variations of

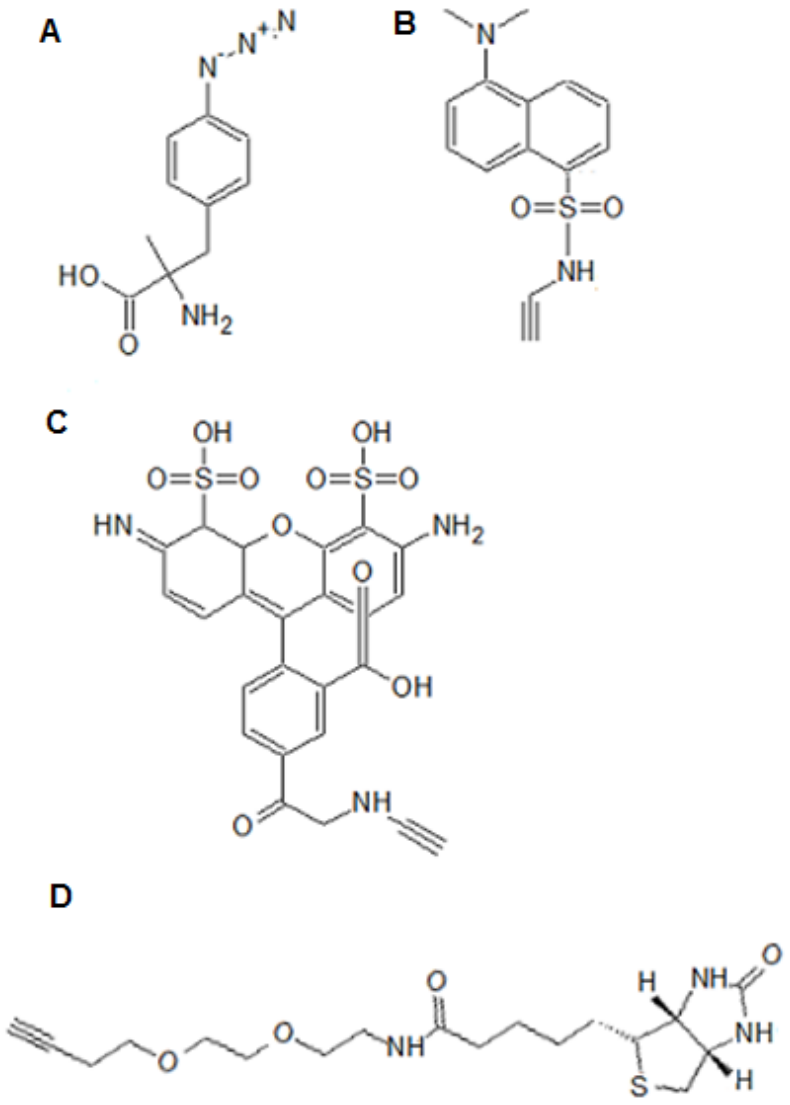

Figure 4.1. Chemical structures of reactants used for click reactions. (A) L-4-azidophenylalanine. (B) Dansyl-alkyne. (C) AlexaFluoro488 alkyne (D) Biotin-PEG4-alkyne.

the approach have been derived[91], including those that no longer require the original $Cu(II)^{2+}$, which can be toxic to living systems[92]. The broad applicability of click chemistry has led to the introduction of an azide and alkyne modifications to metabolites, linkers, fluorescent probes, dendrimers, surfaces, chemotherapeutics, nucleic acids, and amino acids for swift, orthogonal reactions, often resulting in multiple functions within

the same molecule[25-26, 64, 93]. Our group has site-specifically incorporated non-natural amino acids into the bioluminescent flash-emitting photoprotein aequorin with the aim to develop a more extensive catalog of aequorin mutants for applications *in vitro* and *in vivo* as a reporter molecule[3, 34c]. Bioluminescence, or living light, is a natural phenomenon that is non-toxic, requires no outside excitation, and when emitted from photoproteins, can be controlled in an "on" and "off" manner by the addition of the coelenterazine chromophore. By incorporating an L-4-azidophenylalanine into aequorin a position 5, a location previously containing a cysteine used for linking by Sulfo-LC-SPDP linking, we plan to increase the utility of aequorin by introducing orthogonal linking to applications using aequorin. An L-4-azidophenylalanine was site-specifically incorporated into the aequorin using a tRNA/tRNA-synthetase combination with a stop TAG codon at position 5 replacing an introduced cysteine mutation previously used for linking using a Sulfo-LC-SPDP linker. A second position, 69, was chosen for BRET applications by clicking an alkyne-modified fluorophore[44]. The azido group was chosen for incorporation due to its photosensitivity to ensure the group did not degrade prior to the reaction.

To demonstrate the versatility of conjugation via "click" aequorin, three different molecules were chosen for linking (Figure 4.1): biotin-PEG4-alkyne for avidin-biotin binding, 5-(dimethylamino)-N-(prop-2-yn-1-yl)naphthalene-1-Sulfonamide (Dansyl-alkyne) to verify fluorophore linking, and AlexaFluoro488 as the fluorophore receiver in bioluminescence resonance energy transfer (BRET). Biotin-avidin binding is the strongest non-covalent bond known and a widely applied in purification and detection strategies. Aequorin has been used as the bioluminescent source in BRET based imaging using fluorophores linked by methods other than click chemistry. The L-4-

azidophenylalanine was successfully incorporated into aequorin at position 5 and verified by mass spectrometry. All three alkynylated molecules were successfully liked to the PheAz-Aequorin, which maintained bioluminescent activity. To our knowledge, this is the first time aequorin has had an L-4-azidophenylalanine incorporated via TAG codon and the first time aequorin has been clicked to other molecules. Following linking by click chemistry, the biotin-PEG4-alkyne was successfully conjugated to streptavidin, chosen for the previous use of aequorin-streptavidin fusions in bioluminescent assays[94]. Both fluorescent molecules maintained their fluorescent activity after linking, and attempts BRET between the emitted light and the clicked fluorophore were successful, at position 69.

4.2. Materials and Methods

4.2.1 Materials

The pET30Xa/LIC kit, Bug Buster, acetic acid, and glycerol are from EMD Millipore (Darmstadt, Germany). The Terrific Broth (TB) is from Invitrogen (Carlsbad, CA). The Q5 Site-Directed Mutagenesis Kit, BglII and SalI-HF are from New England Biolabs (Boston, MA). The Xa Factor Cleavage Capture Kit and Lysonase are from Novagen (Madison, WI). The pEVOL-pAzF plasmid is from Addgene (Cambridge, MA). Agarose, ascorbate, IPTG, $MgSO_4$, $CaCl_2$, Dansyl chloride, anhydrous dichloromethane, triethylamine, propargylamine, and all antibiotics are from Sigma-Aldrich (St. Louis, MO). Sodium phosphate is from Amresco (Solon, OH). Imidazole is from Alfa Aesar (Ward Hill, MA). The $CuSO_4$, $MgCl_2$, Tris HCl, EDTA, LB agar, and DMSO are from Fischer Scientific (Fair Lawn, NJ). NaCl is from Calbiochem (LaJolla, CA). The

coelenterazine is from Gold Biotechnology (St. Louis, MO). The sodium dodecyl sulfate (SDS) is from Curtin Matheson Scientific Inc. (Houston, TX). The neutravidin, streptavidin, and Sulfo-LC-SPDP are from Thermo Scientific (Waltham, MA). The L-4-azidophenylalanine is from Bachem (Bubendorf, Switzerland). NaOH is from Mallinckrodt Chemicals (Phillipsburg, NJ). The AlexaFluoro488 Alkyne (Alexa Fluor 488 5-Carboxamido-(Propargyl), Bis(Triethylammonium Salt)), 5-isomer and biotin-PEG4-alkyne linker are from Life Technologies (Carlsbad, CA). The Protein Reaction Buffer Kit is from Click Chemistry Tools (Scottsdale, AZ).

4.2.2 Apparatus

Cells were grown in a Thermo-Fisher Scientific orbital shaker incubator. Cell cultures were harvested using a Beckman J2-MI centrifuge. Ni-NTA Agarose beads are from Qiagen (Venlo, Netherlands). Amicron Ultra-15 Centrifugal Filter Units are from EMD (Billerica, MA). Purity of the protein was confirmed by sodium dodecyl sulfate-polyacrylamide gel electrophoresis (SDS-PAGE) using a Novex Mini-cell apparatus from Invitrogen and staining with Coomassie Brilliant Blue. Slide-A-Lyzer Dialysis Cassette 3,500 MWCO 0.5-3 mL are from Thermo Scientific (Waltham, MA). Aequorin activity was measured using an Optocomp I luminometer (MGM Biomedical Hamden, CT). The emission spectra of the aequorins were determined using a custom made SpectroScan instrument (ScienceWares, Falmouth, MA), which is capable of obtaining spectra from flash reactions of luminescent samples that emit in the 400-700 nm range. Half-life scans were taken using a Polarstar 96 well microplate reading luminometer (BMG Labtech, Ortenberg, Germany). Fluorescence measurements were taken using a QuantaMaster 40

steady state spectrofluorometer and Felix32 software purchased from Photon Technology International (Birmingham, NJ).

4.2.3 Synthesis of the Dansyl-alkyne

The Dansyl-alkyne fluorophore was synthesized using a procedure adapted from previous protocols[89]. One gram of dansyl chloride was dissolved in 12 mL of anhydrous dichloromethane, followed by the addition of 469 mg triethylamine and 255 mg of propargylamine. The mixture was stirred at room temperature for 4 hours under argon, and then quenched with 3 x 50 mL of deionized water. The organic phase was dried with $MgSO_4$, filtered and evaporated in vacuum, yielding the compound as a sticky yellow solid.

4.2.4 Construction of the pEVOL-pAzF-pET30AEQ5TAG and pEVOL-pAzF-pET30AEQ69TAG Expression Strains

The pEVOL-AzF plasmid for L-4-azidophenylalanine were transformed into *E. coli* DH10B cells and transformants were selected by plating on LB agar medium containing chloramphenicol (35 μg/mL) and kanamycin (35 μg/mL). The presence of pEVOL was confirmed by plasmid isolation, restriction enzyme digestion, and DNA gel electrophoresis.

pETAEQ5TAG was prepared by inserting the TAG codon into a pET30AEQ5Cys.

The following primers were used for the PCR using the Q5 kit.

AeqTAG5for

5'-GTGAAACTGACCTAGGACTTCGACAACCCA-3’

And *AeqTAG5Rev*

5'-TGGGTTGTCGAAGTCCTAGGTCAGTTTCAC-3’

The PCR product was treated with DpnI then transformed into NEB 5-alpha Competent *E. coli* cells. The plasmid was then isolated via plasmid prep and the sequence verified.

pEVOL-pAzF and pET30AEQ5TAG vectors were cotransformed into chemically competent *E. coli* BL21(DE3) Selection for transformants was performed by plating on LB agar medium containing both chloramphenicol (35 µg/mL) and kanamycin (35 µg/mL).

Identical steps were taken for the creation of the pEVOL-pAzF and pET30AEQ69TAG expression strains with the exception of different primers.

The following primers were used for the PCR using the Q5 kit.

AEQTAG69For

5’-CTTCGGAGGATAGGGAATGAAATATGGTG-3’

And AEQTGT69Rev

5’-AAGGCTTCTACAGCATCTTTG-3’

4.2.5 Expression and Isolation of Aequorin Mutants from pET30AEQ5TAG and pET30AEQ69TAG

The cells were grown in 25 mL of Terrific broth (TB) containing chloramphenicol (35 µg/mL) and kanamycin (35 µg/mL) overnight at 37 ºC at 250 rpm while being

shielded from light. The overnight cultures were used to inoculate 500 mL of TB broth containing the appropriate antibiotics and the cultures were grown at 37 ºC at 250 rpm. After growing to an OD_{600} between 0.4-0.6, the L-4-azidophenylalanine was added to a final concentration of 1 mM. The culture was allowed to grow for 1 hour and then induced with 1 mM IPTG and left to grow overnight.

The culture was centrifuged at 15,300 xg for 20 min and the pellet was lysed for 20 min in Bug Buster with Lysonase while being shielded from light. The lysed pellet was centrifuged again and the supernatant added to 1 mL of suspended Ni-NTA agarose beads and rotated on a Mini Labroller (Labnet, Woodridge, NJ) at room temperature for 2 hours. The protein was eluted using a PBS Buffer with 20 mM imidazole at pH=8.0 under red light and digested with Xa factor according to manufacturer's instructions until all the protein was cleaved while being light protected. The Xa factor was removed with Xa factor Agarose capture beads. The cleaved aequorin was then concentrated using Amicron Ultra spin columns.

4.2.6 Determination of Activities of Aequorin

Aequorin was diluted with 30 mM Tris-HCl, pH 7.5, containing 2 mM EDTA, to $1x10^{-7}$ M to ensure the amount of light produced was within the linear range of the instrument. Aequorin activity was triggered by injecting 100 µL of 100 mM Tris-HCl, pH 7.5, containing 100 mM $CaCl_2$. Bioluminescence intensity was measured at 0.1 s intervals for up to 6 s.

4.2.7 Emission Spectra of Aequorin

A 1 x 10^{-6} M sample of aequorin was charged by incubating overnight at 4 °C with 2 x 10^{-6} M of native coelenterazine. The charged aequorin was pipetted into a 96-well microtiter plate and following injection of 100 µL of 100 mM Tris-HCl, pH 7.5, containing 100 mM $CaCl_2$, the emission spectra was collected for 10 seconds from 400-700 nm in 1.5 nm increments.

4.2.8 Half-life Determination of Aequorin

A 1x10^{-6} M sample of aequorin was charged overnight with 2 x 10^{-6} M of the coelenterazine analog used during the collection of emission spectra. A Polarstar 96 well microplate luminometer (BMG Labtech, Ortenberg, Germany) was utilized for the half-life measurements. The bioluminescence signal of a 50 µL sample was collected for 30s, following the injection of 100 µL of triggering buffer (100 mM Tris-HCl, pH 7.5, containing 100 mM $CaCl_2$). The mean bioluminescence decay spectra was fit with an exponential decay equation using GraphPad Prism 5.0 (GraphPad Software, San Diego, CA), and an equation for first order decay kinetics was used to calculate the bioluminescence half-life of the aequorin.

4.2.9 Copper-based Click Reaction

Method 1: A 0.5 mg sample of aequorin or PheAz-aequorin was reacted with the fluorophore at a ratio of 3.5 molar in a solution 2% molar ascorbate/ 2% molar $CuSO_4$. The sample was light protected and left to react at 23° C overnight. One mL of the sample was loaded into a Slide-A-Lyzer Dialysis Cassette MWCO 3,500, then placed in

1 L of 30 mM Tris-HCl, 2 mM EDTA, pH=7.5 for 2 hours. The buffer was then replaced for a total of 8 L.

Method 2: A 0.5 mg sample of aequorin or PheAz-Aequorin was reacted with an alkyne containing compound in accordance with the instructions provided with the Protein Reaction Buffer Kit and left to react overnight. Samples were then purified using buffer exchange. One mL of the sample was loaded into a Slide-A-Lyzer Dialysis Cassette MWCO 3,500, then placed in 1 L of 30 mM Tris-HCl, 2 mM EDTA, pH=7.5 for 2 hours. The buffer was then replaced for a total of 8 L.

4.2.10 Streptavidin-Biotin Conjugation

A 1 mL 1 x 10^{-6} M sample of aequorin in30 mM Tris-HCl, 2 mM EDTA, pH=7.5 was incubated with a sample of streptavidin at ratio of 1:1, 1:3, or 1:10 at 23 °C overnight.

4.2.11 Fluorescence Measurement of Aequorin-Fluoro Conjugates

A 1 x 10^{-6} M sample of aequorin was charged by incubating overnight at 4 °C with 2 x 10^{-6} M of native coelenterazine. Xe-lamp irradiation passed through the excitation monochromator of the spectrofluorometer in the entire volume of a quartz cuvette 1 cm x 1 cm x 3.5 cm. Excitation was set to 495 nm and the emission was set to 514-564 nm.

4.2.12 Mass Spectrometry

Proteins were run on SDS-PAGE and cut out of the stained gels. Gel pieces were digested with trypsin, and an LC-ESI-MS-MS was performed using a ThermoFinnigan LTQ. Resulting MS-MS spectra were searched against proteins in the Swiss-Prot database using the X!Tandem search engine.

4.3 Results and Discussion

The ability to selectively modify target molecules in biological samples is a valuable tool for biological and chemical studies. Click chemistry is an orthogonal reaction that can be used for selective modifications that uses two different reactive groups with characteristics suitable for uses in biological samples: an azido group and an alkyne. Azido groups and alkynes do not react with chemical structures found in biological samples, yet are highly reactive with each other, and bond covalently, making the bond irreversible. The expanded applications of click chemistry have led to the development of a large number of molecules that can be used for click reactions, including linkers, fluorophores, dendrimers, metabolites, and non-natural amino acids. Non-natural amino acids can be site-specifically incorporated into proteins using a method developed by the Schultz laboratory that utilizes a modified tRNA/tRNA-synthetase combinations encoded by a plasmid that is incorporated into the cell line expressing the gene for the protein of choice, including aequorin[58]. Aequorin is a photoprotein used in a variety of applications as a luminescent reporter molecule. Though copper is not strictly necessary for click chemistry, copper assisted reactions were chosen to maximize the amount of product generated *in vitro*. L-4-Azidophenylalanine was successfully expressed at two different

positions: position 5, for conjugation to linker molecules, and position 69, for BRET applications.

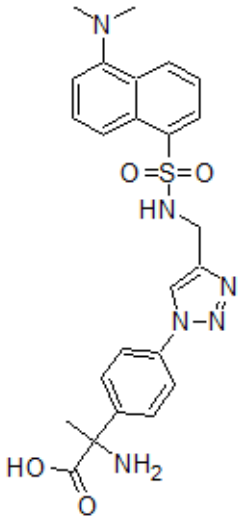

Sequence Mass: 58,792

AA Coverage: 112 of 189 (61%)

VKLTSDFDNP RWIGRHKHMF NFLDVNHNGK ISLDEMVYKA

SDIVINNLGA TPEQAKRHKD AVEAFFGGAG MKYGVETDWP

AYIEGWKKLA TDELEKYAKN EPTLIRIWGD ALFDIVDKDQ

NGAITLDEWK AYTKAAGIIQ SSEDCEETFR VCDIDESGQL

DVDEMTRQHL GFWYTMDPAC EKLYGGAVP

KLTS*DFDNPRW

Figure 4.2. The structure of L-4-azidophenylalanine clicked to the Dansyl-alkyne and the accompanying mass spectrometry data confirming the conjugation. Amino acids in red were detected by mass spectrometry.

The click reaction was verified by mass spectrometry using the Dansyl-alkyne, absorption wavelength 315 nm (Figure 4.2). To our knowledge, this is the first time L-4-azido-phenylalanine has been site-specifically incorporated into aequorin and the first time azide-alkyne cycloaddition has been done in aequorin. Also present in the sample was aequorin with a reduced version of the L-4-azidophenylalanine yielding L-4-aminophenylalanine. This is not unexpected as click chemistry reactions using proteins have not been shown to have a 100% product yield. Reactions to attach the fluorophore were performed with both aequorin and PheAz-Aequorin to show the linking is only successful in substituted aequorin.

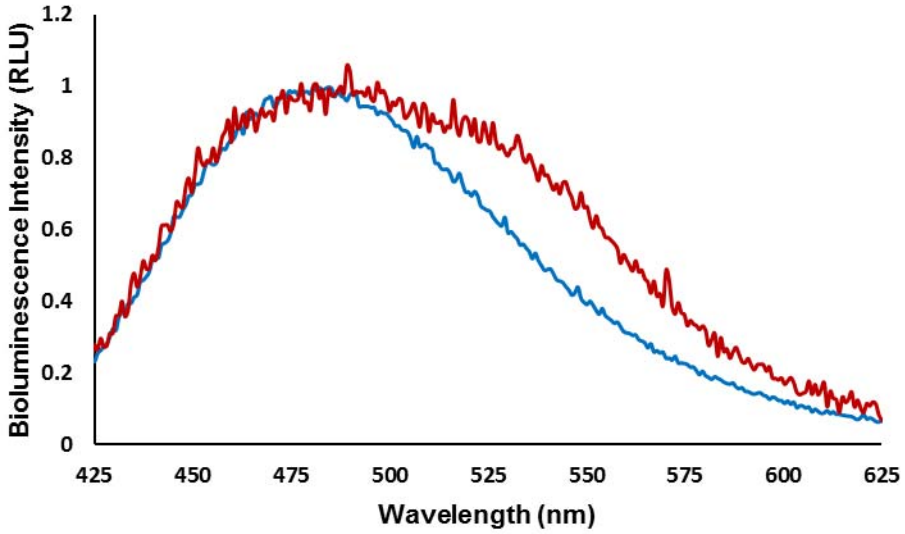

Figure 4.3. (A) Bioluminescence spectra of click aequorin clicked to AlexaFluoro488 alkyne in blue. The peak emission of the aequorin is slightly red-shifted compared to the cysteine-free aequorin. The expected peak at 525 nm generated by BRET is not present. (B) Fluorescence emission spectrum of PheAz-Aequorin after incubation with AlexaFluoro488 alkyne, background subtracted.

Activity test showed the L-4-azidophenylalanine substituted aequorin to maintain a high level of bioluminescence after linking (Figure 4.3A). However, there does not appear to be BRET taking place between the emitted light and the AlexaFluoro488, as the bioluminescent spectra shows an emission peak at approximately 525 nm, a 21 nm shift for the emission peak of cysteine-free aequorin at 469 nm, but not a second peak at anticipated Alexa 488 emission peak of 525 nm. Based on previous work in our lab wherein it was determined that positions 69 and 70, positions in close proximity to the coelenterazine, are best for BRET using aequorin, the fluorophore is most likely too far from the coelenterazine at position 5.

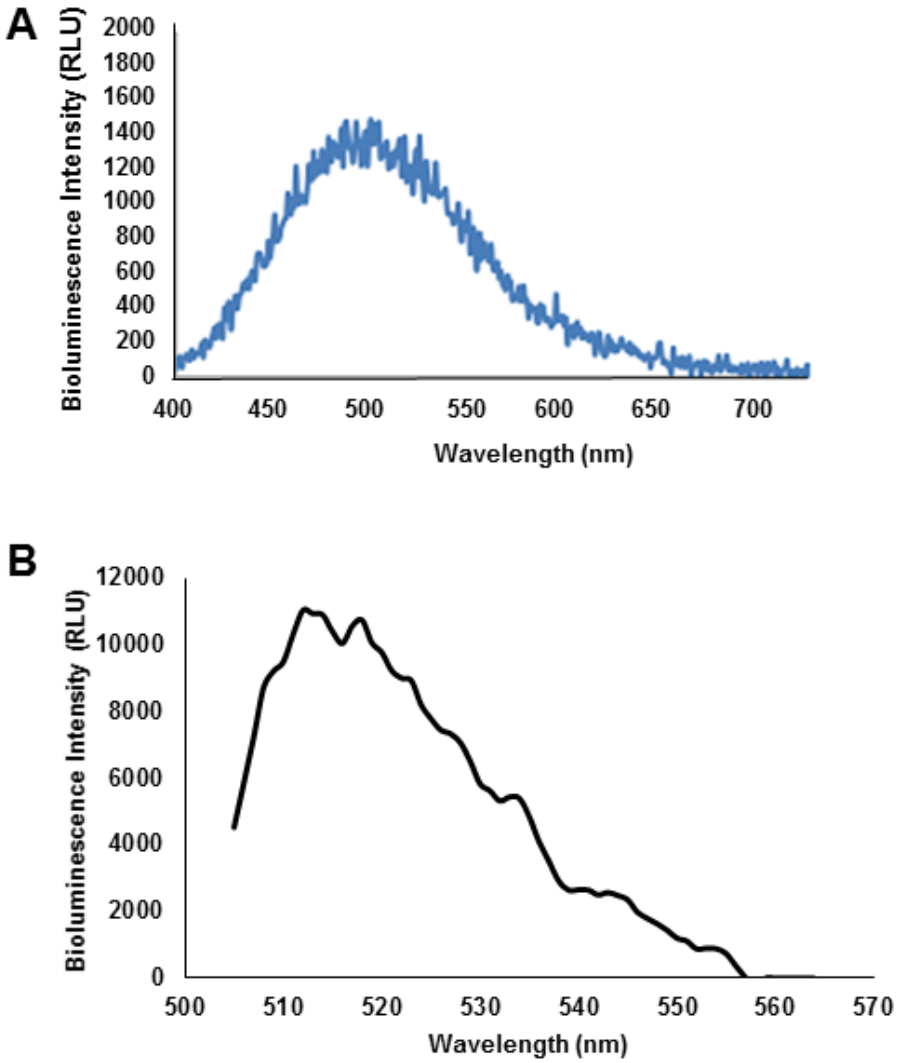

Figure 4.4. Normalized emission spectra of aequorin and PheAz-Aequorin with AlexaFluoro488 alkyne clicked at position 69. Aequorin is in blue and PheAz-Aequorin with the ALexaFluoro488 is in dark red.

Click reactions at position using the AlexaFluoro 488 alkyne showed a change in fluorescence indicating the linking of the fluorophore to the azido group within the aequorin protein despite the lack of BRET (Figure 4.3B). The fluorescence was not seen in aequorin without the azido group. The TAG codon was moved to position 69 to better facilitate BRET. Following click with AlexaFluoro488, a yellow tinge could be seen in

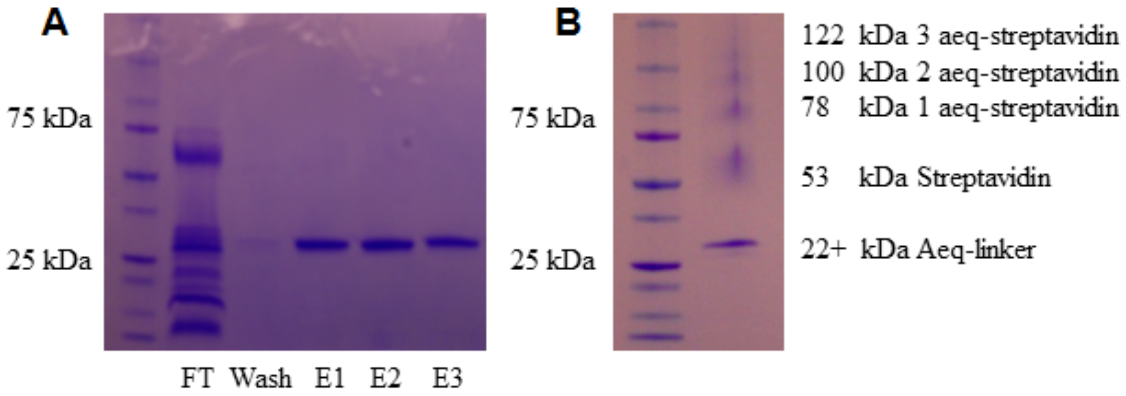

Figure 4.5. SDS-PAGE gels with PheAz-Aequorin. A) Lane 1 1 kDa Ladder, Lane 2 Flow through, Lane 3 Wash, Lane 4-Lane 6 PheAz-Aequorin elutions. B) Lane 1 1 kDa Ladder, Lane 2, PheAz-Aequorin after linking with the biotin-PEG4-alkyne and incubation with streptavidin.

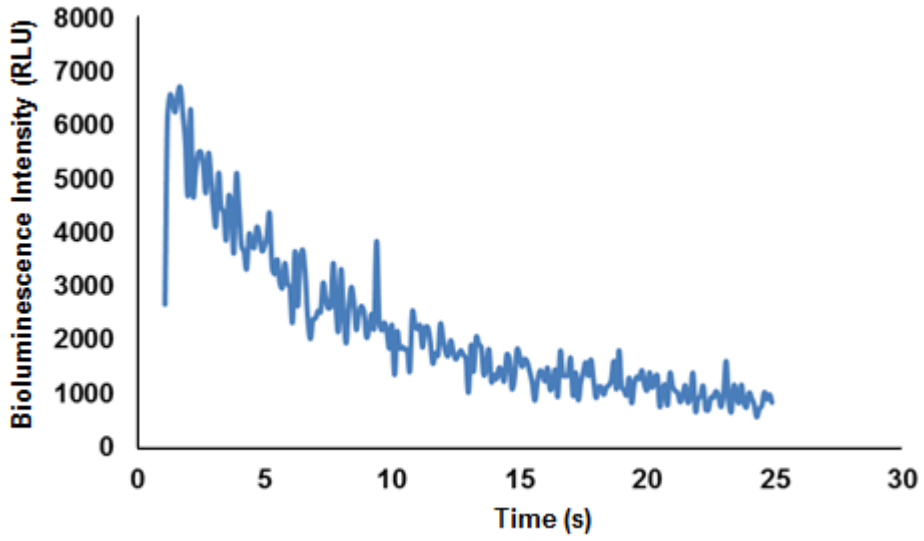

Figure 4.6. Half-life of click aequorin clicked to the linker and conjugated to streptavidin.

the sample, showing confirmation of the signal was available using the naked eye, and specific activity was found to be 2.1 x 10^{14} RLU/mole. Attempts at BRET using the new position at 69 were successful, showing a large second peak in a bimodal spectra at 525 nm as expected (Figure 4.4), and the half-life as measured to be 1.25 s. This the first of evidence of BRET using clicked aequorin.

PheAz-Aequorin was linked to the biotin-PEG4-alkyne linker, then incubated with streptavidin. SDS-PAGE of the reaction revealed the successful conjugation of PheAz-Aequorin to the linker and subsequent reaction between biotin and streptavidin (Figure 4.5), yielding streptavidin with up to four bound aequorin. An activity test confirmed the bioluminescent activity after the click reaction and biotin-streptavidin conjugation, and a half-life test found an increase in the half-life of this conjugated aequorin to be approximately 7 s (Figure 4.6). This demonstrates the suitability of click chemistry as a method of conjugating aequorin to other molecules to create larger, multifunctional structure.

4.4 Conclusions

In conclusion, by utilizing amber suppression to site-specifically incorporate the non-natural amino acid L-4-azidophenylalanine into aequorin using plasmids developed by the Schultz laboratory, the azido group can be inserted into the photoprotein aequorin, a valuable reporter molecule, for click chemistry applications. This exploits the bio-orthogonal nature of the reaction using two reactive groups not normally found in biological samples for labeling, capture, and other forms of molecule modification. To show the applicability of these substituted aequorin, two fluorophores, Dansyl-alkyne and AlexaFluoro488 alkyne, and a heterofunctional linker molecule, biotin-PEG4-alkyne were attached. Aequorin was successfully substituted with the L-4-azidophenylalanine, and shown to maintain its activity before and after linking, and both fluorophores maintained their fluorescent signal. A BRET signal was generated using the AlexaFluoro488 clicked a position 69. Aequorin was also clicked to the biotin-PEG4-

alkyne molecule. The aequorin and linker were then conjugated to streptavidin, showing the usefulness of click chemistry as a starting step in creating larger multi-functional molecules. To our knowledge, this is the first time L-4-azidophenylalanine has been incorporated into aequorin for click chemistry applications, increasing the versatility of aequorin and opening the door for more multifunctional molecules containing aequorin with bio-orthogonal linking capabilities.

CHAPTER 5. BIOLUMINESCENT *IN VIVO* IMAGING OF NEOVASCULARIZATION IN THE RETINA USING A LASER INDUCED WET MACULAR DEGENERATION MODEL AND A VEGFADARPIN-AEQUORIN FUSION PROTEIN

5.1 Overview

Age-related macular degeneration (AMD) is a major health problem world-wide, accounting for 8.7% of all blindness and is the most common cause of blindness in developed countries. Approximately 10% of all people 80 years old or older have late-stage macular degeneration in countries such as the US, France, Australia, Singapore, and Japan[67]. An estimated 196 million people will have AMD by 2020 with number increasing to 288 million by 2040 as the world's population grows and ages. In the US, the total annual direct cost associated with AMD is expected to be $575-733 million[31, 73b, 101]. Late-stage age-related macular degeneration is linked to significant functional loss, reduced quality of life, and depression. Despite the prevalence of AMD, treatments are still limited to a few options, particularly pharmaceutical targeting vascular endothelial growth factor A (VEGFA), most notably as ranibizumab (Lucentis)[71] and bevacizumab (Avastin)[72], which was originally developed as a drug for colon cancer. However, treatments remain expensive and not all patients have access to therapy[69b]. Furthermore, genetic factors, cardiovascular disease, and life-style risks such as cigarette smoking complicate prevention and treatment[68]. Given the lesser impact of early age-related macular degeneration versus the late stages, early detection and treatment is important.

Imaging is a critical part of the management of AMD, in particular the "wet" macular degeneration (wet MD) caused by neovascularization of the retina. Dye-based angiographies are typically used to map blood flow and identify lesions by following dye leakage, but require outside excitation that can be complicated by background fluorescence from molecules like melanin[74]. Optical coherence tomography (OCT)[75] is a newer alternative that forgoes dye in favor of applying near-infrared light and analyzing light scattering to generate cross-sectional images, but does not allow for distinguishing the neovasculature from scarring or hemorrhaging[73b]. However, given that VEGF is a key regulator of angiogenesis[70], triggers angiogenesis in animals, including humans[102], and is the target of the anti-angiogenesis pharmaceuticals that are the standard of care for neovascularization and used for multiple types of age-related macular degeneration, there is a lack of an *in vivo* imaging system that yields information at the molecular level and allows for the detection of VEGF directly.

The In Vivo Imaging System (IVIS) is capable of imaging whole animals and detecting bioluminescence signals *in vivo,* providing a means of detecting a signal from a bioluminescent molecular reporter designed to target endogenous VEGFA. The high-throughput imaging of several live animals that is capable of taking images of bioluminescent signals in only 60 s per image acquisition, providing a swift means of imaging at the molecular level using bioluminescent probes linked to a targeting molecule for VEGFA[34c, 34d, 36].

Wet AMD can be generated in a mouse model by creating laser-induced lesions on the retina[76a]. Post laser photocoagulation occurs most significantly in the retinal

pigmentation layer (RPE) and outer retina, and the VEGFA levels do not return to pre-photocoagulation levels until approximately 72 hours later, creating a suitable time frame for *in vivo* imaging[103]. The In Vivo Imaging System (IVIS) (PerkinElmer, Waltham,

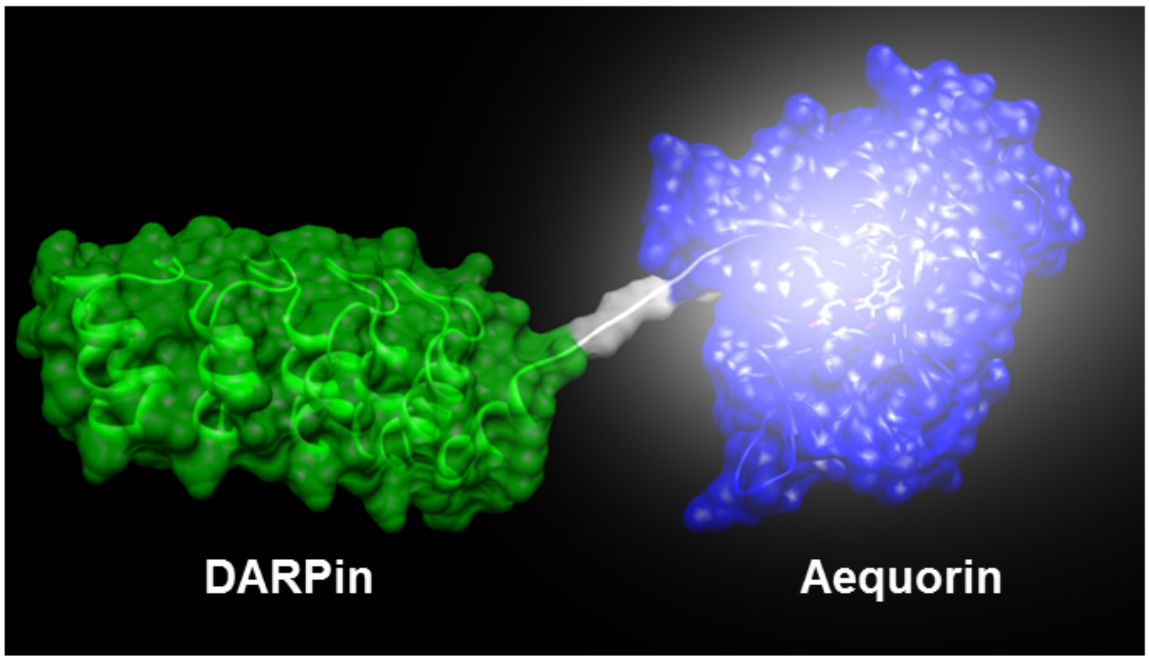

Figure 5.1. Aequorin with native coelenterazine fused by a SGGGGS linker sequence to a generic DARPin scaffold. Aequorin: PDB 1EJ3. DARPin: PDB 4DUI. (Image made in Discovery Studio 3.5, UCSF Chimera 1.5.2, GimpShop).

MA) is capable of imaging whole animals and detecting bioluminescence signals *in vivo,* providing a means of detecting a signal from a bioluminescent molecular reporter designed to target endogenous VEGFA. The high-throughput imaging of several live animals simultaneously as well as taking images of bioluminescent signals in only 60 s per image acquisition, provides a swift means of imaging at the molecular level using bioluminescent probes linked to a targeting molecule for VEGFA[34c, 34d, 36].

Herein, we describe the development of a fusion protein consisting of the cysteine-free variant of the bioluminescent protein aequorin from *Aequorea victoria*[104], and a designed

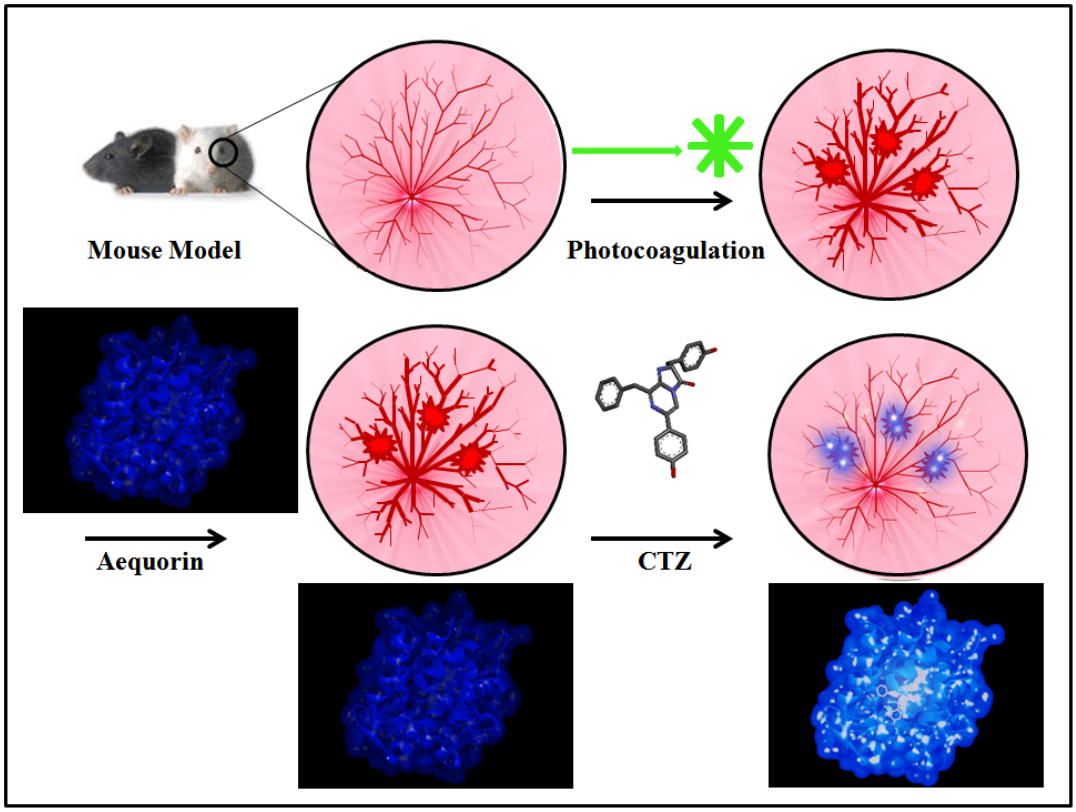

Figure 5.2. Schematic of photocoagulation and imaging with VEGFADARPin-Aequorin after the addition coelenterazine.

ankyrin repeat protein (DARPin) specifically targeted to VEGFA to perform imaging at the molecular level (Figure 5.1)[76a]. Bioluminescence is preferable to fluorescence *in vivo* in that it is not present in most animals, including humans, and does not require an external excitation source[6]. Aequorin and aequorin variants have been engineered for the purposes of *in vivo* imaging by several groups [5, 15-16, 36, 45, 78, 105]. Furthermore, the bioluminescence emission of aequorin can be controlled by withholding the light emitting luciferin, coelenterazine, which comes in many synthetic analogs, and is cell membrane permeable, until the signal is desired[106]. The benefits of pairing bioluminescence and DARPins together for protein detection has been utilized before for a proof of concept biosensor for the detection of isomeric forms of c-Jun N-terminal

kinases (JNK) *in vitro* and in mammalian cells [23]. The DARPin chosen for this investigation, a 15 kDa protein known as MP0112, has a picomolar binding affinity and been shown to effectively target VEGFA in clinical human trials [8, 76a], and the DARPin selected for comparison, targeting HER2, has been applied in *in vivo* mouse models[107]. The DARPin is comprised of cysteine-free anti-parallel alpha-helical repeat modules[17b, 19, 95]. DARPins have comparable specificities and affinities to their target epitopes as antibodies, great robustness and stability, express readily as soluble monomers in *E. coli*, and can be easily genetically fused to other proteins and can be further modified by crosslinking reactions[21c-e, 93c, 108].

The cysteine-free VEGFADARPin-Aequorin was shown to be active with native coelenterazine, and it binds selectively to the soluble VEGF isoform VEGFA (VEGF165). It was also shown to bind competitively with VEGFA in assays, and be used for the bioluminescent *in vivo* detection of VEGFA associated with lesions in the eyes of mice with a laser induced wet MD model (Figure 5.2)[109].

5.2 Materials and Methods

5.2.1 Materials

The bacterial expression constructs for VEGFADARPin-Aequorin fusion proteins and HER2DARPin-Aequorin fusion were special ordered in pReceiver-B01 OmicsLink™ Expression-Ready ORF cDNA Vectors and the DARPin alone is in a pReceiver-B02 from Genecopoeia (Rockville, MD). The Terrific Broth (TB) is from Invitrogen (Carlsbad, CA). Agarose, glucose, $MgCl_2$, $CaCl_2$, human and mouse

recombinant VEGFA and human VEGFC, and all antibiotics, are from Sigma-Aldrich (St. Louis, MO). Sodium phosphate is from Amresco (Solon, OH). Lysonase and pet30 Xa/LIC Kit are from Novagen (Madison, WI). Imidazole is from Alfa Aesar (Ward Hill, MA). The Tris-HCl, EDTA, LB agar, and LB broth are from Fischer Scientific (Fair Lawn, NJ). NaCl is from Calbiochem (LaJolla, CA). The Nunc C8 White MaxiSorp 96-well plates are from Thermo Scientific (Waltham, MA).The HEPES is from BDH (West Chester PA). The native coelenterazine and IPTG are from Gold Biotechnology (St. Louis, MO). Coelenterazine v is from Nanolight (Pinetop, AZ). The sodium dodecyl sulfate (SDS) is from Curtin Matheson Scientific Inc. (Houston, TX). The HEPES is from BDH (West Chester, PA). NaOH is from Mallinckrodt Chemicals (Phillipsburg, NJ). The BugBuster, acetic acid and glycerol is from EMD Millipore (Darmstadt, Germany). The T7 Express Competent *E. coli* (High Efficiency) are from New England Biolabs (Boston, MA). BD Cytofix/Cytoperm Plus is from BD Biosciences (Franklin Lakes, NJ). The Alexa555 NHS ester and 5 mL 7,000 MWCO Zeba Columns are from Life Technologies (Waltham, MA). Cells were analyzed on a FACSCalibur flow cytometer (BDIS, CA).

5.2.2 Apparatus

Cells were grown in a Thermo-Fisher Scientific orbital shaker incubator at what degree and how long, and to what optical density. Cell cultures were harvested using a Beckman J2-MI centrifuge. Ni-NTA Agarose beads are from Qiagen (Venlo, Netherlands). Amicron Ultra-15 Centrifugal Filter Units are from EMD (Billerica, MA). Purity of the protein was confirmed by sodium dodecyl sulfate-polyacrylamide gel electrophoresis (SDS-PAGE) using a BioRad Mini-cell apparatus from Invitrogen and

staining with Coomassie Brilliant Blue. Aequorin activity was measured using an Optocomp I luminometer (MGM Biomedical Hamden, CT). The emission spectra of the aequorins were determined using a custom made SpectroScan instrument (ScienceWares, Falmouth, MA), which is capable of obtaining spectra from flash reactions of luminescent samples that emit in the 400-700 nm range. Half-life scans were taken using a Polarstar 96 well microplate reading luminometer (BMG Labtech, Ortenberg, Germany). Circular Dichroism measurements were taken using a Jasco J-810 Spectropolarimeter (Easton, MD).

5.2.3 Gene Sequences of DARPins and DARPin-Aequorin Fusion Proteins

The fusion proteins were designed to include a SGGGGS linker sequence (underlined) and contain a RGS His6x Tag (bold) built in two the N-Cap. The sequence of all constructs was confirmed by sequencing using the service of the sequencing core at the University of Miami Miller School of Medicine Hussman Institute for Human Genomics (HIHG).

VEGFADARPin

ATG**CGTGGCAGCCATCATCACCACCATCAT**GGCAGCGATCTGGGCAAAAA
ACTGCTGGAAGCTGCGCGTGCGGGCCAGGATGACGAAGTGCGTATTCTGATG
GCGAATGGAGCGGACGTCAACGCGACCGCGGATAGCACCGGATGGACCCCA
TTACATTTAGCGGTGCCGTGGGGCCATCTGGAAATTGTAGAAGTGCTGCTGA
AATATGGCGCCGATGTTAATGCGAAAGATTTTCAGGGCTGGACGCCTCTGCA
CCTGGCCGCAGCTATTGGCCACCAGGAGATCGTGGAGGTGTTGCTTAAAAAC

GGCGCAGATGTAAATGCGCAGGATAAATTCGGCAAAACCGCGTTTGATATTA
GCATTGATAATGGCAATGAAGATCTGGCGGAAATTTTGCAGAAACTGAATTA
G

VEGFADARPin-Aequorin

ATG**CGTGGCAGCCATCATCACCACCATCAT**GGCAGCGATCTGGGCAAAAA
ACTGCTGGAAGCTGCGCGTGCGGGCCAGGATGACGAAGTGCGTATTCTGATG
GCGAATGGAGCGGACGTCAACGCGACCGCGGATAGCACCGGATGGACCCCA
TTACATTTAGCGGTGCCGTGGGGCCATCTGGAAATTGTAGAAGTGCTGCTGA
AATATGGCGCCGATGTTAATGCGAAAGATTTTCAGGGCTGGACGCCTCTGCA
CCTGGCCGCAGCTATTGGCCACCAGGAGATCGTGGAGGTGTTGCTTAAAAAC
GGCGCAGATGTAAATGCGCAGGATAAATTCGGCAAAACCGCGTTTGATATTA
GCATTGATAATGGCAATGAAGATCTGGCGGAAATTTTGCAGAAACTGAATTC
AGGTGGAGGAGGTTCAGTGAAACTGACCAGCGACTTCGACAACCCAAGATG
GATTGGACGACACAAGCATATGTTCAATTTCCTTGATGTCAACCACAATGGA
AAAATCTCTCTTGACGAGATGGTCTACAAGGCATCTGATATTGTCATCAATAA
CCTTGGAGCAACACCTGAGCAAGCCAAACGACACAAAGATGCTGTAGAAGC
CTTCTTCGGAGGAGCTGGAATGAAATATGGTGTGGAAACTGATTGGCCTGCA
TATATTGAAGGATGGAAAAAATTGGCTACTGATGAATTGGAGAAATACGCCA
AAAACGAACCAACGCTCATCCGTATATGGGGTGATGCTTTGTTTGATATCGTT
GACAAAGATCAAAATGGAGCCATTACACTGGATGAATGGAAAGCATACACC
AAAGCTGCTGGTATCATCCAATCATCAGAAGATTCCGAGGAAACATTCAGAG
TGTCCGATATCGATGAAAGTGGACAACTCGATGTTGATGAGATGACAAGACA

ACATTTAGGATTTTGGTACACCATGGATCCTGCTTCCGAAAAGCTCTACGGTG
GAGCTGTCCCCTAA

HER2DARPin-Aequorin

ATGATTCAGGGCCGC**CGCGGCAGCCATCATCATCATCATCAT**GGCAGCGAT
CTGGGCAAAAAACTGCTGGAAGCGGCGCGCGCGGGCCAGGATGATGAAGTG
CGCATTCTGATGGCGAACGGCGCGGATGTGAACGCGAAAGATGAATATGGCC
TGACCCCGCTGTATCTGGCGGCGGCGCATGGCCATCTGGAAATTGTGGAAGT
GCTGCTGAAAAACGGCGCGGATGTGAACGCGAACGATACCCGCGGCATTACC
CCGCTGCATCTGGTGGCGTATAGCGGCCATCTGGAAATTGTGGAAGTGCTGC
TGAAACATGGCGCGGATGTGAACGCGCAGGATAAATTTGGCAAAACCGCGTT
TGATATTAGCATTGATAACGGCAACGAAGATCTGGCGGAAATTCTGCAGAAA
CTGTCAGGTGGAGGAGGTTCAGTGAAACTGACCAGCGACTTCGACAACCCAA
GATGGATTGGACGACACAAGCATATGTTCAATTTCCTTGATGTCAACCACAAT
GGAAAAATCTCTCTTGACGAGATGGTCTACAAGGCATCTGATATTGTCATCA
ATAACCTTGGAGCAACACCTGAGCAAGCCAAACGACACAAAGATGCTGTAG
AAGCCTTCTTCGGAGGAGCTGGAATGAAATATGGTGTGGAAACTGATTGGCC
TGCATATATTGAAGGATGGAAAAAATTGGCTACTGATGAATTGGAGAAATAC
GCCAAAAACGAACCAACGCTCATCCGTATATGGGGTGATGCTTTGTTTGATAT
CGTTGACAAAGATCAAAATGGAGCCATTACACTGGATGAATGGAAAGCATAC
ACCAAAGCTGCTGGTATCATCCAATCATCAGAAGATTCCGAGGAAACATTCA
GAGTGTCCGATATCGATGAAAGTGGACAACTCGATGTTGATGAGATGACAAG

ACAACATTTAGGATTTTGGTACACCATGGATCCTGCTTCCGAAAAGCTCTACG
GTGGAGCTGTCCCCTAA

5.2.4 Expression and Isolation of Aequorin, VEGFADARPin, and VEGFADARPin-Aequorin and HER2DARPin-Aequorin Fusions

The cells were grown in 4 mL of Terrific broth (TB) containing ampicillin (100 µg /mL) for the pR-B01 and pR-B02 vectors overnight at 30 ^{o}C at 250 rpm, and containing kanamycin (35 µg/mL) for the pET30Xa/LIC vector containing the gene for the cysteine-free aequorin overnight at 37 ^{o}C at 250 rpm. The overnight cultures were used to inoculate 500 mL of TB broth containing the appropriate antibiotics and the cultures were grown at 30 ^{o}C if expressing a fusion or 37 ^{o}C as started if only the DARPin at 250 rpm. After growing to an OD_{600} between 0.4-0.6, the culture was induced with 1 mM IPTG and left to grow overnight.

The culture was centrifuged at 15,300 xg for 20 min and the pellet was lysed for 20 min in Bug Buster with Lysonase. The lysed pellet was centrifuged again and the supernatant added to 1 mL of suspended Ni-NTA agarose beads and rotated on a Mini Labroller (Labnet, Woodridge, NJ) at room temperature. The protein was eluted off the column using a PBS Buffer with 20 mM imidazole at pH=8.0. The protein was then dialyzed with Slide-A-Lyzer Dialysis Cassette MWCO 3,500 into 30 mM Tris-HCl, 2 mM EDTA, pH=7.5 for luminescence activity tests, into HEPES Buffered Saline-NaCl (HBS-N), 0.01 M HEPES, 0.15 M NaCl, for affinity studies using BiaCore and *in vivo* studies.

5.2.5 Determination of the Bioluminescence Activity of VEGFADARPin-Aequorin

Aequorin-DARPin was diluted with 30 mM Tris-HCl, pH 7.5, containing 2 mM EDTA, to $1x10^{-7}$ M to ensure the amount of light produced was within the linear range of the luminometer. VEGFADARPin-Aequorin activity was triggered by injecting 100 µL of 100 mM Tris-HCl, pH 7.5, containing 100 mM $CaCl_2$. Bioluminescence intensity was measured at 0.1 s intervals for up to 6 s in triplicate.

5.2.6 Emission Spectra of VEGFADARPin-Aequorin

A 1 x 10^{-6} M sample of VEGFADARPin-Aequorin was charged by incubating overnight at 4 °C with 2 x 10^{-6} M native coelenterazine. The charged aequorin was pipetted into a 96-well microtiter plate, and 100 µL of 100 mM Tris-HCl, pH 7.5, containing 100 mM $CaCl_2$, were injected and the emission spectra was collected for 10 seconds from 400-700 nm in 1.5 nm increments. The experiments was performed in triplicate and the mean calculated.

5.2.7 Dose Response Curves and Cross-Reactivity of DARPin-Aequorin Fusion Proteins

The wells of a MaxiSorp coated plates Thermo Scientific (Waltham, MA) were coated with 150 µL of a 10 nM dilution of human recombinant VEGFA in 50 mM Tris-HCl, 150 mM NaCl, at pH=7.4, incubated by shaking at 250 rpm overnight at 4 °C, and washed three times with 300 uL of 10 mM, Na_2HPO_4, 150 mM, 0.05% Tween at pH=7.4. The VEGFADARPin-Aequorin were conjugated at a concentration of 10 nM in 50 mM Tris-HCl, 150 mM NaCl, at pH=7.4 with 2 mM EDTA was charged overnight with

coelenterazine. A blocking buffer consisting of 50 mM Tris-HCl, 150 mM NaCl, and 0.5% BSA at pH=7.4 was added to a final volume of 300 uL and incubated for 1 hour at room temperature. The competing human and mouse VEGFA and human VEGFC were serially diluted in 50 mM Tris-HCl, 150 mM NaCl, at pH=7.4 with 20 mM EDTA over a range of 10 nM to 0.1 pM. A volume of 75 uL of 10 nM the aequorin-DARPin conjugate was added to 75 uL of each serial dilution and incubated at 4 ºC two hours. Each dilution was then added to a well of the VEGFA coated plate to a final volume of 150 uL and incubated for 20 min at room temperature. A well with aequorin without a DARPin was included as a blank. The plates were then washed 3 times with buffer. A 100 uL volume of triggering buffer was added immediately before bioluminescence emission and data was collected with a Polarstar Luminometer (BMG Labtech, Ortenberg, Germany). The light was collected over 7 seconds and the mean of the triplicate measurements plotted.

5.2.8 Determination of VEGFADARPin-Aequorin Binding to Bound VEGFA Human

The wells of a MaxiSorp coated plates Thermo Scientific (Waltham, MA) were coated sequentially with 150 □L of $5x10^{-9}$ M to $5x10^{-15}$ M dilution of human recombinant VEGFA in 50 mM Tris-HCl, 150 mM NaCl, at pH=7.4, incubated by shaking at 250 rpm overnight at 4 ºC, and washed three times with 300 uL of 10 mM, Na_2HPO_4, 150 mM, 0.05% Tween at pH=7.4. The VEGFADARPin-Aequorin were conjugated at a concentration of 10 nM in 50 mM Tris- HCl, 150 mM NaCl, at pH=7.4 with 2 mM EDTA was charged overnight with coelenterazine. A blocking buffer consisting of 50 mM Tris-HCl, 150 mM NaCl, and 0.5% BSA at pH=7.4 was added to a

final volume of 300 uL and incubated for 1 hour at room temperature. The human VEGFA was diluted in 50 mM Tris-HCl, 150 mM NaCl, at pH=7.4 with 20 mM EDTA to 10 nM. A volume of 75 uL of each serial dilution of the DARPin-Aequorin conjugate was added to 75 uL of 10 nM VEGFA and incubated at 4 ^{o}C two hours. Each dilution was then added to a well of the VEGFA coated plate to a final volume of 150 uL and incubated for 20 min at room temperature. A well with aequorin without a DARPin was included as a blank. The plates were then washed 3 times with buffer. A 100 uL volume of triggering buffer was added immediately before bioluminescence emission and data was collected with a Polarstar Luminometer (BMG Labtech, Ortenberg, Germany). The light was collected over 7 seconds and the mean of the triplicate measurements plotted.

5.2.9 Conjugation of Alexa555 NHS Ester to Aequorin, VEGFADARPin, VEGFADARPin-Aequorin, and HER2DARPin-Aequorin

Alexa555 was dissolved in anhydrous DMSO to a final concentration of 10 nM. All three protein samples were suspended in 50 mM PBS Buffer, pH=7.5 at a concentration of 10 mM. The samples were reacted at a 1:30 ratio by volume (15 µL of Alexa555 to 9.7 nM, 500 µL of protein to 290 µM) at room temperature overnight. The samples were purified using Zeba columns (5 mL, 7,000 MWCO). The degree of ligation (DOL) was calculated using the following equations:

$$\text{Protein M} = \frac{[A_{280} - (A_{555} \times C_{280})]}{\varepsilon \text{ Protein}}$$

$$C_{280} = \frac{\varepsilon_{280}}{\varepsilon_{555}}$$

$$DOL = \frac{A_{555}}{\text{Ɛ Alexa}_{555} \times \text{Protein M}}$$

5.2.10 HeLa Cells Preparation and Flow Cytometry

HeLa cells were harvested and aliquots of 800,000 per Eppendorf tube were washed in 50 mM PBS, pH=7.5 twice and spun at 900 xg for 1 min. Cells were suspended in 250 µL of Fixation/Permeabilization solution for 20 min at 4 ^{o}C. Cells were washed twice with 1 mL of 1x BD Perm/Wash. The cells were spun down and resuspended in 50 µL of BD Perm/Wash buffer only, or 0.2 µg of Alexa555 labeled aequorin, VEGFADARPin, or VEGFADARPin-Aequorin, and incubated for 30 min at 4 ^{o}C, protected from light. Cells were washed twice with 1 mL 1x BD Perm/Wash and resuspended in 100 µL of 50 mM PBS Buffer, pH=7.5. Cells were analyzed on a FACSCalibur flow cytometer (BDIS, CA), and 20,000 ungated events were acquired, and analyzed using CellQuestPro software.

5.2.11 Half-life Determination of Aequorin and VEGFADARPin-Aequorin and HER2DARPin-Aequorin Fusion Proteins

A 1 x 10^{-6} M sample of each aequorin was charged overnight with 1 x 10^{-6} M of the native coelenterazine used during the collection of emission spectra. A Polarstar 96 well microplate luminometer (BMG Labtech, Ortenberg, Germany) was utilized for the half-life measurements. The bioluminescence signal of a 100 µL sample was collected for 35 s, in triplicate following the injection of 100 µL of triggering buffer (100 mM Tris-HCl, pH 7.5, containing 100 mM $CaCl_2$). The mean bioluminescence decay spectra was fit with an exponential decay equation using GraphPad Prism 5.0 (GraphPad Software,

San Diego, CA), and an equation for first order decay kinetics was used to calculate the bioluminescence half-life of each aequorin-coelenterazine pair.

5.2.12 *In Vivo* Imaging

The aequorin and VEGFADARPin-Aequorin were dissolved in a HEPES Buffer (10 mM HEPES, 0.15 M NaCl, 5 mM $MgCl_2$, 1.8 mM $CaCl_2$, at pH=7.4) at concentration from 0.14 mg/mL and 0.21 mg/mL respectively. C57BL outbred female mouse 6-8 weeks old purchased from Taconic (Germantown, NY) were anesthetized with a 0.1 mL ketamine/xylazine injection 90-100 mg/ +5-10 mg/kg of mouse via intraperitoneal (IP) injection and the eyes were dilated with one drop of Phenylephrine Hydrochloride Ophthalmic Solution (company, concentration). The Nidek GYC-1000 laser (Gamagori, Aichi, Japan) was set to 100 mW and the duration of the shot was 0.10 miliseconds to create 4 lesions for testing aequorin and VEGFADARPin-Aequorin binding. One mouse was not subjected to the laser treatment as a control. The aequorin samples were injected into one right eye and the VEGFADARPin-Aequorin samples into the left via intrastromal injection in volumes to add a total of 5 μg of each protein. Native coelenterazine was diluted in PBS Buffer to a volume of 2.3×10^{-4} M and dropped onto the surface of each eye in 1 μL volumes via pipetter. The same conditions were to create 3 lesions and 5 lesions in the right eye of the mice to test for a greater bioluminescence signal from VEGFADARPin-Aequorin binding in the presence of greater amounts of laser induced VEGFA overexpression. After 2 hours, the mice were then placed in a Caliper/Xenogen IVIS® SPECTRUM (Caliper, Hopkinton, MA) imaging system in the IVIS Small Animal Imaging Facility at the Oncogenomics Core Facility, Miller School of

Medicine, University of Miami with oxygen flowing. Images were taken over 30 s to 60 s. All animal experiments were conducted based on protocols approved by Institutional Animal Care and Use Committee of the University of Miami.

5.3 Results and Discussion

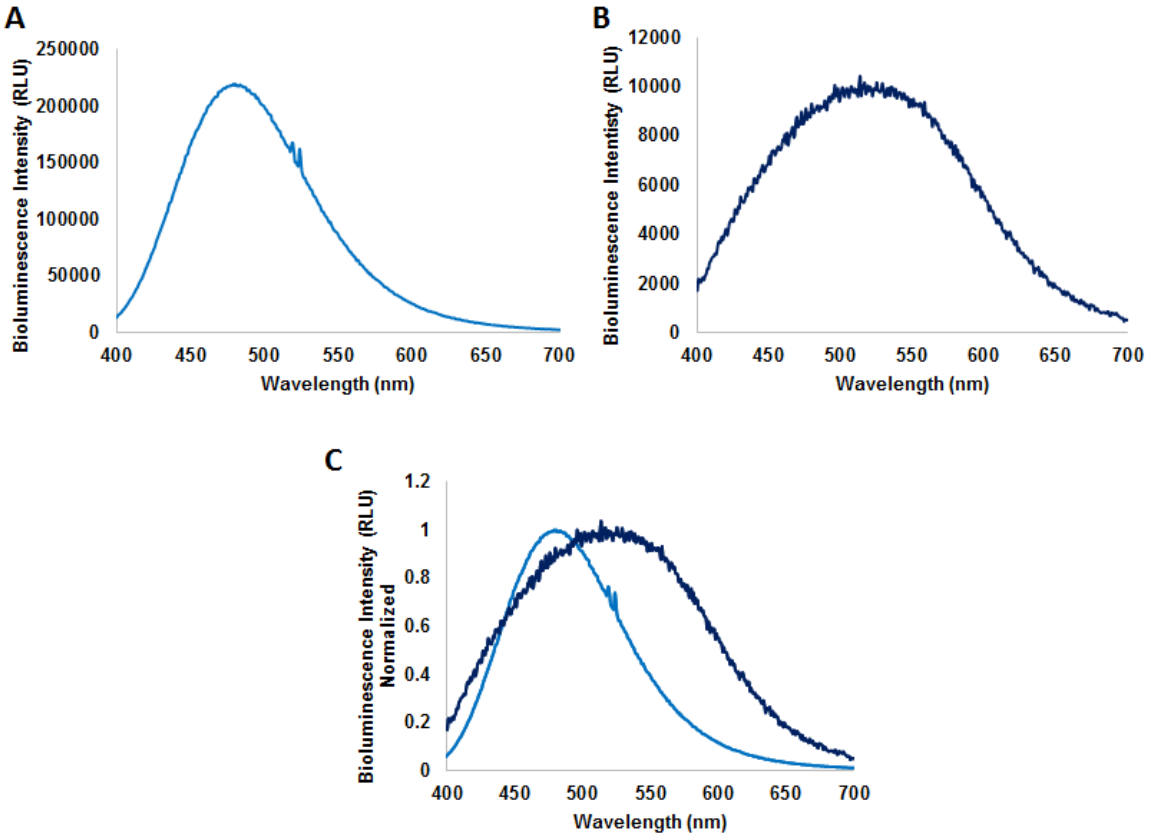

Figure 5.3. Bioluminescence spectra of the aequorin genetically fused to the VEGFADARPin-Aequorin fusion protein. (A) Bioluminescence spectra of VEGFADARPin-Aequorin with native coelenterazine. (B) Bioluminescence spectra of VEGFADARPin-Aequorin with coelenterazine *v*. (C) Normalized bioluminescence spectra of VEGFADARPin-Aequorin with native coelenterazine and coelenterazine *v*.

Herein, bioluminescent based *in vivo* imaging system for the expression of VEGFA in the retina has been developed. We designed a fusion protein combining the DARPin targeting VEGFA, which has been evaluated for efficacy and safety in human trials for AMD, and the bioluminescent photoprotein aequorin, for visualizing VEGFA *in vivo*. A

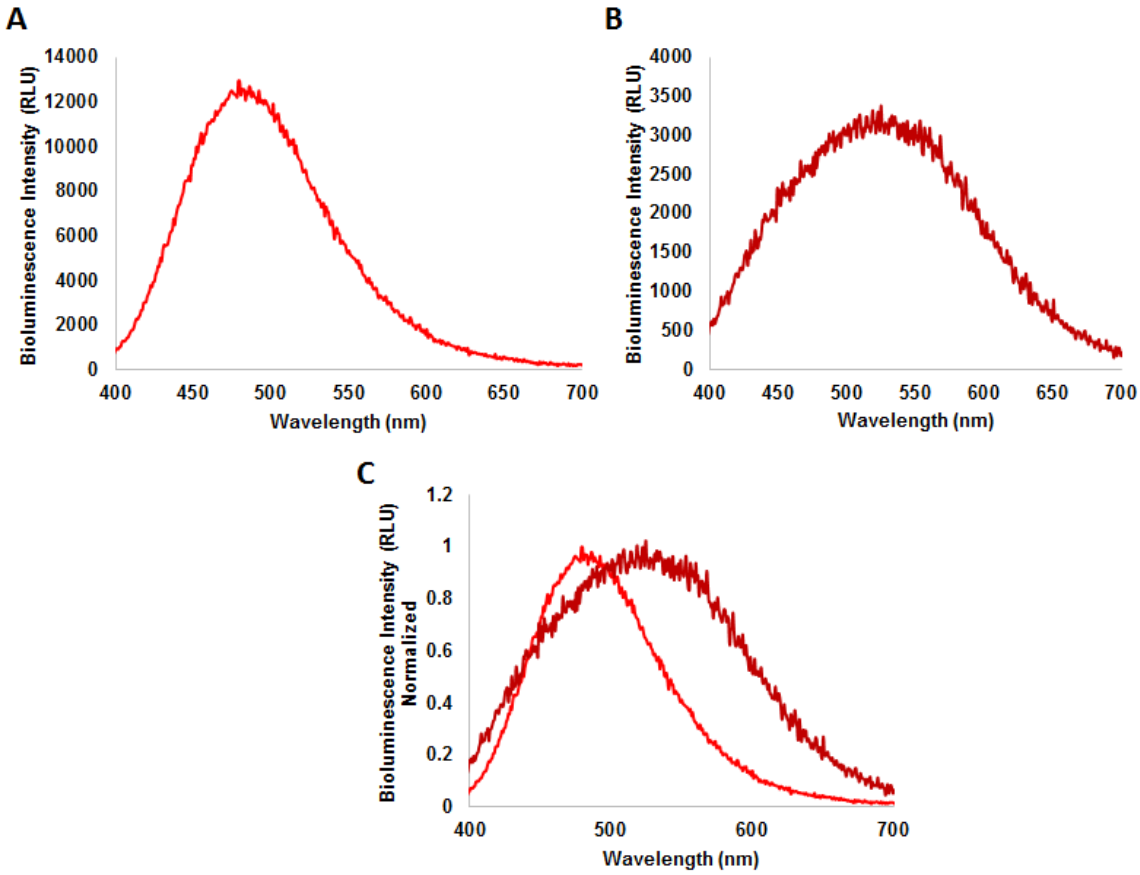

Figure 5.4. Bioluminescence spectra of the aequorin genetically fused to the HER2DARPin-Aequorin fusion proteins. (A) Bioluminescence spectra of HER2DARPin-Aequorin with native coelenterazine. (B) Bioluminescence spectra of HER2DARPin-Aequorin with coelenterazine *v*. (C) Normalized bioluminescence spectra of HER2DARPin-Aequorin with native coelenterazine and coelenterazine *v*.

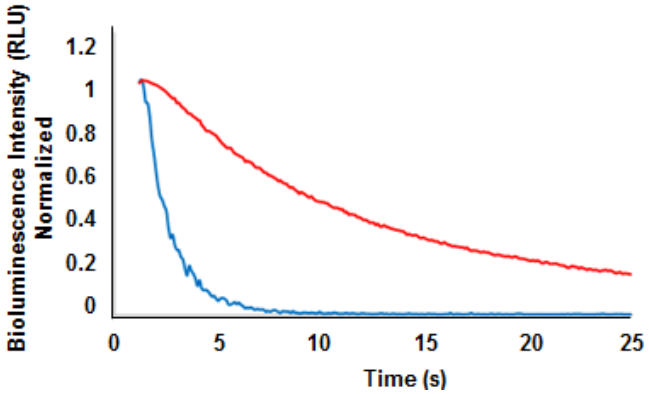

Figure 5.5. Normalized bioluminescent half-life of VEGFADARPin-Aequorin fusion proteins with two different coelenterazines. VEGFADARPin-Aequorin with native coelenterazine (*blue*) and VEGFADARPin-Aequorin with coelenterazine *v* (*red*).

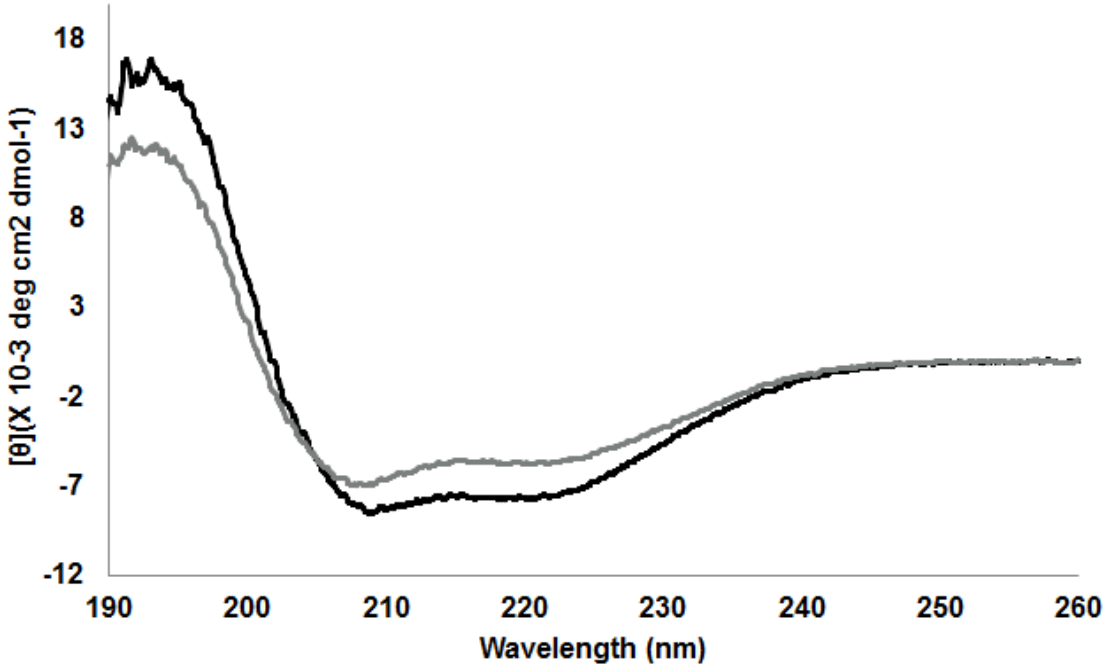

Figure 5.6. Far-UV CD absorbance of VEGFADARPin-Aequorin. The VEGFADARPin-Aequorin is in (*black*) and the DARPin in (*grey*). Three accumulations were averaged for each sample at RT. The response for each blank was subtracted from the response for the corresponding sample, and the resulting spectra are shown.

laser induced wet MD model in mice creating photocoagulation in the retina was used to induce the overexpression of the VEGFA peptide. The bioluminescence generated by the VEGFADARPin-Aequorin was successfully imaged in IVIS. The DARPin and soluble cysteine-free DARPin-Aequorin fusion protein was expressed in T7 Express *E. coli* and yielded a purified concentration of approximately 2 mg/L, much lower than the DARPin alone. Expression tests revealed growing the DARPin at a 37 ^{o}C and IPTG 1 mM caused the DARPin portion to fold improperly and the fusion protein to be found in the insoluble fraction. A lower temperature of 30 ^{o}C and 0.1 mM IPTG was used to express VEGFADARPin-Aequorin and HER2DARPin-Aequorin that were soluble. The both DARPin-Aequorin fusion proteins maintain high levels of bioluminescent activity with

native coelenterazine with a calculated specific activity of 9.15 x 10^{18} RLU/mole compared to native aequorin[48a]. Both fusion proteins were determined to have a peak emission wavelength slightly red-shifted from the wild-type wavelength at 480 nm versus 469 nm and a slightly lengthened bioluminescent half-life at approximately 1 s versus 0.5 s, respectively (Figure 5.3, Figure 5.4, Figure 5.5). Coelenterazine *v* is found to have the same red-shift in the fusion as it does in other luciferases at approximately 530 nm (Figure 5.3B, Figure 5.4B)[14, 110], a 40 nm shift versus the native coelenterazine (Figure 5.3C, Figure 5.4C) and a half-life of around 8 s with the previously reported drop in specific activity to 3.2 x 10^{16} RLU/mole, and 7.4 x 10^{14} RLU/mole for VEGFADARPin-Aequorin and HER2DARPin-Aequorin, respectively. This is the first data regarding coelenterazine *v* with DARPin-Aequorin fusion proteins. CD data taken of the DARPin and VEGFADARPin-Aequorin shows peaks at 208 and 220, indicating the alpha-helix structures of both (Figure 5.6).

The specificity of the VEGFADARPin-Aequorin was confirmed by adding the fusion protein to competitive binding assays against VEGFA from mouse and VEGFC human. The VEGFADARPin-Aequorin showed a lesser affinity for these VEGFs, particularly the VEGFC, but maintained its cross-reactivity with the VEGFA of mice (Figure 5.7A). The DARPin targeting HER2 was selected to compare the binding of a second DARPin-Aequorin fusion to the VEGFA peptide target. The HER2DARPin-Aequorin also displayed a high amount of bioluminescent activity (1.3 x 10^{18} RLU/mole) in solution and was found to not bind the VEGFA peptide in the same completion assay. This suggests the loss of bioluminescence is due to the lack of binding of HER2DARPin-Aequorin to human VEGFA and not lack of signal from aequorin. The binding curve of

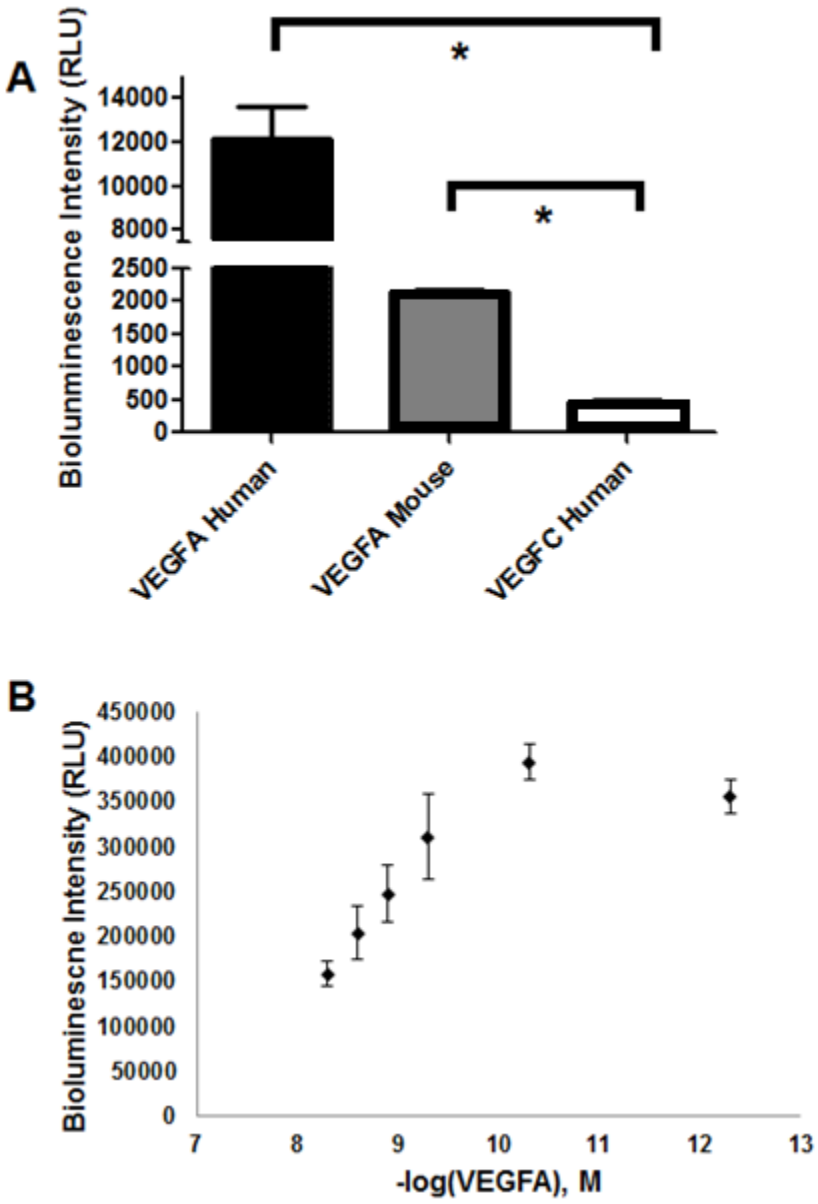

Figure 5.7. The binding of VEGFADARPin-Aequorin against different members of the VEGF family. (A) Binding of VEGFADARPin-Aequorin against VEGFA human, VEGFA mouse, and VEGFC human at 10 nM VEGF family member and 2 pM VEGFADARPin-Aequorin. (B) Bioluminescent competitive binding of VEGFADARPin-Aequorin against VEGFA at a range of concentrations.

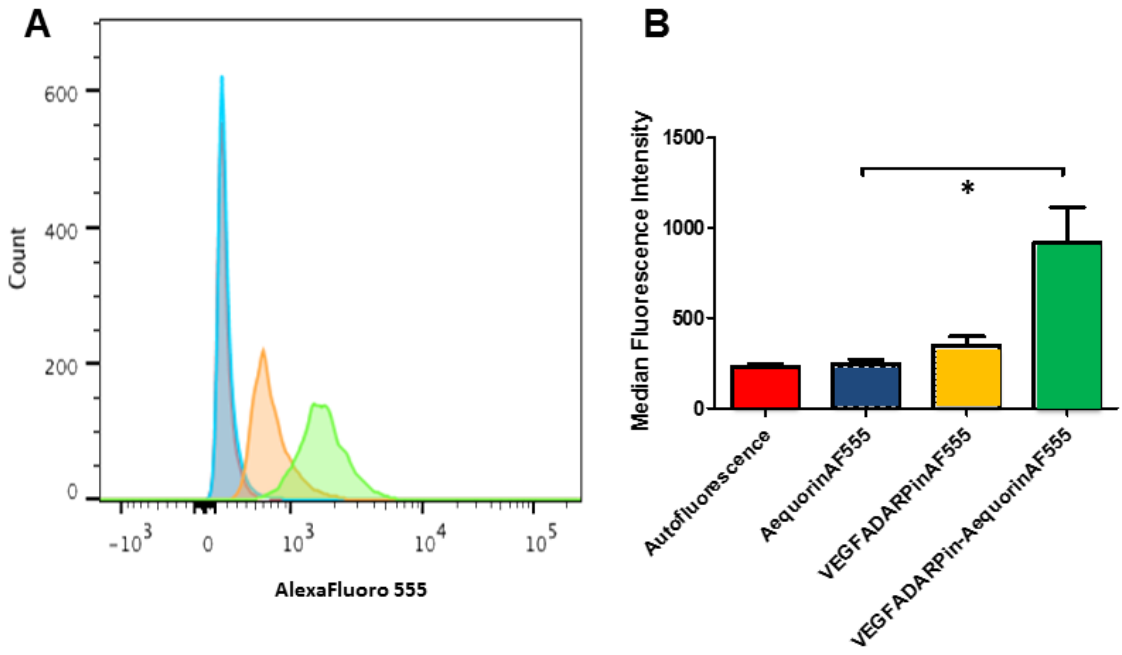

Figure 5.8. Flow cytometry of AlexaFluoro555 conjugated targets in HeLa cells. (A) Flow cytometry data of VEGFADARPin-Aequorin in HeLa cells. *Red* Hela cells only, autofluorescence; *Blue* AequorinAF555, negative control; *Orange* VEGFADARPin555, positive control; *Green* VEGFADARPin-Aequorin555, sample. The red aequorinAF555 autofluorescence signal is partially hidden by the blue negative control signal. (B) Average and standard deviation of fluorescence maximum of flow cytometry data. HeLa cells are used for the autofluorescenct signal, aequorin555 as the negative control, VEGFADARPinAF555as the postive control, and VEGFADARPin-AequorinAF555 as the sample.

Table 5.1. Analysis of the Median Fluorescent Intensity (MFI) of each data set using statistics and robust statistics.

Estimate	Auto-fluorescence	AequorinAF555	VEGFADARPin AF555	VEGFADARPin -AequorinAF555
Median	220	238	299	837
Mean MFI	232.3	244.7	348.3	916.3
Std Dev	25.8	44.4	85.4	343.0

the VEGFADARPin-Aequorin to the VEGAF human was confirmed by a competitive binding assay using microtiter plate wells coated with 10 nM VEGFA the according to

the plate manufactures, revealing a binding curve with the bioluminescence inversely proportional to the amount of VEGFA added (Figure 5.7B). The binding affinity was in the lower nanomolar range at 1.78 nM. Flow cytometry was used to verify the binding of the VEGFADARPin-Aequorin intracellularly using chemically conjugated AlexaFluoro555 as the fluorescent molecule (Figure 5.8). Absorption data was used to calculate the concentration of the protein and the degree of ligation (DOL) prior to cell fixation and permeabilization. The AlexaFluoro555 fluorophore conjugated VEGFADARPin was used as a positive control based on previous intracellular fluorescent studies[76a]. The HER2DARPin-Aequorin with AlexaFluoro555 was initially selected as the negative control, but replaced due to low level HER2 expression in HeLa cells giving a false positive signal.

Figure 5.8 show all three flow cytometry data acquisitions using Hela cells and purified aequorinAF555 (DOL = 0.04), VEGFADARPinAF555 (DOL = 0.08), and VEGFADARPin-AequorinAF555 (DOL=0.13) added so that the concentration of Alexa555in each sample was at 0.2 μg/mL. All three experiments show intracellular binding of the VEGFADARPin-AequorinAF555 such that the signal is greater than that of the positive control. This could be attributed the greater DOL causing the fluorophore to be conjugated to the VEGFADARPin such that binding is inhibited, resulting in protein loss during the wash step. A statistical analysis of the data shows the small difference between the counts from the autofluorescence signal from the HeLa cells alone and the aequorinAF555 negative control and the larger signals from the VEGFADARPinAF555 positive control and VEGFADARPin-AequorinAF555 sample. The activity of the aequorin mutants *in vivo* was confirmed by the injection of aequorin

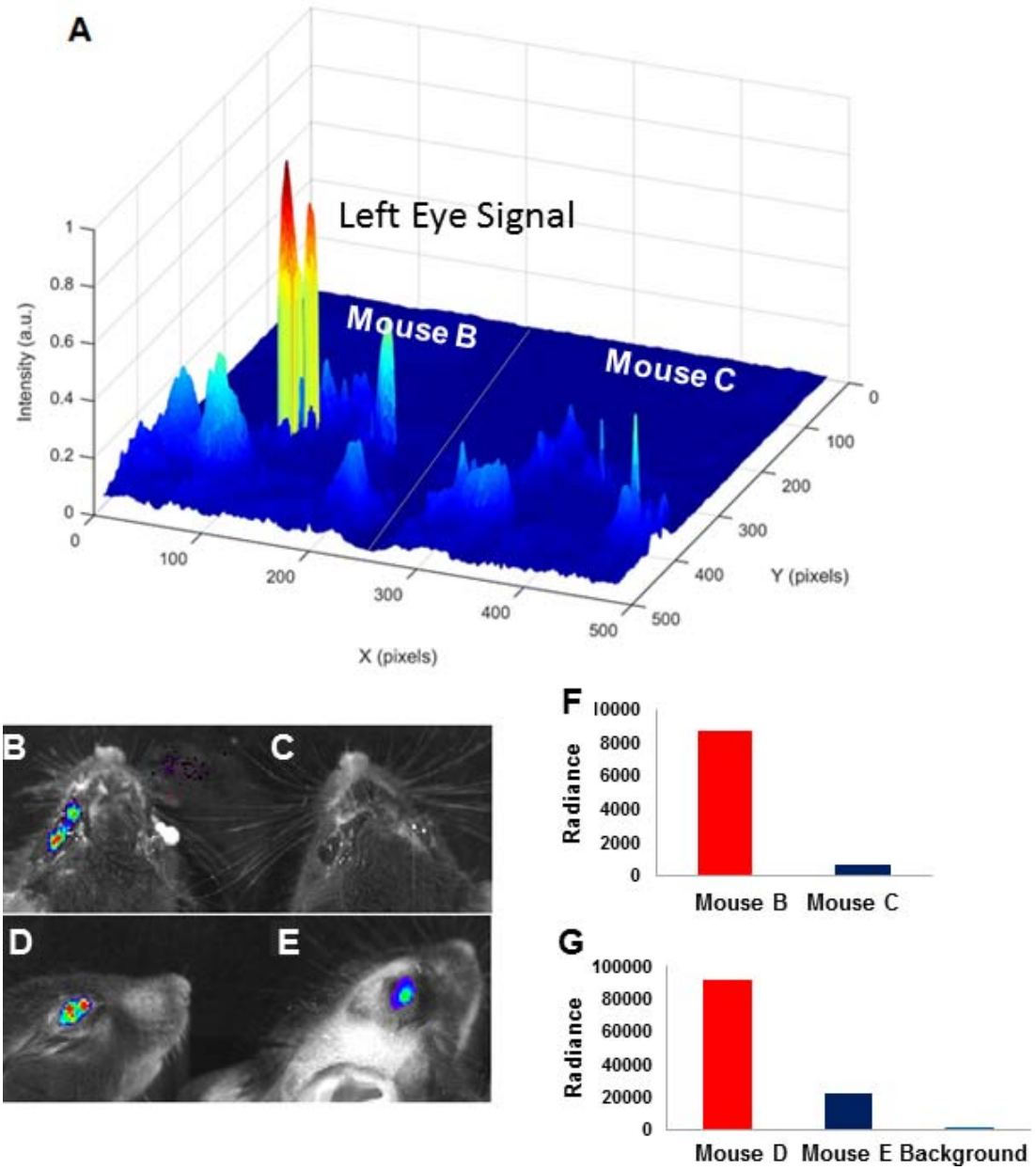

Figure 5.9 Bioluminescence scans of VEGFADARPin-Aequorin and aequorin in IVIS following photocoagulation and the addition of VEGFADARPin-Aequorin or cysteine-free aequorin. (A) Three dimensional image of the mouse B and mouse C. (B) Three laser induced lesions in both eyes. *Left eye* VEGFADARPin-Aequorin. *Right eye* Cysteine-free aequorin. (C) Control mouse with same, no laser. (D) Bioluminescence of VEGFADARPin-Aequorin with 5 laser induced lesions in the eye. (E) Bioluminescence of VEGFADARPin-Aequorin with three laser induced lesions in the eye. Data is in radiance (p/sec/cm^2/sr). (F) Comparison of the radiance counts for left eye of mouse B and mouse C. (G) Comparison of the radiance counts in the right eye of mouse D and mouse E. Background signal is invisible (Background Avg: 500±111, n=3).

into the eyes of anesthetized mice following injury by the laser that were imaged using IVIS. The same was done for a control mouse with no laser-induced lesion induction or injury. Figure 5.9A and B shows the cysteine-free aequorin and VEGFADARPin-Aequorin at the same concentration injected intrastromally. Native coelenterazine was added to the surface of the eye dropwise and the bioluminescence emission was then recorded immediately. External addition of calcium ions was not necessary since the cells and tissues of the eye already contain an abundance of calcium ions. The mice were imaged two hours after injection to allow for unbound aequorin to clear the eye. The images taken in IVIS show that VEGFADARPin-Aequorin binds to the VEGFA in the laser induced wet MD model but not in the eye without the laser induced lesion (Figure 5.9E). Figure 5.9D and E shows two mice with different numbers of laser lesions in the eye. Both mice displayed bioluminescence in the injured eye, with a higher signal in the eye with a larger number of lesions. With further optimization the difference in signal could be measured by taking advantage of the consistent photon counts of aequorin to give quantified values of VEGFA. It should also be noted that the binding of the VEGFADARPin-Aequorin to VEGFA mouse was significantly less than the VEGFA human. Should the VEGFADARPin-Aequorin be moved into human subjects, it can be expected that the binding will be even higher, leading to a better signal. The application of VEGFADARPin-Aequorin in imaging VEGFA in non-optically transparent tissue, such as deep-tissue tumors, would be better facilitated using red-shifted coelenterazine, such as coelenterazine *v*, or non-natural aequorin mutants displaying red-shifts.

5.4 Conclusion

In conclusion, imaging is a critical part of diagnosing and monitoring the treatment of age-related macular degeneration, yet current imaging systems use fluorescent dyes and external excitation sources to monitor changes in blood flow and do not target VEGFA which triggers angiogenesis. An imaging technique that targets the VEGFA directly would provide a means of visualizing the protein that leads to vision loss. This could be especially valuable in measuring the effects of the pharmaceuticals that target VEGFA by imaging the protein directly and not effects like vascular leakage. By using the photoprotein aequorin, a reporter that is dependent on the addition of coelenterazine when used *in vivo* provides control over the timing of the signal, as well as avoiding the background associated with the inherent fluorescence in biological samples by removing a need for an excitation source. The DARPin MP0112 selected for this study because it was shown to be an effective VEGFA targeting molecule in mouse models and in human trials for wet MD. A VEGFADARPin-Aequorin fusion protein was shown to specifically bind VEGFA *in vitro* and *in vivo*. This is the first time a bioluminescent based system has been used to image the presence of VEGFA *in vivo* using a DARPin as the targeting molecule.

CHAPTER 6. A BIOLUMINESCENT SEROTONIN DETECTION ASSAY USING THE PHOTOPROTEIN AEQUORIN AS THE BIOLUMINESCENT REPORTER MOLECULE

6.1 Overview

Bioluminescent proteins have been utilized in a variety of approaches to the detection and quantification of target molecules in biological samples. Bioluminescent proteins have many characteristics that make them preferable to other types of signal source. Bioluminescent proteins are non-radioactive, non-toxic, and therefore safe for use in humans with no requirements for special handling or disposal. Unlike fluorescent reporters, bioluminescent molecules do not require an outside excitation source to generate a luminescent signal, lowering background signal, raising detection limits, and preventing unwanted effects like photobleaching or damage to light sensitive tissues. Photoproteins are a class of bioluminescent proteins that have the additional benefit of not exhibiting the typical luciferin-luciferase kinetics of other bioluminescence proteins, displaying a signal proportional to the amount of protein present.

Aequorin is a photoprotein that incorporates the luciferin coelenterazine into a hydrophobic pocket made by four EF-hands consisting of the helix-turn-helix motifs commonly found in calcium binding proteins[9d, 12b, 95]. When calcium binds to aequorin in the presence of an oxygen molecule, the EF-hands change conformation, resulting in a half-second flash of light in the blue wavelength range (469 nm). Aequorin has already been utilized as the reporter molecule *in vitro* and *in vivo* [15], particularly when the target of interest is calcium ions[3, 24, 42a]. Furthermore, aequorin can have its emission

characteristics tuned to create a catalog of mutants to allow for the detection of multiple analytes simultaneously.

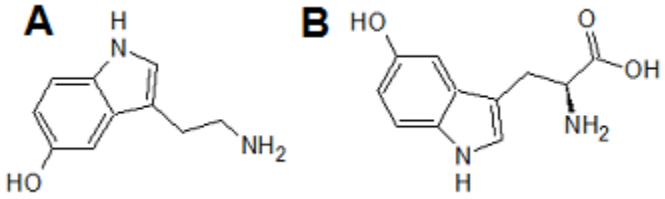

Figure 6.1. The chemical structures of (A) serotonin and its precursor molecule, (B) tryptophan.

Serotonin (5-Hydroxytryptamine) is a monoamine neurotransmitter and neuromodulator synthesized from the essential amino acid tryptophan by the enzyme tryptophan hydroxylase (Figure 6.1). The greatest concentration of serotonin is found in gastrointestinal tract where it is synthesized by enterochromaffin cells, with most serotonin moved to storage in the blood platelets[96].

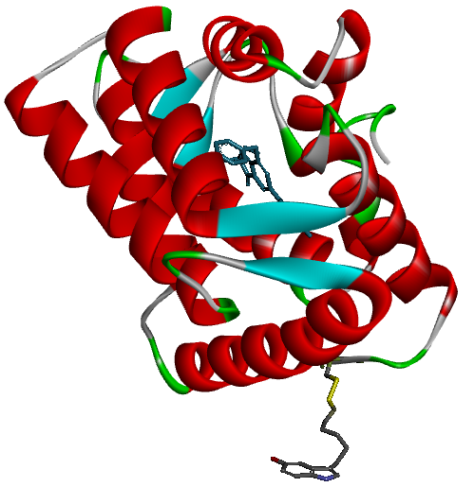

Figure 6.2. Aequorin with a serotonin molecule connected by a Sulfo-LC-SPDP linker.

The remaining serotonin is found with the brain[97]. Serotonin is linked to a wide variety of processes in the body, including muscle contraction, irritable bowel syndrome

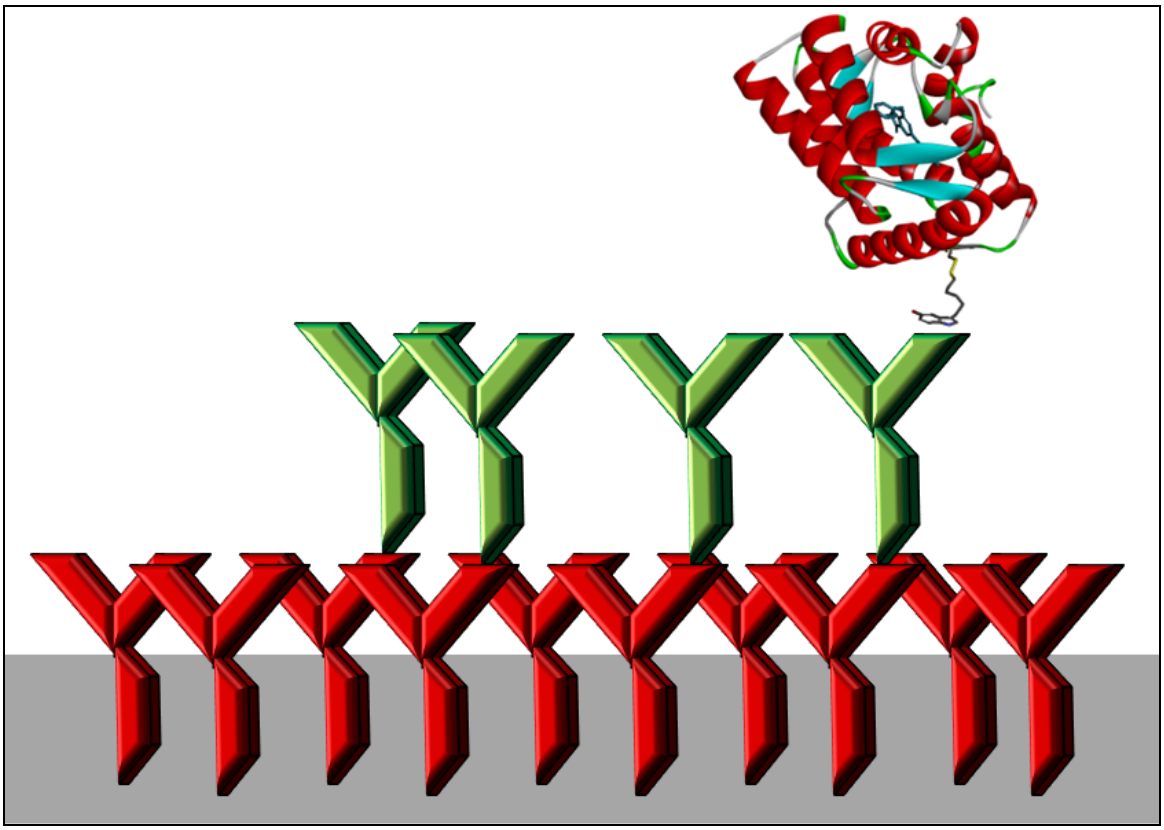

Figure 6.3. A schematic of the competitive bioluminescent serotonin assay. Primary antibodies, rabbit anti-aequorin, are in green and secondary antibodies, goat anti-rabbit, are in red. The primary antibodies detect the serotonin linked to aequorin, providing an inverse bioluminescent signal to the amount of serotonin in the sample.

(IBS), irritable bowel disease (IBD), liver regeneration, endocrine regulation, sleep regulation, depression, obsessive-compulsive disorder, anxiety disorders, eating disorders, infantile autism, and psychosis[98]. The link between serotonin and biological processes has made the determination of the serotonin concentration important part of research and diagnostics for over 50 years. Previous work in our laboratory used two different semi-synthetic aequorin for the detection of 6-keto-prostaglandin-FI-r and angiotensin II, two important cardiovascular molecules[47b]. Based on this, aequorin was linked to the antibodies by two chemical methods, Sulfo-SPDP-LC linkers that covalently bond to the aequorin at a cysteine inserted at position 5, and by cysteine-free aequorin

using BS3 (Sulfo-DSS) linkers (Figure 6.2)[99].To further increase the applications of mutant aequorin and make them usable for further multiplexing, serotonin was selected as a target analyte with the ultimate goal of expanding the assay to include other small molecules related to serotonin, such as dopamine and tryptophan, reducing investments in time and costs during analysis. Herein, the bioluminescent competitive serotonin assay is described (Figure 6.3).

6.2 Materials and Methods

6.2.1 Materials

The pET30Xa/LIC kit, acetic acid, and glycerol are from EMD Millipore (Darmstadt, Germany). The Terrific Broth (TB) is from Invitrogen (Carlsbad, CA). The Q5 Site-Directed Mutagenesis Kit was from New England Biolabs (Boston, MA). The Xa Factor Cleavage Capture Kit is from Novagen (Madison, WI). Agarose, arabinose, sodium phosphate, serotonin HCl, $MgSO_4$, $CaCl_2$, IPTG, glycine, ninhydrin, methanol, powdered milk, and all antibiotics are from Sigma-Aldrich (St. Louis, MO). Sodium phosphate is from Amresco (Solon, OH). Imidazole is from Alfa Aesar (Ward Hill, MA). The $MgCl_2$, Tris-HCl, EDTA, and LB agar, are from Fischer Scientific (Fair Lawn, NJ). NaCl is from Calbiochem (LaJolla, CA). The coelenterazine is from Gold Biotechnology (St. Louis, MO). The sodium dodecyl sulfate (SDS) is from Curtin Matheson Scientific Inc. (Houston, TX). The neutravidin, Pierce NeutrAvidin Coated and Protein G Coated 96-Well Plates, BS3, Sulfo-LC-SPDP are from Thermo Scientific (Waltham, MA). NaOH is from Mallinckrodt Chemicals (Phillipsburg, NJ). Polyclonal goat anti-rabbit

biotin (IgG H&L), rabbit anti-aequorin, and mouse anti-serotonin are from Abcam (Cambridge, England).

6.2.2 Apparatus

Cells were grown in a Thermo-Fisher Scientific orbital shaker incubator. Cell cultures were harvested using a Beckman J2-MI centrifuge. Ni-NTA Agarose beads are from Qiagen (Venlo, Netherlands). Purity of the protein was confirmed by sodium dodecyl sulfate-polyacrylamide gel electrophoresis (SDS-PAGE) using a Novex Mini-cell apparatus from Invitrogen and staining with Coomassie Brilliant Blue. Zeba Spin Desalting Columns 7k MWCO and Slide-A-Lyzer Dialysis Cassette 3,500 MWCO 0.5-3 mL are from Thermo Scientific (Waltham, MA) Western Blots were run using a Mini Trans-Blot cell from BioRad (Hercules, CA). TLC Plates are from Sigma –Aldrich (St. Louis, MO). Aequorin activity was measured using an Optocomp I luminometer (MGM Biomedical Hamden, CT). The emission spectra of the aequorins were determined using a custom made SpectroScan instrument (ScienceWares, Falmouth, MA), which is capable of obtaining spectra from flash reactions of luminescent samples that emit in the 400-700 nm range. Bioluminescence measurements were taken using a Polarstar 96 well microplate reading luminometer (BMG Labtech, Ortenberg, Germany).

6.2.3 Expression and Isolation of Aequorin

The cells were grown in 25 mL of Terrific broth (TB) containing ampicillin (100 μg/mL) for the OmpA containing pIN4 vector with the gene for cysteine-free aequorin and kanamycin (35 μg/mL) for the pET30Xa/LIC vector containing the gene for the

aequorin with a cysteine inserted a position 5 overnight at 37 ^{o}C at 250 rpm while being shielded from light. The overnight cultures were used to inoculate 500 mL of TB broth containing the appropriate antibiotics and the cultures were grown at 37 ^{o}C at 250 rpm. After growing to an OD_{600} between 0.4-0.6. The culture was induced with 1 mM arabinose or IPTG and left to grow overnight.

The culture was centrifuged at 15,300 xg for 20 min. Cysteine-free aequorin was harvested from the supernatant by acid precipitation and then resuspended in Tris Buffer. The pellet of aequorin with a cysteine at position 5 as boiled for 20 min in Native Purification Buffer (50 mM NaH_2PO_4, 0.5 M NaCl, 1 mM Imidazole, pH = 8.0). The lysed pellet was centrifuged again and the supernatant added to 1 mL of suspended Ni-NTA agarose beads and rotated on a Mini Labroller (Labnet, Woodridge, NJ) at room temperature for 2 hours. The protein was eluted off the column using a PBS Buffer with 40 mM imidazole at pH=8.0 and digested with Xa factor according to manufacturer's instructions until all the protein was cleaved. The Xa factor was removed with Xa factor Agarose capture beads. The aequorin was then transferred to PBS buffer for crosslinking using Zeba Desalting Spin Columns.

6.2.4 Determination of Activity of Aequorin

Aequorin was diluted with 30 mM Tris-HCl, pH 7.5, containing 2 mM EDTA, to $1x10^{-7}$ M to ensure the amount of light produced was within the linear range of the instrument. Aequorin activity was triggered by injecting 100 µL of 100 mM Tris-HCl, pH 7.5, containing 100 mM $CaCl_2$. Bioluminescence intensity was measured at 0.1 s intervals for up to 6 s.

6.2.5 Emission Spectra of Aequorin

A 1 x 10^{-6} M sample of aequorin was charged by incubating overnight at 4 °C with 2 x 10^{-6} M of native coelenterazine. The charged aequorin was pipetted into a 96-well microtiter plate and following injection of 100 µL of 100 mM Tris-HCl, pH 7.5, containing 100 mM $CaCl_2$, the emission spectra was collected for 10 seconds from 400-700 nm in 1.5 nm increments.

6.2.6 Half-life Determination of Aequorin

A 1 x 10^{-6} M sample of aequorin was charged overnight by incubating overnight at 4 °C with 1x10^{-4} M of the coelenterazine analog used during the collection of emission spectra. A Polarstar 96 well microplate luminometer (BMG Labtech, Ortenberg, Germany) was utilized for the half-life measurements. The bioluminescence signal of a 50 µL sample was collected for 30s, following the injection of 100 µL of triggering buffer (100 mM Tris-HCl, pH 7.5, containing 100 mM $CaCl_2$). The mean bioluminescence decay spectra was fit with an exponential decay equation using GraphPad Prism 5.0 (GraphPad Software, San Diego, CA), and an equation for first order decay kinetics was used to calculate the bioluminescence half-life of the aequorin.

6.2.7 Crosslinking Aequorin to Serotonin

Aequorin with a cysteine at position 5 was crosslinked to serotonin following the protocols provided by the manufacturers. The crosslinkers and serotonin were reacted at ratio of 1:1.1, with the concentration of serotonin at 0.5 mM in PBS Buffer. The aequorin and conjugated linker and serotonin were reacted at a ratio of 1:3, with the conjugated

linker and serotonin at a final concentration of 5 x 10^{-3} mM in PBS Buffer. Crosslinking was confirmed via ninhydrin reaction run on a thin layer chromatography plate and Dot Blot. The product was then purified by Slide-A-Lyzer Dialysis Cassette MWCO 3,500, then placed in 1 L of 30 mM Tris-HCl, 2 mM EDTA, pH=7.5 for 2 hours. The buffer was then replaced to a total of 8 L.

6.2.8 Calibration Plot of Serotonin-Aequorin Constructs

The biotin conjugated goat anti-rabbit antibody was diluted in 25 mM Tris, 150 mM NaCl, 0.1% BSA at pH=7.2 to a concentration of 10 μg/mL. One hundred μL of the biotinylated antibody was added to each well of the neutravidin coated plates. The plates were shaken at 250 rpm for 1 hour at room temperature. The wells were then washed 3 times with 200 μL of 25 mM Tris, 150 mM NaCl, 0.1% BSA at pH=7.2 buffer. A rabbit anti-serotonin antibody was diluted in 25 mM Tris, 150 mM NaCl, 0.1% BSA at pH=7.2 to a concentration of 5 μg/mL. One hundred μL of the antibody was added to each well and shaken at 250 rpm for 1 hour at room temperature then washed with 200 uL of 25 mM Tris, 150 mM NaCl, 0.1% BSA at pH=7 with 2 mM EDTA. Serotonin-aequorin conjugate charge overnight with native coelenterazine and then serially diluted over a range of (1 x 10^{-8} M)-(1 x 10^{-5} M) in 25 mM Tris, 150 mM NaCl, 0.1% BSA at pH=7 with 2 mM EDTA. A volume of 100 μL was added to each well and shaken at 250 rpm for 1 hour at room temperature. The plates were then washed 3 times with 25 mM Tris, 150 mM NaCl, 0.1% BSA at pH=7.2 with 2 mM EDTA. A 100 uL volume of triggering buffer (100 mM $CaCl_2$) was added immediately before bioluminescence emission data was collected with a Polarstar Luminometer. The light was collected over 7 seconds and

the mean of the triplicate measurements plotted. For Protein G coated plates, the same procedure was followed but without the addition of the primary antibody.

6.2.9 Checkerboard Titration Optimization of Primary and Secondary Antibodies

The biotin conjugated goat anti-rabbit antibody was serially diluted by halves in 25 mM Tris, 150 mM NaCl, 0.1% BSA at pH=7.2 at a concentration of 2 µg/mL, 1 µg/mL, 0.5 µg/mL, and 0.25 ug/mL. Fifty uL of each of the biotinylated antibody dilutions was added to each well of the neutravidin coated plates lengthwise following the rows. The plates were shaken at 250 rpm for 1 hour at room temperature. The wells were then washed 3 times with 200 µL of 25 mM Tris, 150 mM NaCl, 0.1% BSA at pH=7. A rabbit anti-serotonin antibody was serially diluted by halves in buffer starting with a concentration of 1 µg/mL. Fifty µL of each of the antibody dilutions was added to each well downwards following the columns and shaken at 250 rpm for 1 hour at room temperature then washed with 200 µL of 25 mM Tris, 150 mM NaCl, 0.1% BSA at pH=7 with 2 mM EDTA. Serotonin-aequorin conjugate charged overnight with native coelenterazine was added at concentration of 1 x 10^{-5} M in 25 mM Tris, 150 mM NaCl, 0.1% BSA at pH=7 with 2 mM EDTA. A volume of 100 µL was added to each well and shaken at 250 rpm for 1 hour at room temperature. The plates were then washed 3 times with 25 mM Tris, 150 mM NaCl, 0.1% BSA at pH=7 with 2 mM EDTA. A 100 µL volume of triggering buffer was added immediately before bioluminescence emission data was collected with a Polarstar Luminometer. The light was collected over 3 seconds and measurements plotted.

6.2.10 Dose Response Curves of Serotonin-Aequorin Constructs

The wells of a neutravidin coated plates were coated with 100 µL of a 10 µg/mL dilution of the biotinylated goat anti-rabbit antibody in 25 mM Tris, 150 mM NaCl, 0.1% BSA at pH=7.2 then incubated by shaking at 250 rpm for 1 hour at room temperature then washed three times with 200 µL of 25 mM Tris, 150 mM NaCl, 0.1% BSA at pH=7.2. A rabbit anti-serotonin antibody was serially diluted in 25 mM Tris, 150 mM NaCl, 0.1% BSA at pH=7 with 2 mM EDTA to a concentration of 5 µg/mL. One hundred µL of each of the serial antibody dilution was added to each well then washed with 150 mM NaCl, 0.1% BSA at pH=7 with 2 mM EDTA. Serotonin-aequorin conjugate at concentration of 1 x 10^{-5} M in 25 mM Tris, 150 mM NaCl, 0.1% BSA at pH=7 with 2 mM EDTA was charged overnight with coelenterazine. Serial dilutions were made of serotonin over and range of (1 x 10^{-4} M) - (1 x 10^{-13} M). A volume of 50 µL of the serotonin-aequorin conjugate was added to the well with a dilution of the serotonin and shaken at 250 rpm for 1 hour at room temperature. A well without any serotonin but with the serotonin-aequorin conjugate was included as a blank. The plates were then washed 3 times with buffer. A 100 uL volume of triggering buffer was added immediately before bioluminescence emission data was collected with a Polarstar Luminometer. The light was collected over 7 seconds and the mean of the triplicate measurements plotted.

6.3 Results and Discussion

Bioluminescent proteins are a non-radioactive, non-toxic, option for use in the detection and quantification of biological molecules. Bioluminescent molecules do not require an outside excitation source, increasing signal sensitivity by lowering background

signal and protecting light-sensitive molecules and tissues from irradiation damage. Bioluminescent photoproteins do not exhibiting the typical substrate-enzyme kinetics of other bioluminescence protein, providing a one to one signal ratio between the amount of photoprotein and the luminescent signal. Aequorin is a photoprotein that has been utilized as the reporter molecule *in vitro* and *in vivo* in a variety of diagnostic and imaging applications. Aequorin can also be modified through genetic engineering and the incorporation of coelenterazine analogs generate aequorin with a range of emissions characteristics, allowing it to be tailored to a specific application to use it to discriminate multiple bioluminescent signals in a single sample simultaneously.

Figure 6.4. TLC plates with a ninhydrin reaction confirming the presence of serotonin and the conjugation of the serotonin and linkers. The Sulfo-LC-SPDP linker shows superior linking compared to the BS3. Lane 1 Serotonin, Lane 2 BS3-serotonin, Lane 3 Sulfo-LC-SPDP linker, Lane 4 Sulfo-LC-SPDP-serotonin.

Serotonin (5-Hydroxytryptamine) is a neurotransmitter and neuromodulator synthesized in the body from the essential amino acid tryptophan. Serotonin is linked to a large number of physiological functions including muscle contraction and wound healing and the determination of the presence and levels of serotonin yields valuable information in the study, diagnosis, and treatment of conditions from sleep disorders to autism. Our

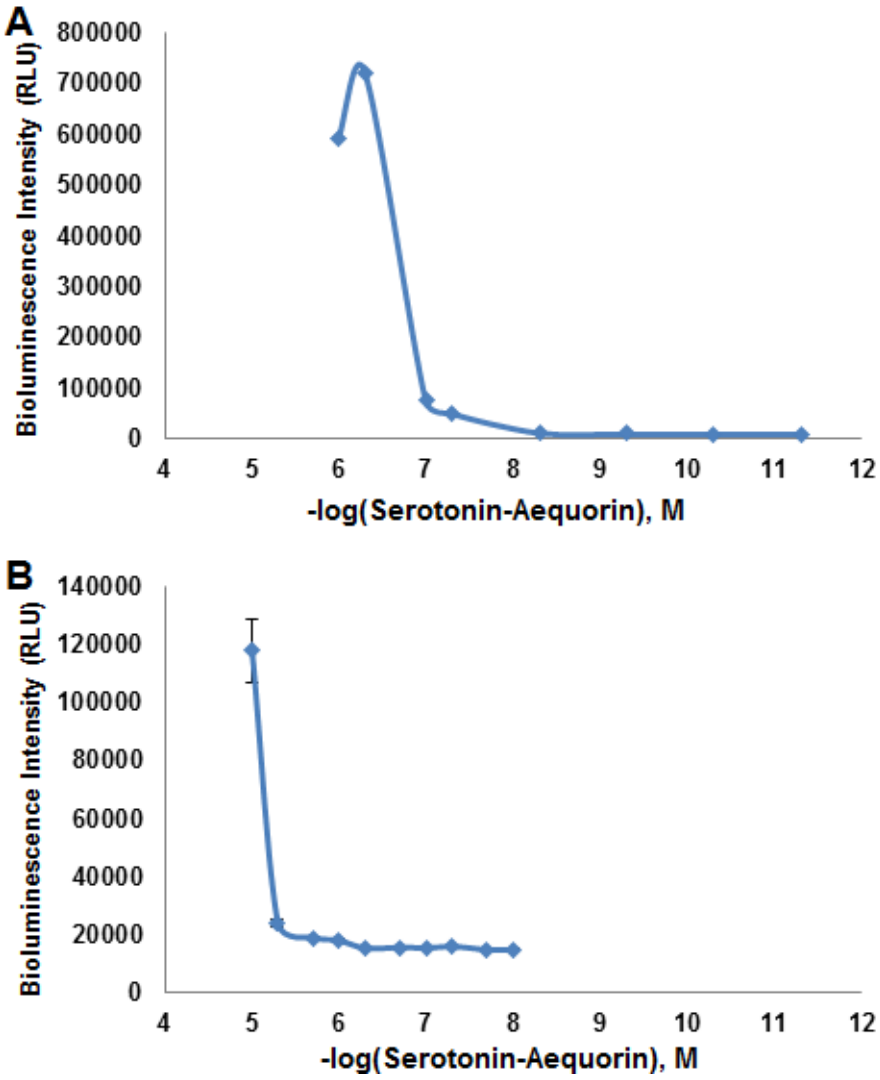

Figure 6.5. The dilution curve for aequorin-serotonin. (A) Dilution curve using a neutravidin plate. Error bars are too small to be visible. (B) Dilution curve using a Protein G plate.

lab has developed a bioluminescent assay to simultaneously measure compounds such as 6-keto-prostaglandin-FI-r and angiotensin II[100].

The detection of serotonin using aequorin as part of a competitive bioluminescent assay provides low detection limits and sensitivity with the ability to expand the assay to detect multiple analytes simultaneously. Aequorin was linked via BS3 and Sulfo-SPDP-

LC to serotonin to determine the preferable linking method. The Sulfo-SPDP-LC crosslinking with aequorin containing a unique cysteine at position 5 was found to have greater reproducibility and confirmed via the appearance of color blue via Dot Blot (not shown) and TLC (Figure 6.4).

The aequorin-serotonin conjugate maintained its activity and has a specific activity of 9.15 x 10^{16} RLU/mole. A biotinylated anti-serotonin antibody from goat against rabbit IgG was immobilized on a neutravidin coated plate then incubated with a rabbit anti-serotonin primary antibody. The serotonin-aequorin conjugate was incubated with free serotonin before addition to the plate to create a competitive binding assay. Therefore, the amount of bioluminescence is inversely proportional to the amount of serotonin added, providing information on the presence and amount of serotonin present.

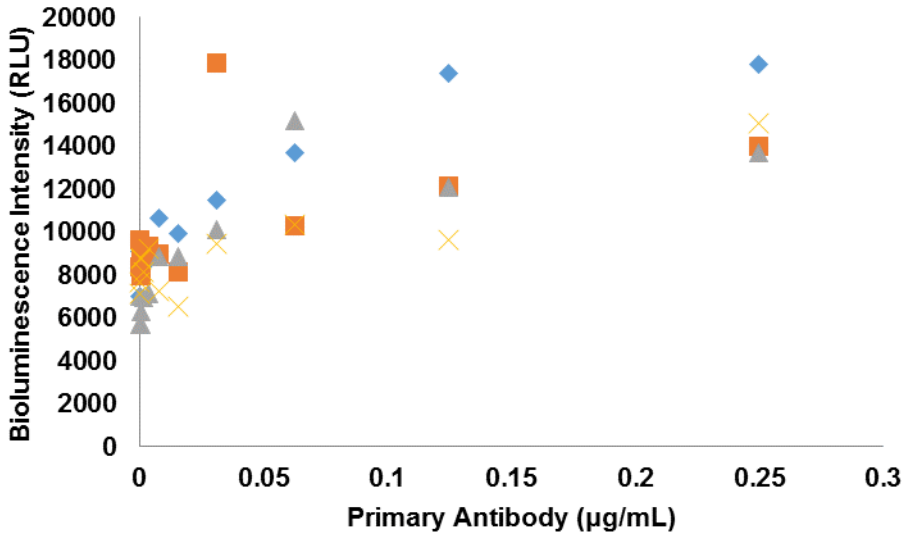

Figure 6.6. Results of the checkerboard titration of the primary and secondary antibodies. Secondary antibody in total to each well: *Blue diamonds* 1 µg/mL, *Orange squares* 0.5 µg/mL, *Grey triangles* 0.25 µg/mL, *Yellow Xs* 0.125 µg/mL.

Two different plates were selected to test the binding to test the binding of the conjugate, a neutravidin plate and a Protein G plate. The Protein G plate was found to have lower binding capacity then the neutravidin plate. A calibration study was performed using the neutravidin plate to optimize the amount of aequorin-serotonin conjugate added, specifically 1 x 10^{-7} M was the minimal concentration for maximum signal (Figure 6.5).

A checkerboard-titration was performed to determine the proper amount of each antibody. From this it was determined that the concentrations were 10 µg/mL of the secondary antibody and 5 µg/mL of the primary antibody at a volume of 100 µL each (Figure 6.6).

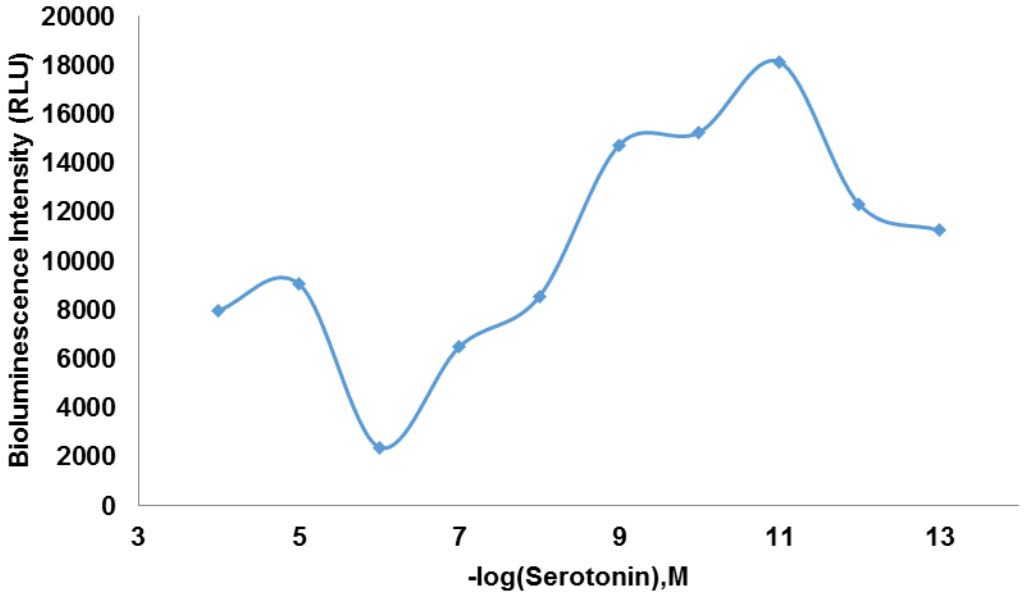

Figure 6.7. The dose response curve of serotonin using competitive binding.

The dose response curve obtained for the assay shoes that the bioluminescence signal from the aequorin-serotonin conjugate was dependent on the concentration of free serotonin and inversely proportional to this concentration (Figure 6.7). In addition, the serotonin assay developed demonstrated a detection limit of 0.017 nM, or 1.76 pg/μL of serotonin. This is within the range of lower detection limits of commercially available detection kits.

6.4 Conclusions

In conclusion, a competitive assay for the detection of serotonin using an aequorin-serotonin was developed on a 96-well plate. The detection limit was found to be as low as 1.76 pg/μL and the tunability of aequorin will allow for the number of target molecules to be increased to expand the number of analytes detected in a single sample to create a multiplexing assay. Serotonin is an important neurotransmitter that's presence and level in a sample provide valuable information in research and diagnostic settings. The sensitivity and low detection limit of an aequorin based reporter combined with the flexibility of multiplexing provides means of further combining several test into one combined multiples assays, reducing testing time and cost.

CHAPTER 7. CONCLUSIONS AND FUTURE PERSPECTIVES

Protein engineering takes advantage of the molecular machinery found in nature to create designer proteins with characteristics tailored to specific applications. Gene sequence of proteins found in nature are recreated in the laboratory and engineered for a wide range of applications. Luminescent proteins in particular make excellent reporters in biosensors, especially bioluminescent photoproteins.

Bioluminescent photoproteins do not require outside excitation, have a signal proportional to the amount of charged protein present, and can have the triggering of their signal controlled by not adding the luciferin substrate and Ca^{2+} until a signal is desired. Among bioluminescent proteins, the photoprotein aequorin is among the most well-characterized. Aequorin is 189 amino acid long, globular, contains four helix-turn-helix EF-hands characteristic of calcium-binding proteins, and can be subjected to protein engineering including deletions, insertions, and substitutions. The introduction of non-natural amino acids, such that variety of peak wavelength emissions, half-lives, and specific activities can be generated[12c]. Aequorin can also be genetically and chemically linked to other molecules and it is non-toxic in mammalian cells[111]. Aequorin is therefore a desirable reporter molecule and has been utilized in *in vitro* assays, human cells, and whole animals. While antibodies are the most common targeting molecules and have been frequently applied with aequorin, antibodies have several drawbacks such as, leading to the development of alternative targeting molecules, most notable the robust, easily expressed, DARPins.

Chapters Two and Three describe the development of aequorin variants with a variety of peak emission wavelengths and bioluminescent half-lives to create a catalog of aequorins for multiplexing and *in vivo* imaging. Using an sophisticated genetic amber suppression system, the non-natural amino acids were incorporated at a single position (replacing Trp86) or concurrently at positions two positions (Tyr82 and Trp86), using four different non-natural amino acids (L-4-aminophenylalanine, L-4-bromophenylalanine, L-iodophenylalanine, and L-4-methoxyphenylalanine) with both types of substitutions confirmed by mass spectrometry. Four different non-natural amino acids were incorporated into aequorin in a site-specific manner and charged with native coelenterazine and eight different coelenterazine analogs to create active mutants with emission wavelengths red-shifted as far as 56 nm from the wild-type and half-lives extended from 0.5 s to up to 60 s. A fifth non-natural amino was incorporated at position 86, but rendered the aequorin non-functional. Two of these aequorin, dual substituted L-4-methoxyphenylalanine and L-4-iodophenylalanine, chosen for their red-shift and long half-life respectively, were injected into the eyes of mice to prove their activity *in vivo*. This is the first reported instance of aequorin with non-natural amino acids being active *in vivo*.

Future work related to the work described in these two chapters should look to expand the catalog further by incorporating more non-natural amino acids as they become available to further push the emission towards the red for use *in vivo*. The ability to the engineered tRNA/tRNA-synthetase combination to incorporate non-natural amino acids

by Amber Suppression is only limited by the initiative to develop them. In particular, the effect iodine molecules and methoxy groups on the red-shift and half-life suggest more amino acids with these types of substitutions may push the peak emission wavelengths even further. Additionally, in the here described experiments only native coelenterazine was used *in vivo*. The coelenterazine analogs have different traits that affect their use *in vivo* including membrane permeability and influence on the calcium binding sensitivity. Further tailoring of each mutant to a given application would benefit from analysis of the effect of the coelenterazine analogs on bioluminescent signal generation and fusing red-shifted aequorin to the DARPins.

Chapter Four describes the development of an aequorin capable of orthogonal linking in biological samples utilizing "click" chemistry. Modifying molecules is often the first step in analyzing samples, with the modification generating molecules that are susceptible for capturing, isolation and measuring amounts and activity. Often these analytes are found in in biological samples where crosslinking reactions that utilize side groups found in nature would result in non-specific binding and undesirable reaction side products. Click chemistry provides an orthogonal crosslinking in the form of cycloaddition between an alkyne and an azide. The reactive groups do not occur naturally in nature and therefore do not generate unwanted reactions giving non-specific labeling even complex sample, making click chemistry an appealing option for labeling biological molecules. Using a tRNA/tRNA-synthetase combination and Amber Suppression, an L-4-azidophenylalanine was site-specifically incorporated into position 5 of aequorin and clicked to three different alkynylated molecules: a Dansyl-alkyne, AlexaFluoro488 alkyne, and Biotin-PEG4-alkyne. The aequorin and biotin linker were then bound to

neutravidin, demonstrating the potential of aequorin click reactions as the beginning step in creating larger molecules for purification, labeling, detection or the nanoassembly of designer engineered multi-functional macromolecules. The aequorin and fluorophores maintained their activity following conjugation, and attempts to use the light produced by aequorin for BRET were successful.

Future work involving the "click" aequorin would continue to apply click chemistry to create larger, multifunctional molecules, such as by clicking aequorin to a DARPin, or clicking a cytotoxic molecule to a VEGFADARPin-Aequorin genetic fusion. The specificity of click chemistry has led to a large number of linkers, fluorophores, and metabolites for applications in fields ranging from materials science to drug development. Any of these approaches would take advantage of the ease of attaching "click" aequorin for use as a reporter molecule, or simply as a calcium sensor, to a platform, as part of protein-protein interaction studies, BRET, or as part of a larger drug delivery system. The cysteine-free aequorin could also be engineered to include other non-natural amino acids using site-specific methods that target sequence other than TAG to synthesize aequorin with different bioluminescent characteristics for use in click conjugations.

Chapter Five covers the development of an *in vivo* bioluminescent VEGFA imaging system utilizing the MP0112 DARPin targeting VEGFA and cysteine-free aequorin. Cysteine-free aequorin and the VEGFADARPin were fused genetically with a short SGGGGS linker and a His6x Tag. The fusion maintained both its bioluminescent and specific targeting capabilities *in vitro* and *in vivo*. A wet MD model was generated in mice using a laser to create four lesions in the retina. The VEGFADARPin-Aequorin was

injected into one eye and non-conjugated aequorin into the other. After two hours, the bioluminescent signal was only in the eye with the VEGFADARPin, indicating the presence of VEGFA.

Future work with respect to Chapter Five should include testing the half-life of the VEGFADARPin-Aequorin *in vivo*. Current work would suggest the DARPin stays in the eye for days. Another area of possible improvement is optimizing the amount of fusion protein added and the optimal time-line of the procedure, as determined by the amount of time required for unbound protein to clear the eye. Since the amount of signal is directly proportional to the amount of coelenterazine charged aequorin, determining the amount of time required to collect all possible bioluminescence could be used to quantify the amount of VEGFA present to account for the amount of time required for the diffusion of coelenterazine through the tissues of the eye.

Chapter Six describes the development of a competitive bioluminescence based aequorin assay for the detection and quantification of serotonin. An otherwise cysteine-free aequorin with a single cysteine at position five was linked to serotonin using a Sulfo-LC-SPDP linker. In this assay, a biotinylated secondary anti-body was linked to the plate via a biotin-neutravidin on a neutravidin coated plate. A primary antibody to serotonin was added for the detection of free serotonin against the competing aequorin-serotonin conjugate. Hence, an assay was developed with a sensitivity up to 1.76 pg/μL, which falls within the range of lower detection limits is commercially available serotonin ELISA kits.

Future work with the aequorin based detection of serotonin using an assay would include optimizing incubation times and performing further replicates of existing data to verify the results. Additionally, serotonin is often in samples with other similar molecules, such as dopamine, or the precursor molecule tryptophan. Using multiple different aequorins with non-natural amino acids substitutions would provide multiplex detection capable of detecting up two or three different small targets like serotonin and its related molecules by discriminating different signal wavelengths and/or half-lives. Finally, the assay requires validation using serum samples.

In conclusion, the bioluminescent photoprotein aequorin was engineered in multiple ways to be used as sensor and imaging tool for several applications of biomedical relevance. First, four different non-natural amino acids were site-specifically incorporated into aequorin and the protein charged with nine different coelenterazines to create a catalog of red-shifted flash emission characteristics suitable for *in vitro* and *in vivo* analyte detection. An L-4-azidophenylalanine was also successfully site-specifically incorporated into an aequorin variant for the purpose of bio-orthogonal linking via click chemistry and shown to successfully link to several alkynylated molecules. A VEGFADARPin-Aequorin conjugate capable of targeting VEGFA in the retina for the purposes of imaging neovascularization has been generated, and demonstrated to be applicable as sensor for VEGFA in a wet MD models in mice.

REFERENCES

1. (a) Schott, H.; Fischer, D.; Kossel, H., Synthesis of four undecanucleotides complementary to a region of the coat protein cistron of phage fd. *Biochemistry* **1973,** *12* (18), 3447-53; (b) Hutchison, C. A., 3rd; Edgell, M. H., Genetic assay for small fragments of bacteriophage phi X174 deoxyribonucleic acid. *Journal of virology* **1971,** *8* (2), 181-9.

2. (a) Rowe, L.; Dikici, E.; Daunert, S., Engineering bioluminescent proteins: Expanding their analytical potential. *Analytical chemistry* **2009,** *81* (21), 8662-8668; (b) Chiesa, A.; Rapizzi, E.; Tosello, V.; Pinton, P.; de Virgilio, M.; Fogarty, K. E.; Rizzuto, R., Recombinant aequorin and green fluorescent protein as valuable tools in the study of cell signalling. *The Biochemical journal* **2001,** *355* (Pt 1), 1-12; (c) Inouye, S.; Noguchi, M.; Sakaki, Y.; Takagi, Y.; Miyata, T.; Iwanaga, S.; Tsuji, F. I., Cloning and sequence analysis of cDNA for the luminescent protein aequorin. *Proceedings of the National Academy of Sciences of the United States of America* **1985,** *82* (10), 3154-8.

3. Prendergast, F. G., Bioluminescence illuminated. *Nature* **2000,** *405* (6784), 291-3.

4. Widder, E. A., Bioluminescence in the ocean: Origins of biological, chemical, and ecological diversity. *Science* **2010,** *328* (5979), 704-708.

5. Scott, D.; Dikici, E.; Ensor, M.; Daunert, S., Bioluminescence and its impact on bioanalysis. *Annu Rev Anal Chem (Palo Alto Calif)* **2011,** *4*, 297-319.

6. Prescher, J. A.; Contag, C. H., Guided by the light: visualizing biomolecular processes in living animals with bioluminescence. *Current opinion in chemical biology* **2010,** *14* (1), 80-9.

7. (a) Hastings, J. W., Chemistries and colors of bioluminescent reactions: A review. *Gene* **1996,** *173* (1), 5-11; (b) Hall, M. P.; Unch, J.; Binkowski, B. F.; Valley, M. P.; Butler, B. L.; Wood, M. G.; Otto, P.; Zimmerman, K.; Vidugiris, G.; Machleidt, T.; Robers, M. B.; Benink, H. A.; Eggers, C. T.; Slater, M. R.; Meisenheimer, P. L.; Klaubert, D. H.; Fan, F.; Encell, L. P.; Wood, K. V., Engineered luciferase reporter from a deep sea shrimp utilizing a novel imidazopyrazinone substrate. *ACS chemical biology* **2012,** *7* (11), 1848-57; (c) Nakatsu, T.; Ichiyama, S.; Hiratake, J.; Saldanha, A.; Kobashi, N.; Sakata, K.; Kato, H., Structural basis for the spectral difference in luciferase bioluminescence. *Nature* **2006,** *440* (7082), 372-

8. Crofcheck, C. L.; Grosvenor, A. L.; Anderson, K. W.; Lumpp, J. K.; Scott, D. L.; Daunert, S., Detecting biomolecules in picoliter vials using aequorin bioluminescence. *Analytical chemistry* **1997,** *69* (23), 4768-72.

9. (a) Stepanyuk, G. A.; Golz, S.; Markova, S. V.; Frank, L. A.; Lee, J.; Vysotski, E. S., Interchange of aequorin and obelin bioluminescence color is determined by substitution of one active site residue of each photoprotein. *FEBS letters* **2005,** *579* (5), 1008-14; (b) van Oort, B.; Eremeeva, E. V.; Koehorst, R. B. M.; Laptenok, S. P.; van Amerongen, H.; van Berkel, W. J. H.; Malikova, N. P.; Markova, S. V.; Vysotski, E. S.; Visser, A. J. W. G.; Lee, J., Picosecond Fluorescence Relaxation Spectroscopy of the Calcium-Discharged Photoproteins Aequorin and Obelin. *Biochemistry* **2009,** *48* (44), 10486-10491; (c) Ohmiya, Y.; Hirano, T., Shining the light: the mechanism of the bioluminescence reaction of calcium-binding photoproteins. *Chemistry & biology* **1996,** *3* (5), 337-47; (d) Vysotski, E. S.; Lee, J., Ca2+-regulated photoproteins: structural insight into the bioluminescence mechanism. *Accounts of chemical research* **2004,** *37* (6), 405-15.

10. (a) Shimomura, O., A short story of aequorin. *The Biological bulletin* **1995,** *189* (1), 1-5; (b) The Royal Swedish Academy of Sciences, The Nobel Prize in Chemistry 2008-Press Release. **2008**.

11. Strynadka, N. C.; James, M. N., Crystal structures of the helix-loop-helix calcium-binding proteins. *Annu Rev Biochem* **1989,** *58*, 951-98.

12. (a) Deng, L.; Vysotski, E. S.; Markova, S. V.; Liu, Z. J.; Lee, J.; Rose, J.; Wang, B. C., All three Ca2+-binding loops of photoproteins bind calcium ions: the crystal structures of calcium-loaded apo-aequorin and apo-obelin. *Protein science : a publication of the Protein Society* **2005,** *14* (3), 663-75; (b) Charbonneau, H.; Walsh, K. A.; McCann, R. O.; Prendergast, F. G.; Cormier, M. J.; Vanaman, T. C., Amino acid sequence of the calcium-dependent photoprotein aequorin. *Biochemistry* **1985,** *24* (24), 6762-71; (c) Head, J. F.; Inouye, S.; Teranishi, K.; Shimomura, O., The crystal structure of the photoprotein aequorin at 2.3 A resolution. *Nature* **2000,** *405* (6784), 372-6.

13. Ohmiya, Y.; Ohashi, M.; Tsuji, F. I., Two excited states in aequorin bioluminescence induced by tryptophan modification. *FEBS letters* **1992,** *301* (2), 197-201.

14. Shimomura, O.; Kishi, Y.; Inouye, S., The relative rate of aequorin regeneration from apoaequorin and coelenterazine analogs. *The Biochemical journal* **1993,** *296 (Pt 3)*, 549-51.

15. Webb, S. E.; Karplus, E.; Miller, A. L., Retrospective on the development of aequorin and aequorin-based imaging to visualize changes in intracellular free [Ca]. *Molecular reproduction and development* **2013**.

16. (a) Curie, T.; Rogers, K. L.; Colasante, C.; Brulet, P., Red-shifted aequorin-based bioluminescent reporters for in vivo imaging of Ca2 signaling. *Molecular imaging* **2007,** *6* (1), 30-42; (b) Roda, A.; Pasini, P.; Mirasoli, M.; Michelini, E.; Guardigli, M., Biotechnological applications of bioluminescence and chemiluminescence. *Trends in biotechnology* **2004,** *22* (6), 295-303.

17. (a) Pancer, Z.; Amemiya, C. T.; Ehrhardt, G. R.; Ceitlin, J.; Gartland, G. L.; Cooper, M. D., Somatic diversification of variable lymphocyte receptors in the agnathan sea lamprey. *Nature* **2004,** *430* (6996), 174-80; (b) Pluckthun, A., Designed Ankyrin Repeat Proteins (DARPins): Binding Proteins for Research, Diagnostics, and Therapy. *Annual review of pharmacology and toxicology* **2015,** *55*, 489-511.

18. Barford, D., The Role of Multiple Sequence Repeat Motifs in the Assembly of Multi-protein Complexes. In *Macromolecular*, Springer Netherlands: 2012; pp 43-49.

19. Li, J.; Mahajan, A.; Tsai, M. D., Ankyrin repeat: a unique motif mediating protein-protein interactions. *Biochemistry* **2006,** *45* (51), 15168-78.

20. (a) Bork, P., Hundreds of ankyrin-like repeats in functionally diverse proteins: mobile modules that cross phyla horizontally? *Proteins* **1993,** *17* (4), 363-74; (b) Walker, R. G.; Willingham, A. T.; Zuker, C. S., A Drosophila mechanosensory transduction channel. *Science* **2000,** *287* (5461), 2229-34; (c) Binz, H. K.; Amstutz, P.; Pluckthun, A., Engineering novel binding proteins from nonimmunoglobulin domains. *Nature biotechnology* **2005,** *23* (10), 1257-68.

21. (a) Wetzel, S. K.; Ewald, C.; Settanni, G.; Jurt, S.; Pluckthun, A.; Zerbe, O., Residue-resolved stability of full-consensus ankyrin repeat proteins probed by NMR. *Journal of molecular biology* **2010,** *402* (1), 241-58; (b) Wetzel, S. K.; Settanni, G.; Kenig, M.; Binz, H. K.; Pluckthun, A., Folding and unfolding mechanism of highly stable full-consensus ankyrin repeat proteins. *Journal of molecular biology* **2008,** *376* (1), 241-57; (c) Binz, H. K.; Amstutz, P.; Kohl, A.; Stumpp, M. T.; Briand, C.; Forrer, P.; Grutter, M. G.; Pluckthun, A., High-affinity binders selected from designed ankyrin repeat protein libraries. *Nature biotechnology* **2004,** *22* (5), 575-82; (d) Kohl, A.; Binz, H. K.; Forrer, P.; Stumpp, M. T.; Pluckthun, A.; Grutter, M. G., Designed to be stable: crystal structure of a consensus ankyrin repeat protein. *Proceedings of the National Academy of Sciences of the United States of America* **2003,** *100* (4), 1700-5; (e) Interlandi, G.; Wetzel, S. K.; Settanni, G.; Pluckthun, A.; Caflisch, A., Characterization and further stabilization of designed ankyrin repeat proteins by combining molecular dynamics simulations and experiments. *Journal of molecular biology* **2008,** *375* (3), 837-54.

22. Goldstein, R.; Sosabowski, J.; Livanos, M.; Leyton, J.; Vigor, K.; Bhavsar, G.; Nagy-Davidescu, G.; Rashid, M.; Miranda, E.; Yeung, J.; Tolner, B.; Pluckthun, A.; Mather, S.; Meyer, T.; Chester, K., Development of the designed ankyrin repeat protein (DARPin) G3 for HER2 molecular imaging. *European journal of nuclear medicine and molecular imaging* **2015,** *42* (2), 288-301.

23. Parizek, P.; Kummer, L.; Rube, P.; Prinz, A.; Herberg, F. W.; Pluckthun, A., Designed ankyrin repeat proteins (DARPins) as novel isoform-specific intracellular inhibitors of c-Jun N-terminal kinases. *ACS chemical biology* **2012,** *7* (8), 1356-66.

24. Lewis, J. C.; Daunert, S., Photoproteins as luminescent labels in binding assays. *Fresen J Anal Chem* **2000,** *366* (6-7), 760-768.

25. Agarwal, P.; Bertozzi, C. R., Site-specific antibody-drug conjugates: The nexus of bioorthogonal chemistry, protein engineering, and drug development. *Bioconjugate chemistry* **2015**.

26. Best, M. D., Click chemistry and bioorthogonal reactions: unprecedented selectivity in the labeling of biological molecules. *Biochemistry* **2009,** *48* (28), 6571-84.

27. (a) Mirasoli, M.; Deo, S. K.; Lewis, J. C.; Roda, A.; Daunert, S., Bioluminescence immunoassay for cortisol using recombinant aequorin as a label. *Analytical biochemistry* **2002,** *306* (2), 204-11; (b) Chong, T. J.; Victorino, G. P., Angiotensin II subtype AT1 and AT2 receptors regulate microvascular hydraulic permeability via cAMP and cGMP. *The Journal of surgical research* **2006,** *131* (1), 105-10.

28. (a) Deo, S. K.; Lewis, J. C.; Daunert, S., Bioluminescence detection of proteolytic bond cleavage by using recombinant aequorin. *Analytical biochemistry* **2000,** *281* (1), 87-94; (b) Lizano, S.; Ramanathan, S.; Feltus, A.; Witkowski, A.; Daunert, S., Bioluminescence competitive binding assays for biotin based on photoprotein aequorin. *Methods in enzymology* **1997,** *279*, 296-303.

29. (a) Scott, D.; Hamorsky, K. T.; Ensor, C. M.; Anderson, K. W.; Daunert, S., Cyclic AMP receptor protein-aequorin molecular switch for cyclic AMP. *Bioconjugate chemistry* **2011,** *22* (3), 475-81; (b) Hamorsky, K. T.; Ensor, C. M.; Pasini, P.; Daunert, S., A protein switch sensing system for the quantification of sulfate. *Analytical biochemistry* **2012,** *421* (1), 172-80; (c) Teasley Hamorsky, K.; Ensor, C. M.; Wei, Y.; Daunert, S., A bioluminescent molecular switch for glucose. *Angew Chem Int Ed Engl* **2008,** *47* (20), 3718-21.

30. (a) Deroose, C. M.; De, A.; Loening, A. M.; Chow, P. L.; Ray, P.; Chatziioannou, A. F.; Gambhir, S. S., Multimodality imaging of tumor xenografts and metastases in mice with combined small-animal PET, small-animal CT, and bioluminescence imaging. *Journal of nuclear medicine : official publication, Society of Nuclear Medicine* **2007,** *48* (2), 295-303; (b) Smith-Bindman, R.; Miglioretti, D. L.; Johnson, E.; Lee, C.; Feigelson, H. S.; Flynn, M.; Greenlee, R. T.; Kruger, R. L.; Hornbrook, M. C.; Roblin, D.; Solberg, L. I.; Vanneman, N.; Weinmann, S.; Williams, A. E., Use of Diagnostic Imaging Studies and Associated Radiation Exposure for Patients Enrolled in Large Integrated Health Care Systems, 1996-2010. *Jama-J Am Med Assoc* **2012,** *307* (22), 2400-2409; (c) van Essen, M.; Sundin, A.; Krenning, E. P.; Kwekkeboom, D. J., Neuroendocrine tumours: the role of imaging for diagnosis and therapy. *Nat Rev Endocrinol* **2014,** *10* (2), 102-114.

31. Iglehart, J. K., Health insurers and medical-imaging policy--a work in progress. *The New England journal of medicine* **2009,** *360* (10), 1030-7.

32. Choy, G.; O'Connor, S.; Diehn, F. E.; Costouros, N.; Alexander, H. R.; Choyke, P.; Libutti, S. K., Comparison of noninvasive fluorescent and bioluminescent small animal optical imaging. *BioTechniques* **2003,** *35* (5), 1022-6, 1028-30.

33. (a) Ozawa, T.; Yoshimura, H.; Kim, S. B., Advances in Fluorescence and Bioluminescence Imaging. *Analytical chemistry* **2012**; (b) Shetty, R. S.; Deo, S. K.; Liu, Y.; Daunert, S., Fluorescence-based sensing system for copper using genetically engineered living yeast cells. *Biotechnology and bioengineering* **2004,** *88* (5), 664-70.

34. (a) Bhaumik, S.; Gambhir, S. S., Optical imaging of Renilla luciferase reporter gene expression in living mice. *Proceedings of the National Academy of Sciences of the United States of America* **2002,** *99* (1), 377-82; (b) Bhaumik, S.; Lewis, X. Z.; Gambhir, S. S., Optical imaging of Renilla luciferase, synthetic Renilla luciferase, and firefly luciferase reporter gene expression in living mice. *Journal of biomedical optics* **2004,** *9* (3), 578-86; (c) Close, D. M.; Xu, T.; Sayler, G. S.; Ripp, S., In vivo bioluminescent imaging (BLI): noninvasive visualization and interrogation of biological processes in living animals. *Sensors* **2011,** *11* (1), 180-206; (d) Hutchens, M.; Luker, G. D., Applications of bioluminescence imaging to the study of infectious diseases. *Cell Microbiol* **2007,** *9* (10), 2315-2322; (e) Godinat, A.; Park, H. M.; Miller, S. C.; Cheng, K.; Hanahan, D.; Sanman, L. E.; Bogyo, M.; Yu, A.; Nikitin, G. F.; Stahl, A.; Dubikovskaya, E. A., A biocompatible in vivo ligation reaction and its application for noninvasive bioluminescent imaging of protease activity in living mice. *ACS chemical biology* **2013,** *8* (5), 987-99.

35. Du, J.; Yu, C.; Pan, D.; Li, J.; Chen, W.; Yan, M.; Segura, T.; Lu, Y., Quantum-dot-decorated robust transductable bioluminescent nanocapsules. *Journal of the American Chemical Society* **2010,** *132* (37), 12780-1.

36. Zinn, K. R.; Chaudhuri, T. R.; Szafran, A. A.; O'Quinn, D.; Weaver, C.; Dugger, K.; Lamar, D.; Kesterson, R. A.; Wang, X.; Frank, S. J., Noninvasive Bioluminescence Imaging in Small Animals. *ILAR Journal* **2008,** *49* (1), 103-115.

37. (a) Chusacultanachai, S.; Yuthavong, Y., Random mutagenesis strategies for construction of large and diverse clone libraries of mutated DNA fragments. *Methods Mol Biol* **2004,** *270*, 319-34; (b) McCullum, E. O.; Williams, B. A.; Zhang, J.; Chaput, J. C., Random mutagenesis by error-prone PCR. *Methods Mol Biol* **2010,** *634*, 103-9.

38. (a) Qu, X.; Rowe, L.; Dikici, E.; Ensor, M.; Daunert, S., Aequorin mutants with increased thermostability. *Analytical and bioanalytical chemistry* **2014,** *406* (23), 5639-43; (b) Tricoire, L., Tsuzuki, K., Courjean, O., *et al*. ., Calcium Dependence of Aequorin Bioluminescnece Dissected by Random Mutagenesis. *cPNAS* **2006,** *103* (25), 5; (c) Tsuzuki, K.; Tricoire, L.; Courjean, O.; Gibelin, N.; Rossier, J.; Lambolez, B., Thermostable mutants of the photoprotein aequorin obtained by in vitro evolution. *Journal of Biological Chemistry* **2005,** *280* (40), 34324-34331.

39. (a) Nomura, M.; Inouye, S.; Ohmiya, Y.; Tsuji, F. I., A C-terminal proline is required for bioluminescence of the Ca(2+)-binding photoprotein, aequorin. *FEBS letters* **1991,** *295* (1-3), 63-6; (b) Dikici, E.; Qu, X.; *al., e.*, Aequorin variants with improved bioluminescence properties. *Protein engineering, design & selection : PEDS* **2009,** *22* (4), 243-8; (c) Tricoire, L.; Tsuzuki, K.; Courjean, O.; Gibelin, N.; Bourout, G.; Rossier, J.; Lambolez, B., Calcium dependence of aequorin bioluminescence dissected by random mutagenesis. *Proceedings of the National Academy of Sciences of the United States of America* **2006,** *103* (25), 9500-5.

40. Ohmiya, Y.; Tsuji, F. I., Bioluminescence of the Ca(2+)-binding photoprotein, aequorin, after histidine modification. *FEBS letters* **1993,** *320* (3), 267-70.

41. Shrestha, S.; Paeng, I. R.; Deo, S. K.; Daunert, S., Cysteine-free mutant of aequorin as a photolabel in immunoassay development. *Bioconjugate chemistry* **2002,** *13* (2), 269-75.

42. (a) Lewis, J. C.; Daunert, S., Bioluminescence immunoassay for thyroxine employing genetically engineered mutant aequorins containing unique cysteine residues. *Analytical chemistry* **2001,** *73* (14), 3227-33; (b) Kurose, K.; Inouye, S.; Sakaki, Y.; Tsuji, F. I., Bioluminescence of the Ca2+-binding photoprotein aequorin after cysteine modification. *Proceedings of the National Academy of Sciences of the United States of America* **1989,** *86* (1), 80-4.

43. Roura, S.; Galvez-Monton, C.; Bayes-Genis, A., Bioluminescence imaging: a shining future for cardiac regeneration. *Journal of cellular and molecular medicine* **2013,** *17* (6), 693-703.

44. Deo, S. K.; Mirasoli, M.; Daunert, S., Bioluminescence resonance energy transfer from aequorin to a fluorophore: an artificial jellyfish for applications in multianalyte detection. *Analytical and bioanalytical chemistry* **2005,** *381* (7), 1387-94.

45. (a) Bakayan, A.; Domingo, B.; Miyawaki, A.; Llopis, J., Imaging Ca activity in mammalian cells and zebrafish with a novel red-emitting aequorin variant. *Pflugers Archiv : European journal of physiology* **2014**; (b) Bakayan, A.; Vaquero, C. F.; Picazo, F.; Llopis, J., Red fluorescent protein-aequorin fusions as improved bioluminescent Ca2+ reporters in single cells and mice. *PloS one* **2011,** *6* (5), e19520.

46. Haddock, S. H.; Rivers, T. J.; Robison, B. H., Can coelenterates make coelenterazine? Dietary requirement for luciferin in cnidarian bioluminescence. *Proceedings of the National Academy of Sciences of the United States of America* **2001,** *98* (20), 11148-51.

47. (a) Shimomura, O.; Musicki, B.; Kishi, Y.; Inouye, S., Light-emitting properties of recombinant semi-synthetic aequorins and recombinant fluorescein-conjugated aequorin for measuring cellular calcium. *Cell calcium* **1993,** *14* (5), 373-8; (b) Rowe, L.; Combs, K.; Deo, S.; Ensor, C.; Daunert, S.; Qu, X., Genetically modified semisynthetic bioluminescent photoprotein variants: simultaneous dual-analyte assay in a single well employing time resolution of decay kinetics. *Analytical chemistry* **2008,** *80* (22), 8470-6.

48. (a) Shimomura, O.; Musicki, B.; Kishi, Y., Semi-synthetic aequorin. An improved tool for the measurement of calcium ion concentration. *The Biochemical journal* **1988,** *251* (2), 405-10; (b) Shimomura, O.; Musicki, B.; Kishi, Y., Semi-synthetic aequorins with improved sensitivity to Ca2+ ions. *The Biochemical journal* **1989,** *261* (3), 913-20.

49. (a) Liu, C. C.; Schultz, P. G., Adding new chemistries to the genetic code. *Annu Rev Biochem* **2010,** *79*, 413-44; (b) Farrell, I. S.; Toroney, R.; Hazen, J. L.; Mehl, R. A.; Chin, J. W., Photo-cross-linking interacting proteins with a genetically encoded benzophenone. *Nature methods* **2005,** *2* (5), 377-84.

50. England, P. M., Unnatural amino acid mutagenesis: a precise tool for probing protein structure and function. *Biochemistry* **2004,** *43* (37), 11623-9.

51. Camarero, J. A.; Hackel, B. J.; de Yoreo, J. J.; Mitchell, A. R., Fmoc-based synthesis of peptide alpha-thioesters using an aryl hydrazine support. *The Journal of organic chemistry* **2004,** *69* (12), 4145-51.

52. Deechongkit, S.; You, S. L.; Kelly, J. W., Synthesis of all nineteen appropriately protected chiral alpha-hydroxy acid equivalents of the alpha-amino acids for Boc solid-phase depsi-peptide synthesis. *Organic letters* **2004,** *6* (4), 497-500.

53. Schwarzer, D.; Cole, P. A., Protein semisynthesis and expressed protein ligation: chasing a protein's tail. *Current opinion in chemical biology* **2005,** *9* (6), 561-9.

54. Bacher, J. M.; Ellington, A. D., Global incorporation of unnatural amino acids in Escherichia coli. *Methods Mol Biol* **2007,** *352*, 23-34.

55. (a) Cirino, P. C.; Tang, Y.; Takahashi, K.; Tirrell, D. A.; Arnold, F. H., Global incorporation of norleucine in place of methionine in cytochrome P450 BM-3 heme domain increases peroxygenase activity. *Biotechnology and bioengineering* **2003,** *83* (6), 729-34; (b) Rubini, M.; Lepthien, S.; Golbik, R.; Budisa, N., Aminotryptophan-containing barstar: structure--function tradeoff in protein design and engineering with an expanded genetic code. *Biochimica et biophysica acta* **2006,** *1764* (7), 1147-58.

56. Singer, R. A.; Johnston, G. C.; Bedard, D., Methionine analogs and cell division regulation in the yeast Saccharomyces cerevisiae. *Proceedings of the National Academy of Sciences of the United States of America* **1978,** *75* (12), 6083-7.

57. (a) Heckler, T. G.; Chang, L. H.; Zama, Y.; Naka, T.; Chorghade, M. S.; Hecht, S. M., T4 RNA ligase mediated preparation of novel "chemically misacylated" tRNAPheS. *Biochemistry* **1984,** *23* (7), 1468-73; (b) Roesser, J. R.; Xu, C.; Payne, R. C.; Surratt, C. K.; Hecht, S. M., Preparation of misacylated aminoacyl-tRNA(Phe)'s useful as probes of the ribosomal acceptor site. *Biochemistry* **1989,** *28* (12), 5185-95.

58. Wang, L.; Brock, A.; Herberich, B.; Schultz, P. G., Expanding the genetic code of Escherichia coli. *Science* **2001,** *292* (5516), 498-500.

59. Noren, C. J.; Anthony-Cahill, S. J.; Griffith, M. C.; Schultz, P. G., A general method for site-specific incorporation of unnatural amino acids into proteins. *Science* **1989,** *244* (4901), 182-8.

60. Nowak, M. W.; Gallivan, J. P.; Silverman, S. K.; Labarca, C. G.; Dougherty, D. A.; Lester, H. A., In vivo incorporation of unnatural amino acids into ion channels in Xenopus oocyte expression system. *Methods in enzymology* **1998,** *293*, 504-29.

61. (a) Ryu, Y.; Schultz, P. G., Efficient incorporation of unnatural amino acids into proteins in Escherichia coli. *Nature Methods* **2006,** *3*, 263-265; (b) Greiss, S.; Chin, J. W., Expanding the genetic code of an animal. *Journal of the American Chemical Society* **2011,** *133* (36), 14196-9; (c) Ibba, M.; Hennecke, H., Relaxing the substrate specificity of an aminoacyl-tRNA synthetase allows in vitro and in vivo synthesis of proteins containing unnatural amino acids. *FEBS letters* **1995,** *364* (3), 272-5.

62. Young, T. S.; Ahmad, I.; Yin, J. A.; Schultz, P. G., An enhanced system for unnatural amino acid mutagenesis in E. coli. *Journal of molecular biology* **2010,** *395* (2), 361-74.

63. Chin, J. W.; Martin, A. B.; King, D. S.; Wang, L.; Schultz, P. G., Addition of a photocrosslinking amino acid to the genetic code of Escherichiacoli. *Proceedings of the National Academy of Sciences of the United States of America* **2002,** *99* (17), 11020-4.

64. Batjargal, S.; Walters, C. R.; Petersson, E. J., Inteins as traceless purification tags for unnatural amino acid proteins. *Journal of the American chemical society* **2015**.

65. (a) Wang, F.; Niu, W.; Guo, J.; Schultz, P. G., Unnatural amino acid mutagenesis of fluorescent proteins. *Angew Chem Int Ed Engl* **2012,** *51* (40), 10132-5; (b) Bae, J. H.; Rubini, M.; Jung, G.; Wiegand, G.; Seifert, M. H.; Azim, M. K.; Kim, J. S.; Zumbusch, A.; Holak, T. A.; Moroder, L.; Huber, R.; Budisa, N., Expansion of the genetic code enables design of a novel "gold" class of green fluorescent proteins. *Journal of molecular biology* **2003,** *328* (5), 1071-81.

66. Rowe, L.; Ensor, M.; Mehl, R.; Daunert, S., Modulating the bioluminescence emission of photoproteins by in vivo site-directed incorporation of non-natural amino acids. *ACS chemical biology* **2010,** *5* (5), 455-460.

67. (a) Coscas, G.; Yamashiro, K.; Coscas, F.; De Benedetto, U.; Tsujikawa, A.; Miyake, M.; Gemmy Cheung, C. M.; Wong, T. Y.; Yoshimura, N., Comparison of exudative age-related macular degeneration subtypes in Japanese and French Patients: multicenter diagnosis with multimodal imaging. *American journal of ophthalmology* **2014,** *158* (2), 309-318 e2; (b) Cheung, C. M.; Li, X.; Cheng, C. Y.; Zheng, Y.; Mitchell, P.; Wang, J. J.; Wong, T. Y., Prevalence, racial variations, and risk factors of age-related macular degeneration in Singaporean Chinese, Indians, and Malays. *Ophthalmology* **2014,** *121* (8), 1598-603; (c) Joachim, N.; Mitchell, P.; Younan, C.; Burlutsky, G.; Cheng, C. Y.; Cheung, C. M.; Zheng, Y.; Moffitt, M.; Wong, T. Y.; Wang, J. J., Ethnic variation in early age-related macular degeneration lesions between white Australians and Singaporean Asians. *Investigative ophthalmology & visual science* **2014,** *55* (7), 4421-9.

68. (a) Smith, W.; Assink, J.; Klein, R.; Mitchell, P.; Klaver, C. C.; Klein, B. E.; Hofman, A.; Jensen, S.; Wang, J. J.; de Jong, P. T., Risk factors for age-related macular degeneration: Pooled findings from three continents. *Ophthalmology* **2001,** *108* (4), 697-704; (b) Seddon, J. M.; Reynolds, R.; Yu, Y.; Daly, M. J.; Rosner, B., Risk models for progression to advanced age-related macular degeneration using demographic, environmental, genetic, and ocular factors. *Ophthalmology* **2011,** *118* (11), 2203-11; (c) Yang, K.; Wang, F. H.; Liang, Y. B.; Wong, T. Y.; Wang, J. J.; Zhan, S. Y.; Wang, N. L., Associations between cardiovascular risk factors and early age-related macular degeneration in a rural Chinese adult population. *Retina* **2014,** *34* (8), 1539-53.

69. (a) Truong, A.; Wong, T. Y.; Khachigian, L. M., Emerging therapeutic approaches in the management of retinal angiogenesis and edema. *Journal of molecular medicine* **2011,** *89* (4), 343-61; (b) Lim, J. H.; Wickremasinghe, S. S.; Xie, J.; Chauhan, D. S.; Baird, P. N.; Robman, L. D.; Hageman, G.; Guymer, R. H., Delay to treatment and visual outcomes in patients treated with anti-vascular endothelial growth factor for age-related macular degeneration. *American journal of ophthalmology* **2012,** *153* (4), 678-86, 686 e1-2.

70. Grisanti, S.; Tatar, O., The role of vascular endothelial growth factor and other endogenous interplayers in age-related macular degeneration. *Progress in retinal and eye research* **2008,** *27* (4), 372-90.

71. Rosenfeld, P. J.; Brown, D. M.; Heier, J. S.; Boyer, D. S.; Kaiser, P. K.; Chung, C. Y.; Kim, R. Y.; Group, M. S., Ranibizumab for neovascular age-related macular degeneration. *The New England journal of medicine* **2006,** *355* (14), 1419-31.

72. El Matri, L.; Bouraoui, R.; Chebil, A.; Kort, F.; Bouladi, M.; Limaiem, R.; Landoulsi, H., Bevacizumab injection in patients with age-related macular degeneration associated with poor initial visual acuity. *Journal of ophthalmology* **2012,** *2012*, 861384.

73. (a) Parmeggiani, F.; Costagliola, C.; Incorvaia, C.; Sebastiani, A.; Gemmati, D., Pharmacogenetic aspects in therapeutic management of subfoveal choroidal neovascularisation: role of factor XIII-A 185 T-allele. *Current drug targets* **2011,** *12* (2), 138-48; (b) Lim, L. S.; Mitchell, P.; Seddon, J. M.; Holz, F. G.; Wong, T. Y., Age-related macular degeneration. *Lancet* **2012,** *379* (9827), 1728-38.

74. (a) Jorzik, J. J.; Bindewald, A.; Dithmar, S.; Holz, F. G., Digital simultaneous fluorescein and indocyanine green angiography, autofluorescence, and red-free imaging with a solid-state laser-based confocal scanning laser ophthalmoscope. *Retina* **2005,** *25* (4), 405-16; (b) Holz, F. G.; Bindewald-Wittich, A.; Fleckenstein, M.; Dreyhaupt, J.; Scholl, H. P.; Schmitz-Valckenberg, S.; Group, F. A.-S., Progression of geographic atrophy and impact of fundus autofluorescence patterns in age-related macular degeneration. *American journal of ophthalmology* **2007,** *143* (3), 463-72.

75. Schmitz-Valckenberg, S.; Steinberg, J. S.; Fleckenstein, M.; Visvalingam, S.; Brinkmann, C. K.; Holz, F. G., Combined confocal scanning laser ophthalmoscopy and spectral-domain optical coherence tomography imaging of reticular drusen associated with age-related macular degeneration. *Ophthalmology* **2010,** *117* (6), 1169-76.

76. (a) Stahl, A.; Stumpp, M. T.; Schlegel, A.; Ekawardhani, S.; Lehrling, C.; Martin, G.; Gulotti-Georgieva, M.; Villemagne, D.; Forrer, P.; Agostini, H. T.; Binz, H. K., Highly potent VEGF-A-antagonistic DARPins as anti-angiogenic agents for topical and intravitreal applications. *Angiogenesis* **2013,** *16* (1), 101-11; (b) Campochiaro, P. A.; Channa, R.; Berger, B. B.; Heier, J. S.; Brown, D. M.; Fiedler, U.; Hepp, J.; Stumpp, M. T., Treatment of diabetic macular edema with a designed ankyrin repeat protein that binds vascular endothelial growth factor: a phase I/II study. *American journal of ophthalmology* **2013,** *155* (4), 697-704, 704 e1-2.

77. Tamaskovic, R.; Simon, M.; Stefan, N.; Schwill, M.; Pluckthun, A., Designed ankyrin repeat proteins (DARPins) from research to therapy. *Methods in enzymology* **2012,** *503*, 101-34.

78. O'Neill, K.; Lyons, S. K.; Gallagher, W. M.; Curran, K. M.; Byrne, A. T., Bioluminescent imaging: a critical tool in pre-clinical oncology research. *J Pathol* **2010,** *220* (3), 317-27.

79. Moschou, E. A.; Sharma, B. V.; Deo, S. K.; Daunert, S., Fluorescence glucose detection: advances toward the ideal in vivo biosensor. *Journal of fluorescence* **2004,** *14* (5), 535-47.

80. Rowe, L.; Ensor, M.; Mehl, R.; Daunert, S., Modulating the bioluminescence emission of photoproteins by in vivo site-directed incorporation of non-natural amino acids. *ACS chemical biology* **2010,** *5* (5), 455-60.

81. Maniatis, T.; Fritsch, E. F.; Sambrook, J., *Molecular cloning : a laboratory manual*. Cold Spring Harbor Laboratory: Cold Spring Harbor, N.Y., 1982; p x, 545 p.

82. Deng, L.; Markova, S. V.; Vysotski, E. S.; Liu, Z. J.; Lee, J.; Rose, J.; Wang, B. C., Crystal structure of a Ca2+-discharged photoprotein: implications for mechanisms of the calcium trigger and bioluminescence. *The Journal of biological chemistry* **2004,** *279* (32), 33647-52.

83. Nijegorodov, N.; Mabbs, R., The influence of molecular symmetry and topological factors on the internal heavy atom effect in aromatic and heteroaromatic compounds. *Spectrochimica acta. Part A, Molecular and biomolecular spectroscopy* **2001,** *57* (7), 1449-62.

84. Dothager, R. S.; Flentie, K.; Moss, B.; Pan, M. H.; Kesarwala, A.; Piwnica-Worms, D., Advances in bioluminescence imaging of live animal models. *Current opinion in biotechnology* **2009,** *20* (1), 45-53.

85. Shimomura, O.; Johnson, F. H.; Saiga, Y., Extraction, purification and properties of aequorin, a bioluminescent protein from the luminous hydromedusan, Aequorea. *Journal of cellular and comparative physiology* **1962,** *59*, 223-39.

86. (a) Dikici, E.; Qu, X.; Rowe, L.; Millner, L.; Logue, C.; Deo, S. K.; Ensor, M.; Daunert, S., Aequorin variants with improved bioluminescence properties. *Protein engineering, design & selection : PEDS* **2009,** *22* (4), 243-8; (b) Rowe, L.; Rothert, A.; Logue, C.; Ensor, C. M.; Deo, S. K.; Daunert, S., Spectral tuning of photoproteins by partnering site-directed mutagenesis strategies with the incorporation of chromophore analogs. *Protein engineering, design & selection : PEDS* **2008,** *21* (2), 73-81; (c) Chatterjee, A.; Xiao, H.; Schultz, P. G., Evolution of multiple, mutually orthogonal prolyl-tRNA synthetase/tRNA pairs for unnatural amino acid mutagenesis in Escherichia coli. *Proceedings of the National Academy of Sciences of the United States of America* **2012,** *109* (37), 14841-6.

87. Eremeeva, E. V.; Markova, S. V.; Westphal, A. H.; Visser, A. J. W. G.; van Berkel, W. J. H.; Vysotski, E. S., The intrinsic fluorescence of apo-obelin and apo-aequorin and use of its quenching to characterize coelenterazine binding. *FEBS letters* **2009,** *583* (12), 1939-1944.

88. Negrin, R. S.; Contag, C. H., In vivo imaging using bioluminescence: a tool for probing graft-versus-host disease. *Nature reviews. Immunology* **2006,** *6* (6), 484-90.

89. Filpponen, I.; Kontturi, E.; Nummelin, S.; Rosilo, H.; Kolehmainen, E.; Ikkala, O.; Laine, J., Generic method for modular surface modification of cellulosic materials in aqueous medium by sequential "click" reaction and adsorption. *Biomacromolecules* **2012,** *13* (3), 736-42.

90. Chang, P. V.; Prescher, J. A.; Sletten, E. M.; Baskin, J. M.; Miller, I. A.; Agard, N. J.; Lo, A.; Bertozzi, C. R., Copper-free click chemistry in living animals. *Proceedings of the National Academy of Sciences of the United States of America* **2010,** *107* (5), 1821-6.

91. Lin, S.; Zhang, Z.; Xu, H.; Li, L.; Chen, S.; Li, J.; Hao, Z.; Chen, P. R., Site-specific incorporation of photo-cross-linker and bioorthogonal amino acids into enteric bacterial pathogens. *Journal of the American chemical society* **2011,** *133* (50), 20581-7.

92. Bostic, H. E.; Smith, M. D.; Poloukhtine, A. A.; Popik, V. V.; Best, M. D., Membrane labeling and immobilization via copper-free click chemistry. *Chem Commun (Camb)* **2012,** *48* (10), 1431-3.

93. (a) Yang, Y.; Verhelst, S. H., Cleavable trifunctional biotin reagents for protein labelling, capture and release. *Chem Commun (Camb)* **2013,** *49* (47), 5366-8; (b) Chin, J. W.; Santoro, S. W.; Martin, A. B.; King, D. S.; Wang, L.; Schultz, P. G., Addition of p-azido-L-phenylalanine to the genetic code of Escherichia coli. *Journal of the American Chemical Society* **2002,** *124* (31), 9026-7; (c) Simon, M.; Frey, R.; Zangemeister-Wittke, U.; Pluckthun, A., Orthogonal assembly of a designed ankyrin repeat protein-cytotoxin conjugate with a clickable serum albumin module for half-life extension. *Bioconjugate chemistry* **2013,** *24* (11), 1955-66.

94. Inouye, S.; Sato, J.; Sasaki, S.; Sahara, Y., Streptavidin-aequorin fusion protein for bioluminescent immunoassay. *Bioscience, biotechnology, and biochemistry* **2011,** *75* (3), 568-71.

95. Ball, J. C.; Scott, D. L.; Lumpp, J. K.; Daunert, S.; Wang, J.; Bachas, L. G., Electrochemistry in nanovials fabricated by combining screen printing and laser micromachining. *Analytical chemistry* **2000,** *72* (3), 497-501.

96. (a) Maurer-Spurej, E.; Dyker, K.; Gahl, W. A.; Devine, D. V., A novel immunocytochemical assay for the detection of serotonin in platelets. *Br J Haematol* **2002,** *116* (3), 604-11; (b) Gershon, M. D., 5-Hydroxytryptamine (serotonin) in the gastrointestinal tract. *Current opinion in endocrinology, diabetes, and obesity* **2013,** *20* (1), 14-21; (c) Mawe, G. M.; Hoffman, J. M., Serotonin signalling in the gut--functions, dysfunctions and therapeutic targets. *Nature reviews. Gastroenterology & hepatology* **2013,** *10* (8), 473-86; (d) O'Mahony, S. M.; Clarke, G.; Borre, Y. E.; Dinan, T. G.; Cryan, J. F., Serotonin, tryptophan metabolism and the brain-gut-microbiome axis. *Behavioural brain research* **2015,** *277*, 32-48; (e) Legay, C.; Faudon, M.; Hery, F.; Ternaux, J. P., 5-HT metabolism in the intestinal wall of the rat-I. The mucosa. *Neurochemistry international* **1983,** *5* (6), 721-7.

97. Lovenberg, W.; Jequier, E.; Sjoerdsma, A., Tryptophan hydroxylation: measurement in pineal gland, brainstem, and carcinoid tumor. *Science* **1967,** *155* (3759), 217-9.

98. (a) Atkinson, W.; Lockhart, S.; Whorwell, P. J.; Keevil, B.; Houghton, L. A., Altered 5-hydroxytryptamine signaling in patients with constipation- and diarrhea-predominant irritable bowel syndrome. *Gastroenterology* **2006,** *130* (1), 34-43; (b) Manocha, M.; Khan, W. I., Serotonin and GI Disorders: An Update on Clinical and Experimental Studies. *Clinical and translational gastroenterology* **2012,** *3*, e13; (c) Daly, E.; Ecker, C.; Hallahan, B.; Deeley, Q.; Craig, M.; Murphy, C.; Johnston, P.; Spain, D.; Gillan, N.; Gudbrandsen, M.; Brammer, M.; Giampietro, V.; Lamar, M.; Page, L.; Toal, F.; Schmitz, N.; Cleare, A.; Robertson, D.; Rubia, K.; Murphy, D. G., Response inhibition and serotonin in autism: a functional MRI study using acute tryptophan depletion. *Brain : a journal of neurology* **2014,** *137* (Pt 9), 2600-10; (d) Lesurtel, M.; Clavien, P. A., Platelet-derived serotonin: translational implications for liver regeneration. *Hepatology* **2014,** *60* (1), 30-3.

99. Inouye, S.; Sato, J., Purification of histidine-tagged aequorin with a reactive cysteine residue for chemical conjugations and its application for bioluminescent sandwich immunoassays. *Protein expression and purification* **2012,** *83* (2), 205-10.

100. Qu, X.; Deo, S. K.; Dikici, E.; Ensor, M.; Poon, M.; Daunert, S., Bioluminescence immunoassay for angiotensin II using aequorin as a label. *Analytical biochemistry* **2007,** *371* (2), 154-61.

101. (a) Smith-Bindman, R.; Miglioretti, D. L.; Johnson, E.; Lee, C.; Feigelson, H. S.; Flynn, M.; Greenlee, R. T.; Kruger, R. L.; Hornbrook, M. C.; Roblin, D.; Solberg, L. I.; Vanneman, N.; Weinmann, S.; Williams, A. E., Use of diagnostic imaging studies and associated radiation exposure for patients enrolled in large integrated health care systems, 1996-2010. *Jama* **2012,** *307* (22), 2400-9; (b) Rein, D. B.; Zhang, P.; Wirth, K. E.; Lee, P. P.; Hoerger, T. J.; McCall, N.; Klein, R.; Tielsch, J. M.; Vijan, S.; Saaddine, J., The economic burden of major adult visual disorders in the United States. *Archives of ophthalmology* **2006,** *124* (12), 1754-60.

102. Kondo, S.; Asano, M.; Suzuki, H., Significance of vascular endothelial growth factor/vascular permeability factor for solid tumor growth, and its inhibition by the antibody. *Biochemical and biophysical research communications* **1993,** *194* (3), 1234-41.

103. Ogata, N.; Ando, A.; Uyama, M.; Matsumura, M., Expression of cytokines and transcription factors in photocoagulated human retinal pigment epithelial cells. *Graefe's archive for clinical and experimental ophthalmology = Albrecht von Graefes Archiv fur klinische und experimentelle Ophthalmologie* **2001,** *239* (2), 87-95.

104. Lewis, J. C.; Lopez-Moya, J. J.; Daunert, S., Bioluminescence and secondary structure properties of aequorin mutants produced for site-specific conjugation and immobilization. *Bioconjugate chemistry* **2000,** *11* (1), 65-70.

105. (a) Ottolini, D.; Cali, T.; Brini, M., Measurements of Ca(2)(+) concentration with recombinant targeted luminescent probes. *Methods Mol Biol* **2013,** *937*, 273-91; (b) Wang, Y.; Iyer, M.; Annala, A.; Wu, L.; Carey, M.; Gambhir, S. S., Noninvasive indirect imaging of vascular endothelial growth factor gene expression using bioluminescence imaging in living transgenic mice. *Physiological genomics* **2006,** *24* (2), 173-80.

106. Shimomura, O., Membrane permeability of coelenterazine analogs measured with fish eggs. *The Biochemical journal* **1997,** *326 (Pt 2)*, 297-8.

107. Zahnd, C.; Kawe, M.; Stumpp, M. T.; de Pasquale, C.; Tamaskovic, R.; Nagy-Davidescu, G.; Dreier, B.; Schibli, R.; Binz, H. K.; Waibel, R.; Pluckthun, A., Efficient tumor targeting with high-affinity designed ankyrin repeat proteins: effects of affinity and molecular size. *Cancer research* **2010,** *70* (4), 1595-605.

108. Eisenstein, M., Something new under the skin. *Nature biotechnology* **2011,** *29* (2), 107-9.

109. Itaya, M.; Sakurai, E.; Nozaki, M.; Yamada, K.; Yamasaki, S.; Asai, K.; Ogura, Y., Upregulation of VEGF in murine retina via monocyte recruitment after retinal scatter laser photocoagulation. *Investigative ophthalmology & visual science* **2007,** *48* (12), 5677-83.

110. Stepanyuk, G. A.; Unch, J.; Malikova, N. P.; Markova, S. V.; Lee, J.; Vysotski, E. S., Coelenterazine-v ligated to Ca2+-triggered coelenterazine-binding protein is a stable and efficient substrate of the red-shifted mutant of Renilla muelleri luciferase. *Analytical and bioanalytical chemistry* **2010,** *398* (4), 1809-17.

111. Blinks, J. R.; Wier, W. G.; Hess, P.; Prendergast, F. G., Measurement of Ca2+ concentrations in living cells. *Progress in biophysics and molecular biology* **1982,** *40* (1-2), 1-114.